Dipartimento di Biologia Vegetale

DOTTORATO DI RICERCA
IN BIOTECOLOGIE VEGETALI
XX Ciclo

Identification and characterisation of new members of pectin methylesterase/invertase inhibitor family in tomato (*Solanum lycopersicum)*

(AGR/07-BIO/04)

Coordinatore: Prof. Stefania Masci

Tutor: Prof. Daniela Bellincampi

Dottorando: Ida Barbara Reca

Tesi in cotutela con/Thèse an co-tutelle avec

L'UNIVERSITE PAUL CEZANNE (AIX-MARSEILLE III)

Identification and characterisation of new members of pectin methylesterase/invertase inhibitor family in tomato (*Solanum lycopersicum)*

En vue d'obtenir le grade de

DOCTEUR de L'UNIVERSITE Paul CEZANNE
Faculté des Sciences et Techniques
Discipline : Nutrition ; Aspects Moléculaires et Cellulaires

Présentée et soutenue publiquement par Mme Ida Barbara RECA
Vendredi 14 Mars

Directeur de thèse : Prof. Daniela Bellincampi
Co-Directeur de thèse : Dr. Thierry Giardina

JURY

Pr. Daniela Bellincampi	Directeur de thèse
Dr Thierry Giardina	Co-Directeur de thèse
Dr. Josette Perrier	Examinateur
Pr. Stefania Masci	Examinateur
Dr. Nathalie Juge	Rapporteur
Pr. Rodolfo Federico	Rapporteur

ANNEE 2008

A nonno Paolo che ancora alimenta il mio spirito

E' difficile in poche righe ricordare tutte le persone che, a vario titolo, hanno contribuito a rendere "migliori" questi anni.

Desidero ringraziare la Pr. Daniela Bellincampi e il Dr Thiery Giardina per la pazienza, la disponibilità, per avermi aiutata nei momenti difficili e per avermi indirizzata sempre verso la strada giusta da intraprendere. Ringrazio la Dr Laura Camardella per la collaborazione e la simpatia tipica napoletana. Vorrei inoltre ringraziare il Prof. Felice Cervone e la Prof Giulia De Lorenzo, il Prof. Renato D'ovidio e la Prof. Stefania Masci per la loro gentilezza e disponibilità. Grazie a Gianni per il prezioso supporto tecnico e a Vera per le lezioni di stile.

Un grazie particolare va a Lucia, Fedra e Flavio, insostituibili compagni con cui ho condiviso gioie e dolori di questo periodo così impegnativo della mia vita. Vorrei ringraziare le compagne di bancone Roberta e Danielina per i consigli e il supporto morale. Ringrazio Lorenzo Manuel e Daniel per le discussioni, costruttive e distruttive su tecniche e attitudini del laboratorio. Un ringraziamento va ad Enzo collega e conterraneo, per la simpatia e per i valori che ci accomunano. Grazie a Francesca per la gentilezza e la simpatia. Vorrei ringraziare anche Alexandra e Andrea, per la collaborazione e tutti i ragazzi di Viterbo per la loro amicizia e disponibilità. Ringrazio in modo particolare Sameh e Sophie indimenticabili amiche francesi, per avermi accompagnata con affetto ed entusiasmo in quella che è stata un'esperienza per me indimenticabile.

Un grandissimo ringraziamento va a mio marito, Alexandre, per essermi stato sempre vicino con amore in questi anni, per avermi sopportata anche nei momenti di gran difficoltà e per avermi convinto a non gettare mai la spugna.

Ringrazio mio padre che, fin da piccola, ha permesso che m'innamorassi delle scienze, mia madre che mi ha insegnato come portare i pantaloni senza dimenticare di essere una donna. Sono grata a nonna Grazia e Zia Nettina, per aver sempre creduto in me e per tutte le volte che mi hanno cucinato le orecchiette. Ringrazio mio fratello Ciro mia cognata Federica e Giovannino, per aver ricreato qui a Roma quell'insostituibile ambiente familiare che mi ha dato la forza di andare avanti. Ringrazio inolre Regine, Faustine e tutta la famiglia francese per avermi fatta sentire sempre parte della "famille".

Grazie a tutti

Barbara

Riassunto

La pectina metilesterasi (PME) e l'invertasi (INV) sono due enzimi chiave del metabolismo dei caboidraiti nelle piante. Oltre al controllo a livello trascrizionale, un importante meccanismo di regolazione dell'attività di questi enzimi è svolto da specifici inibitori proteici. Gli inibitori di invertasi (INH) e di pectina metilesterasi (PMEI) sono degli inibitori proteici raggruppati nella famiglia Pf 04043 in quanto condividono numerose proprietà strutturali. Nonostante queste similitudini strutturali, i diversi inibitori interagiscono in modo specifico con enzimi funzionalmente e strutturalmente diversi. Entrambi gli inhibitori non agiscono su enzimi prodotti da patogeni, indicando un ruolo prevalente nei processi di sviluppo, anche se sembrano partecipare nella difesa delle piante da patogeni.

In questa tesi, attraverso un approccio di genomica funzionale, un inibitore di PME (SolyPMEI) e un inibitore di INV (SolyCIF) sono stati identificati e caratterizzati in pomodoro (*Solanum lycopersicum*).

SolyPMEI ha mostrato essere molto espresso in frutto rosso e, a bassi livelli, anche in fiori e polline. Il cDNA del *SolyPMEI* è stato clonato ed espresso in *Pichia pastoris*. Tutti i tentativi di produrre una proteina ricombinante attiva sono stati vani sebbene, l'analisi CD e dei ponti dusilfuro, rivelassero un corretto ripiegamento della proteina *in vitro*. Al fine di purificare l'inibitore naturale da bacca di pomodoro, è stata realizzata una colonna d'immuno-affinità. L'eluizione sia dell'inibitore sia della PME-1 di pomodoro, indica che *in vivo*, SolyPMEI è coinvolto nella formazione di un complesso stabile con le PME endogene.

SolyCIF è una proteina apoplastica espressa nelle foglie, nei fiori e nei frutti verdi. Il cDNA del *SolyCIF* è stato clonato ed espresso in *Pichia pastoris* e la proteina ricombinante, è stata purificata e caratterizzata biochimicamente L'invertasi di pomodoro era fortemente inibita in maniera dose dipendente dal SolyCIF. Il partner naturale dell'inibitore (l'invertasi vacuolare TIV-1) è stato purificato con una colonna di affinità e caratterizzato biochimicamente. TIV-1 mostrava diversi siti di proteolisi naturali. I frammenti che compongono TIV-1 interagiscono tra loro permettendo all'enzima di funzionare. Il sequenziamento N-terminale dei frammenti e analisi di modeling di TIV-1 mostrano che il sito attivo del'enzima è diviso in due, confermando che l'idrolisi del saccarosio avviene solo quando i frammenti sono associati tra loro.

Abstract

Pectin methylesterase (PME) and invertase (INV) are key enzymes in plant carbohydrate metabolism. An important post-transcriptional mechanism of regulation of these enzymes is represented by proteinaceous inhibitors. PME inhibitors (PMEI) and INV inhibitors (INH), belong to the same structural family Pf 04043. Despite the structural similarity, these two inhibitors act on two structurally and functionally different enzymes, but never both. Both inhibitors do not inhibit fungal enzymes indicating that they are mainly involved in growth and development even if they seems to be also involved in defence against pathogens.

In this thesis through a functional genomics approach a pectin methylesterase inhibitor (SolyPMEI) and an invertase inhibitor (SolyCIF) of *Solanum lycopersicum* have been identified and characterised.

SolyPMEI was mainly expressed in red fruits and, albeit at lower levels, in flowers and pollen. The *SolyPMEI* cDNA was cloned and expressed in *Pichia pastoris*. All attempts to produce active recombinant SolyPMEI protein appeared to be unsuccessful, neverthless CD spectra and disulfide bridges indicated a correct folding of the protein *in vitro*. The immuno-affinity fishing approach was used to purify the natural SolyPMEI from tomato fruits. The isolation of both natural SolyPMEI and PME-1 indicated that SolyPMEIs is *in vivo* engaged in the formation of a stable complex with endogenous PMEs.

SolyCIF was mainly expressed in leaves, flowers and green fruits of the plant and localized in the cell wall compartment. The *SolyCIF* cDNA was cloned and expressed in *Pichia pastoris*. The purified recombinant protein was biochemically characterized. The invertase activity was strongly inhibited in a dose-dependent manner by recombinant SolyCIF.With an affinity chromatography approach, the natural ligand of the inhibitor (the vacuolar invertase namely TIV-1) was purified and characterised. TIV-1 has been shown to be naturally proteolyzed and it was established that the fragments produced have to be tightly associated for its enzymatic activity to occur. N- terminal sequencing of fragments and the molecular model of TIV-1 shows that the fragmentation splits the catalytic site of the enzyme into two halves, which confirms that the enzymatic activity is possible only when the fragments are tightly associated.

SUMMARY

ABREVIATIONS

Amp: Ampicilline

AOX1: Alcool oxydase 1

ATP: Adenosin triphosphate

bp : Base pair

CIF: Cell wall Inhibitor of beta fructosidase

DNA: Desoxy ribonucleic Acid

DNS: 3-5 dinitrosalicylic acid

dNTP: Desoxynucleotid triphosphate

DTT: Dithiothreitol

EDTA: Ethylen diamine tetraacetic acid

GFP: Green Fluorescent Protein

GH: Glycosyl-hydrolase

GUS. β-Glucuronidase

HG: Homogalacturonan

INH: Invertase inhibitor

INV: Invertase

kDa : kiloDalton

LB : Luria Bertani

LRR: Leucin rich repeat

PAGE: Poly-acrylamide gel electrophoresis

PCR: Polymerisation chain reaction

PG: Polygalacturonase

PGIP: Polygalacturonase inhibitor protein

PME: Pectin methylesterase

PMEI: Pectin methylesterase inhibitor protein

PNLIP: Pectate lyase inhibitor protein

PNLP: Pectate lyase

PR: Pathogenesis related (protein)

PVDF: Polyvinylidene difluorure

RNA: Ribonucleic Acid

SDS: Sodium dodecylsulfate

Soly: *Solanum lycopersicon*

SuSy: Sucrose synthase

Taq: Polymerase from *Thermus aquaticus*

TAXI : *Triticum aestivum* xylanase inhibitor

TLXI: Thaumatin like xylanase inhibitor

Tris: Tris-(hydroxyméthyl) aminomethane

VIF: Vacular Inhibitor of beta fructosidase

XEGIP: Xylo-Endoglucanase inhibitor protein

XIP: Xylanase inhibitor protein

XYN/Xyn: Xylanase

FIGURES

TABLES

1. Introduction

1.1. Sugars: energy molecules and cell wall components

Carbohydrates play fundamental roles in plants. They are the principal components of the cell wall as well as energy molecules which, depending on the physiological needs, can be channeled into various pathways in different subcellular compartments for their utilization as source of carbon and energy or converted in polymers for long-term storage. Sugars can also act as signalling molecules whose transduction pathways control gene expression and influence plant growth and development as well as defence responses against pathogens (Côté and Hahn, 1994; Smeekens, 2000; Loreti et al., 2002).

Cell wall is a dynamic interface that changes during the growth and differentiation of the cell and that also participates in cellular responses to exogenous stimuli. Primary cell wall is essentially constituted by cellulose, hemicellulose and pectin. Primary cell wall (Fig.1) is formed during cell division and is continuously modified during cell extension. The middle lamella constitutes the interface between the primary walls of neighbouring cells (Fig. 1).

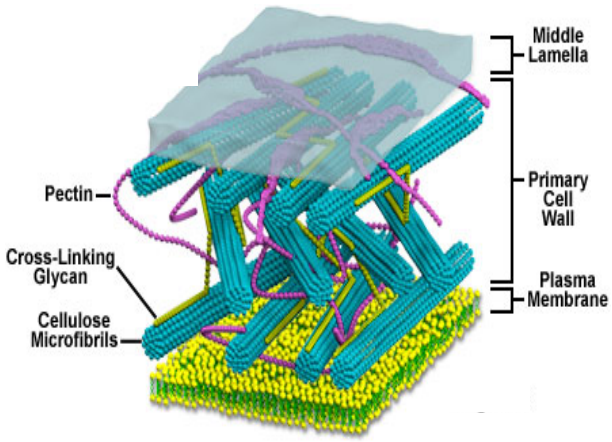

Figure 1. Schematic representation of plant cell wall

Plants produce a number of carbohydrate-active enzymes including glycosidases, transglycosidases, glycosyltransferases, polysaccharide lyases and carbohydrate esterases, which activity and regulation have been a main focus in plant biology. Carbohydrate-active enzymes are also produced by microbial pathogens at the early stages of infection to invade plant tissue and sustain their growth and are important factors of pathogenicity (D'Ovidio et al., 2004a). Plants

synthesize different classes of proteinaceous inhibitors against endogenous carbohydrate-active enzymes as well as against the enzymes produced by pathogens.

1.2. Plant proteinaceous inhibitors directed against exogenous carbohydrate-active enzymes (CAE)

1.2.1. Xyloglucan endoglucanase inhibitor protein (XEGIPs)

Xyloglucan is the quantitatively predominant hemicellulosic polysaccharide in the primary walls of dicots and non-graminaceous monocots. Xyloglucans consist of a β-1,4-linked D-glucose backbone substituted by D-xylose. Xyloglucans interact with cellulose microfibrils by forming hydrogen bonds, thus contributing to the structural integrity of the cellulose network. Endoglucanases (EGs) hydrolyse both xyloglucan and cellulose or carboxymethyl cellulose (CMC) (Jahr et al., 2000; Lev and Horwitz, 2003). A novel class of EGs, the xyloglucan-specific endoglucanases (XEGs) has been discovered whose specific activity toward xyloglucan exceeds the activity toward CMC and/or linear β-glucan by at least ten times (Grishutin et al., 2004). All known XEGs belong to the GH12 and GH74 families (Coutinho and Henrissat, 1999) but information on their properties is scarce (Grishutin et al., 2004).

It has been recently purified from suspension-cultured tomato cells a protein that binds an inhibits fungal GH12 XEGsv (Qin et al., 2003). This protein, termed XEG inhibitor protein (XEGIP), represents the newest class of plant-derived proteins that inhibit carbohydrate-active enzymes. XEGIP is widely expressed in tomato vegetative tissues and is down regulated during ripening. Genes that are homologous to tomato XEGIPs are present in soybean, lotus, carrot, cotton, maize, rice, sorghum, *Medicago trunculata* and Arabidopsis. XEGIPs and related proteins do not show any capacity to inhibit other carbohydrate-active enzymes of either plant or fungal origin (Qin et al., 2003). Today, XEGIP is the only protein inhibitor of EGs, including the cellulases, to have been reported and it remains to be established whether the ability to interact with XEG is a strict specificity of XEGIP-related proteins.

1.2.2. Xylanase Inhibitors

The major hemicellulose polymer in cereals and hardwood is xylan. Xylan consists of a β-1,4-linked D-xylose backbone and can be substituted by different side groups (Zuppini et al., 2005). Endo-β-1,4-xylanase (EC 3.2.1.8, xylanase) is a crucial component that carries out the initial breakdown of the xylan backbone into smaller oligosaccharides. Endoxylanases are classified into six GH different families (GH5, GH7, GH8, GH10, GH11 and GH43). All the family include plant

enzyme with the exception of GH11 family which is exclusively composed by microbial xylanases. The first direct evidence for a role of xylanase in pathogenesis was recently obtained by deleting the gene encoding an endoxylanase from the fungal plant pathogen *B. cinerea*, which severely affected virulence by delaying the appearance of secondary lesions and significantly reducing the average lesion size on tomato leaves and grape berries (Brito et al., 2006). Reintroducing the wild-type gene into the mutant strains the altered phenotype reversed back to wild type (Brito et al., 2006).

Three structurally different classes of endoxylanase inhibitors have been documented in the literature, the TAXI-type (Gebruers et al., 2004), the XIP-type (Juge et al., 2004) and the thaumatin-like (TL-XI) xylanase inhibitor. The two first inhibitors are widely represented in cereals (rye, barley, maize, rice, durum and bread wheat) as multi isoform families (Goesaert et al., 2004). The third type of inhibitor, TL-XI, was recently identified in wheat (Fierens et al., 2007). These are specific inhibitors of microbial (bacterial and fungal) endoxylanases and do not inhibit plant endoxylanases. XIP-type inhibits both GH10 and GH11 microbial endoxylanases (Flatman et al., 2002; Brutus et al., 2005; Furniss et al., 2005) whereas TAXI-type and TL-XI exclusively inhibit GH11 endoxylanases (Gebruers et al., 2001; Fries et al., 2007). Sequence and structural similarities indicate that XIP-I is related to chitinases in the GH18 family, despite its lack of enzymatic activity (Elliott et al., 2002; Payan et al., 2003).

XIP-I in complex with GH10 *Aspergillus nidulans* (PDB code 1TA3) and GH11 *P. funiculosum* (PDB code 1TE1) endoxylanases showed the presence of two independent enzyme-binding sites. The strategy for inhibiting endoxylanases involves substrate-mimicking contacts and interactions occluding the active site (Tahir et al., 2002; Payan et al., 2004).

The structures of TAXI-I, free or in complex with GH11 endoxylanase, were also recently determined (Sansen et al., 2004). TAXI-I is highly similar to the core structure of *Rhizomucor miehei* aspartic proteinase but is proteolytically non-functional; the inhibitor probably divergently evolved at an early stage from a pepsin-like aspartic protease ancestor (Sansen et al., 2004).

The structure of TL-XI has not been determined. Like other PR proteins, thaumatin is predicted to have a mainly β structure, with a high content of β-turns and little helix (Fierens et al., 2007).

Although a direct role remains to be demonstrated, increasing lines of evidence suggest that endoxylanase inhibitors are part of the network of plant defence against pathogens. They inhibit the activity of GH11 endoxylanases secreted by pathogens such as *B. cinerea* (Brutus et al., 2005) and *Fusarium graminearum* in vitro (Sansen et al., 2004).

1.2.3. Inhibitors of pectic enzymes

Pectins are highly heterogeneous polysaccharides whose backbones are highly enriched in α-1,4-linked-D-galacturonic acid residues, with various degrees of methyl esterification. Their structure is continuously modified by pectic enzymes such as pectin lyases (PL), polygalacturonases (PGs), pectin methylesterases (PME). In healthy plants, pectic enzymes participate in the remodelling of the cell wall during plant growth and development. At the early stages of plant infection, pectic enzymes are the first cell wall degrading enzymes produced by fungal and bacterial pathogens and have been demonstrated to be important virulence factors (D'Ovidio et al., 2004a). A number of proteinaceous inhibitors against pectic enzymes have been discovered in plants.

1.2.4. Pectin lyase inhibitor protein

The first evidence of a proteinaceous inhibitor of fungal pectin lyase was obtained in extract of been and cucumber (Bock et al., 1975). Pectin lyases (PNLs; EC 4.2.2.10), catalyse β-elimination cleavage of methylesterified polygalacturonic acid in pectin, the methyl ester, rather than pectate, the anion which is the preferred substrate of pectate lyases, (PeLs; EC 4.2.2.2). Pectin lyases belong to the family 1 of polysaccharide lyases, of which 18 families are known (Henrissat et al., 1995). Although pectate lyases produced by fungal and bacterial pathogens have been shown to be important factors of virulence (Akimitsu et al., 2004), little information is available on the role of PNLs during pathogenicity, apart from a study reporting PNL activity in mallow leaves during the biotrophic and necrotrophic phases of infection (Wei et al., 2002). Sugar beet produces a cell wall PNLIP that inhibits a PNL from *Rhizoctonia solani*, which is a fungal pathogen of sugar beet (Bugbee, 1993). The presence of the PNLIP has been shown to correlate with resistance to root rot caused by R. solani (Bugbee, 1993). The inhibitor, which the mode of inhibition was uncompetitive, is also active against other fungal PNLs from *Phoma betae* and *Aspergillus japonicus* (Bugbee, 1993). No investigations have yet be performed on the inhibitor structure, and its physiological role.

1.2.5. Polygalacturonase-inhibitor proteins (PGIPs)

Polygalacturonases (PG) are the first enzymes to be secreted by pathogens when they encounter plant cell walls and their contribution to the pathogenicity of same fungi and bacteria has been assessed. PGs (EC 3.2.1.15), cleave the linkages between D-galacturonic acid residues in non-methylated homogalacturonan, a major component of pectins. Based on their sequences and their structurally related catalytic folding, PGs have been classified in family 28 of glycoside hydrolases, GH28 (Henrissat and Davies, 1997). To accommodate pathogenesis a variety of different conditions, PGs are highly variable in term of primary structure, specific activity, pH optimum and

mode of action (D'Ovidio et al., 2004b). To counteract the action of PGs, plants have evolved cell wall associated polygalacturonase inhibiting proteins (PGIPs) displaying a high degree of polymorphism. PGIPs are organized into multigene families, clustered in specific chromosomal regions, and encode PGIP isoforms with homologous structure but different specificities (De Lorenzo et al., 2001; D'Ovidio et al., 2004b). PGIPs are typically effective against fungal PGs and ineffective against other pectic enzymes of either bacterial or plant origin. Thibition can be either competitive, non-competitive or mixed, a further indication of the versatility of PGIPs to evolve different recognition specificities (Sicilia et al., 2005).

PGIPs belong to the leucine-rich repeat (LRR) superfamily of proteins whose structure is conserved in many disease resistance genes (R-genes) (Bergelson et al., 2001) and is characteristic of protein–protein interactions (Shanmugam, 2005).

The role of PGIPs as important players in the defence response is now clear: they are induced early during infection, retard PG function, prevent cell wall degradation, and limit fungal growth and colonization. Long-chain oligogalacturonides (OGs), which elicit many defence responses in plants, are produced when fungal PGs activity is controlled by PGIP. For this reason PGIPs are included among the microbe-detecting molecules that are part of the plant immune system (Federici et al., 2006).

Name	Source	Enzyme specificity cAZy[a]	Molecular mass (kDa)	Structural class SCOP fold[b]	Pfam[c]	PDB code
XEGIP	Tomato, carrot, tobacco	Fungal XEG (GH12	51.0	Pepsin like[d]	ND	ND
XIP	Graminaceous monocots	Fungal GH10 and GH11 endoxylanases	29.0	TIM-barrel	PF00704	1OMO, 1TA3, 1TE1
TAXI	Graminaceous monocots	Fungal and bacterial GH11 endoxylanases	40	Pepsin-like	PF00026	1T6E
TL-XI	Wheat	Fungal and bacterial GH11 endoxylanases	18.0	Thaumatin-like[d]	PF00314[d]	ND
PNLIP	Sugar beet	Fungal PNLP (PL1)	57.5	ND	ND	ND
PGIP	Dicots, *Allium porrum*, wheat, rice	Fungal PGs (GH28)	34.0-54.0	LRR	PF00560	1OGQ

Table 1. Different classes of inhibitors directed against carbohydrate-active enzymes (Juge, 2006).
Abbreviation: ND, not determined
[a] Carbohydrate Active Enzyme database (http://www.cazy.org/CAZY)
[b] Structural Classification of Proteins (http://www.scop.berkeleiy.edu)
[c] Pfam protein families database (http://www.sanger.ac.uk/Sotftware.Pfam/)
[d] Based on sequence and homology modelling

1.3. Plant proteinaceous inhibitors directed against endogenous carbohydrate-active enzymes (CAE)

1.3.1. Pectin methylesterase/invertase inhibitor family (PMEI/INH family) Pfam 04043

Recent plant genome sequencing projects have identified a novel structural protein family Pfam04043 (http://pfam.wustl.edu/), formed by invertase inhibitors (INH) and the pectin methylesterase inhibitors (PMEI), the first involved in the carbohydrate metabolism and sugar signalling (Rausch and Greiner, 2004) and the latter involved in the control of pectin metabolism. Common features of this plant-specific family include an N-terminal signal peptide, four conserved cysteine residues involved in the formation of two disulfide bridges and a molecular mass of about 18 kDa. The determination of their three dimensional structures also shown that they are both folded in an asymmetric up-and-down four-helix bundle (Hothorn et al., 2004a; Di Matteo et al., 2005).

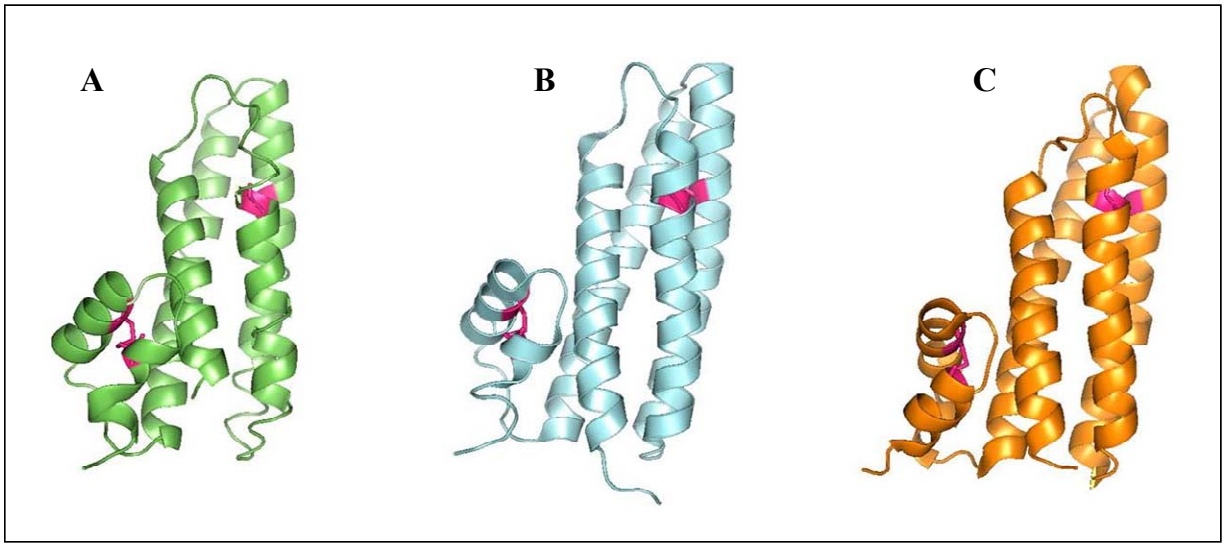

Figure 2. **Pectin methylesterase/invertase inhibitor family (PMEI/INH) Pfam 04043 3D-structures**. (**A**) PMEI from kiwi. (**B**) PMEI from Arabidopsis; (**C**) CIF from *Nicothiana tabacum*; disulfide bridges are in pink (Hothorn et al., 2004a; Hothorn et al., 2004b; Di Matteo et al., 2005).

Despite this structural similarity these two inhibitors act on two structurally and functionally different carbohydrate modifying enzymes, but never both.

1.3.2. Pectin methylesterase (PME)

1.3.2.1. Biochemical features and types of plant PMEs

Pectic polysaccharides are synthesized in the Golgi apparatus and secreted into the wall as highly methylesterified forms. Subsequently, they can then be modified by pectinases such as pectin methylesterases (PMEs, EC 3.1.1.11), which catalyse the demethylesterification of homogalacturonans (HGA), the main pectic cell wall component, releasing acidic pectins, methanol and proton (Fig. 3) (Moustacas et al., 1991).

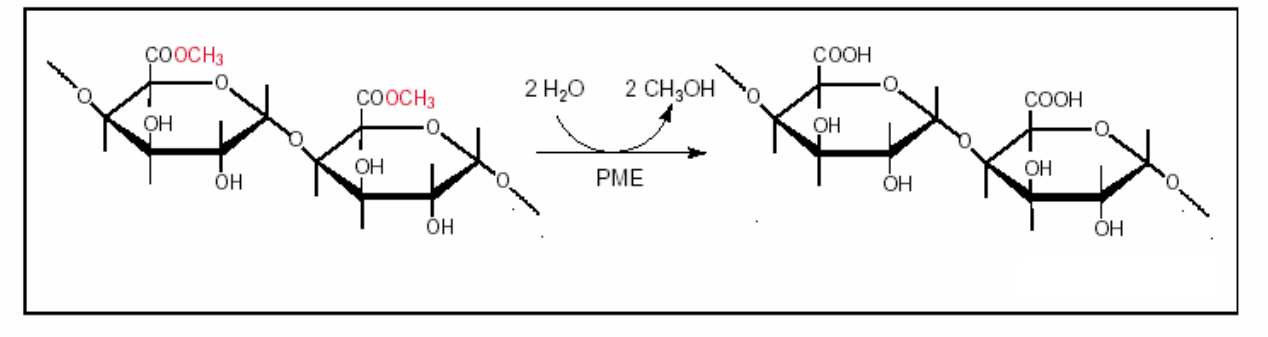

Figure 3. Demethylesterification of pectins by pectin methylesterases (PME) (Micheli et al., 2000).

Several PME isoforms differing in molecular weight, p*I* and biochemical activity were detected in all higher plants examined so far as well as in a number of plant pathogenic fungi and bacteria (Collmer and Keen, 1986; Brady, 1987). Pectin methylesterase, belong to class 8 (CE-8) of the carbohydrate esterase (CAZy, http://www.cazy.org/fam/CE8.html)(Henrissat, 1991). Plants PMEs belong to large multigene families. For instance, in *Arabidopsis thaliana*, 66 ORFs have been annotated as putative full-length PMEs. The PME ORFs of *Populus trichocarpa* are 89 (http://genome.jgi-psf.org/Poptr1_1/Poptr1_1.home.html; (Geisler-Lee et al., 2006) whereas those numbers is substantially lower (35 ORFs) in *Oryza sativa* (http://www.tigr.org/tdb/e2k1/osa1/), probably due to the low level of pectins in their cell wall.

Higher plant PMEs are frequently organised in pre-pro-proteins. The PRE domain leading to the export of PMEs to the cell wall, is formed by a common type signal peptide (SP) and by a transmembrane domain (TM or signal anchor). Different PMEs possess one, both, or neither of these motifs. Those with neither motif are classed as putatively soluble isoforms. The mature, active part of the protein (PME domain, Pfam01095, IPR000070) is preceded by an N-terminal extension (PRO region Pfam04043, IPR006501) that share similarities with the pectin methylesterase inhibitors. The PRO-regions can vary in length and shows a relatively low level of amino acids identity between isoforms (Markovic and Janecek, 2004). In Arabidopsis, the isoelectric point of the

PME domain tends to be basic whereas that of the PRO region is neutral or acidic (Bosch et al., 2005; Bosch and Hepler, 2005). Similar differences in length and isoelectric points between PRO and PME domains have also been found in several other species (Al Qsous et al., 2004; Bosch et al., 2005), and might influence the optimal pH activities of specific isoforms.

PMEs can be classified on the presence or absence of the PRO domain in PMEs type I (500–900 amino acids; 52–105 kDa) which contain 1–3 PRO domains and two or tree introns (Fig. 4), or PMEs type II (250 to 400 amino acids; 27–45 kDa) without PRO domain and with five or six introns (Fig. 4) (Micheli, 2001; Tian et al., 2006). The type II sequences have a structure close to that of the PMEs identified in phytopatogenic organisms (bacteria, fungi).

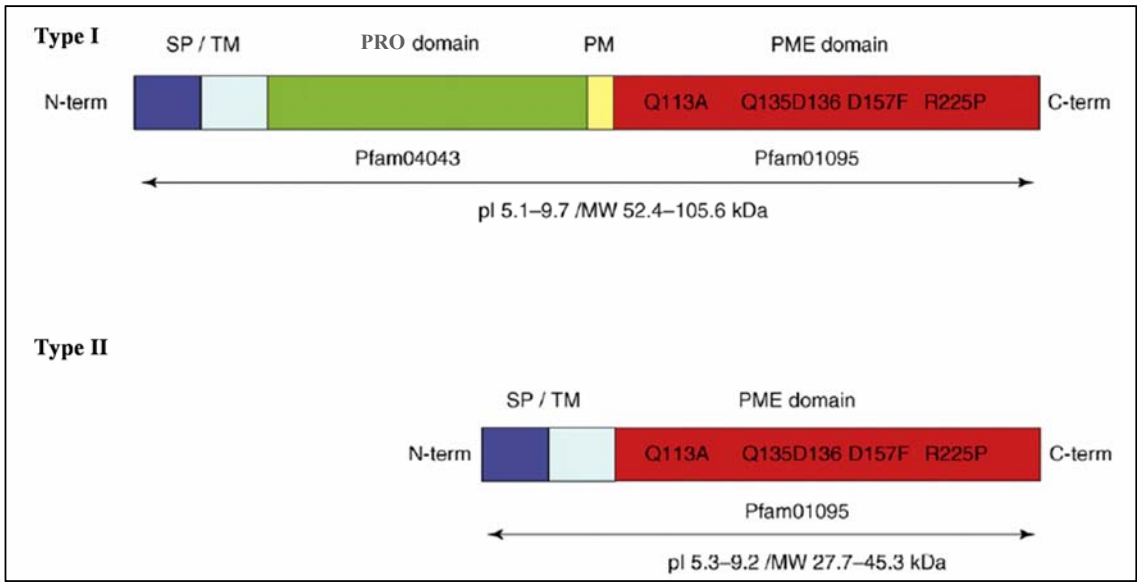

Figure 4. Pectin methylesterase (PME) structural motifs. Type I and Type II PMEs possess a conserved PME domain (Pfam01095) with characteristic, highly conserved amino acid fragments. Type I PMEs possess an N-terminal extension designated the PRO domain and a processing motif (PM) that might be a putative target for subtilisin –like proteases.The targeting to the endomembrane system leading to the export of PMEs to the cell wall is mediated either by a signal peptide (SP) or a transmembrane domain (TM or signal anchor). Different PMEs possess one, both, or neither of these motifs (Pelloux et al., 2007).

1.3.2.2. The role of the PRE-PRO domain in PME targeting and function

PMEs, type I and II, have been found to be localized in *Arabidopsis* pollen tubes (Jiang et al., 2005; Tian et al., 2006) and tobacco cell wall (Li et al., 2002) respectively. The PRE-PRO domain of the protein, has been shown to be necessary for the targeting of *Nicotiana tabacum* tPPME1, a type I protein, to the pollen tube cell wall via the exocytotic pathway (Bosch et al., 2005). However, the absence of a PRO domain in type II proteins does not preclude cell wall targeting (Tian et al., 2006). As initially described for *Phaseolus vulgaris* PME, tobacco PME Q9LEB0 has been shown to possess TM domain (Dorokhov et al., 2006b). Whereas the TM domain

is required for transient binding of the tobacco Q9LEBO PME to endoplasmic reticulum membranes, its transport to the cell surface and export to the cell wall, the PRO-domain between the TM and the PME domain (Fig. 4), does not affect the targeting (Dorokhov et al., 2006b). Because NtPPME1 and Q9LEBO tobacco protein sequences both have TM domains but differ in the presence or absence of the common type signal peptide, the TM domain might be sufficient for the targeting of the protein to the cell wall.

SP/TM and PRO-domain are processed to yield the mature active PMEs. Protein sequence analysis has revealed that the processing motif (MP) might correspond to the sequence R(RK)L(L/M) conserved in plant PMEs. PMEs are likely to be processed inside cells or immediately after export in the apoplast (Fig. 5) (Dorokhov et al., 2006b). In the first case, the pro-domain might be degraded or play a role either inside the cell or in the apoplast (Fig. 5).

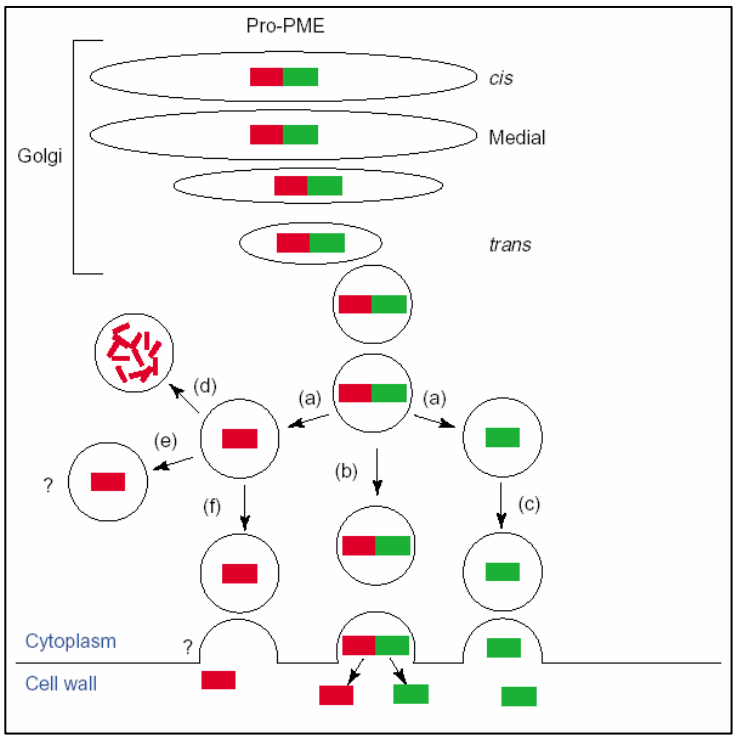

Figure 5. Hypotheses for pectin methylesterase (PME) excretion into the apoplasm and maturation of the protein. The cleavage of the pro region (red) from the mature PME (green) occurred either early on, before excretion of the mature PME into the apoplasm (a,c), or afterwards (b). In the first case, the pro region could be degraded (d) or play a role either inside the cell (e) or in the apoplasm (f)(Micheli et al., 2000).

Although the role of the pro region is not known, several hypotheses are possible. It might play a role: in targeting PMEs towards the cell wall, as an inhibitor of the enzyme activity to prevent pectin demethylesterification before its secretion into the wall. (Bosch et al., 2005). This last

hypothesis agree with the fact that, bacterial PMEs, do not have a pro-peptide, because they did not secrete pectins (Lord, 2000).

1.3.2.3. Three-dimensional structures of PMEs

Major advances facilitating attempts to elucidate the mechanism(s) of action and substrate specificity of PMEs were achieved when 3D crystallographic structures were obtained. Since now three 3D structures have been solved: a bacterial PME, from *Erwinia chrysantemi* (PDB code 1QJV), the same PME in complex with pectin (Jenkins et al., 2001; Fries et al., 2007) and two plant PMEs, are from *Daucus carota* (PDB code 1GQ8) and the other from *Solanun Lycopersicon* (Fig. 7A) (Di Matteo et al., 2005). The enzyme folds into a right handed parallel β-helix, first observed in pectate lyase C (Yoder et al., 1993) and typical of pectic enzymes (Jenkins and Pickersgill, 2001).

The 3D structures of the carrot and tomato PMEs show striking similarities, and are almost entirely structurally superimposable (Fig. 6/A) (Di Matteo et al., 2005) In addition, both of these plant PMEs show similar folding topology to PME from *Erwinia chrysanthemi*, although one major difference lies in the length of turns protruding from the β-helix in proximity of the substrate cleft (Fig. 6/B), in particular, turns that protrude out of the β-helix are much longer in the bacterial enzyme, making its putative active site cleft deeper and narrower than that of plant PMEs (Fig. 6).

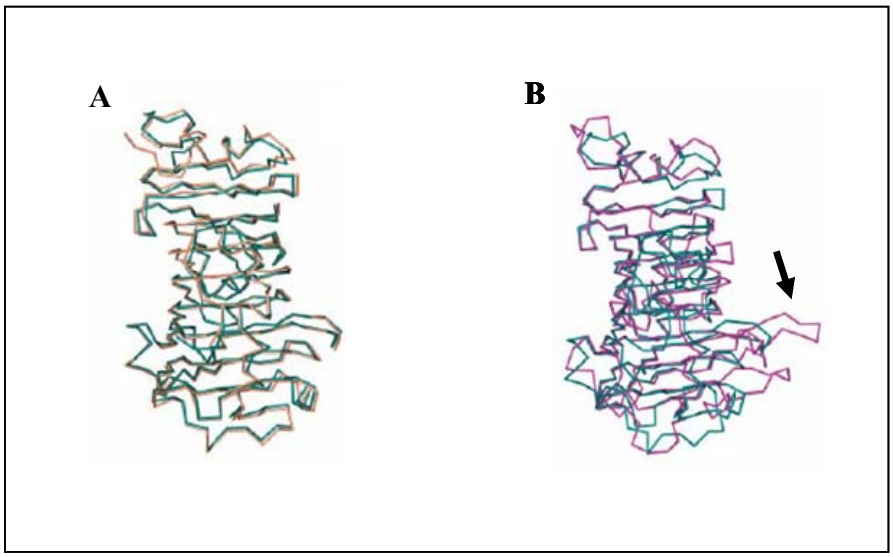

Figure 6. Comparison of the known structures of PMEs. (**A**) Overlay of the Cα trace of PME from tomato (green) and PME from carrot (orange). Structures are almost completely superimposable. (**B**) Superimposition of PME from tomato (green) and PME from *E. chrysanthemi* (violet). Although the β-helices are completely superimposable, main differences (showed by arrow) are located in the length of the turns protruding out from the β-helix in proximity of the putative active site cleft (Di Matteo et al., 2005).

In tomato PME-1 the β-helix consists of seven complete coils, which have different lengths because the number of amino acids located in the loops connecting the β-strands is variable. Each

coil consists of three β-strands that line up to form three extended parallel β-sheets called PB1, PB2, and PB3 (Fig.7). The N-terminal region of PME is composed by a short α-helix followed by a β-strand that lines up with PB1. The C-terminal region has an extended conformation in which a long tail and four short and distorted α-helices protrude out of the parallel β-helix flanking PB1 (Fig. 7/A).

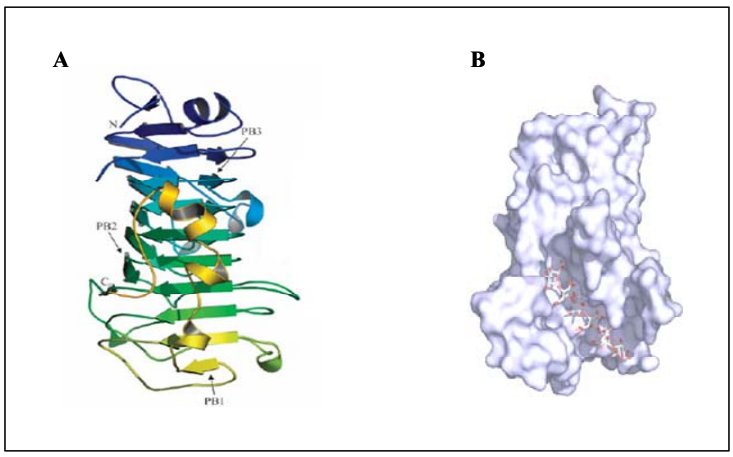

Figure 7: PMEs 3D structure (**A**) Three-dimensional structure of PME-1 from tomato; (**B**) Surface representation of *Erwinia chrisantemi* PME together with stick representation of hexasacharide II showing the shape and position of the substrate-binding cleft (Di Matteo et al., 2005; Fries et al., 2007).

The putative active site of PME is located on the PB3. Many aromatic residues (Phe80, Tyr135, Phe156, Tyr218, Trp223, and Trp248) putatively involved in substrate binding are located in this pocket (Johansson et al., 2002). These residues are well conserved in plant PMEs (Markovic and Janecek, 2004). Tyr135, Phe156, and Trp223 are also conserved in PME of *E. chrysanthemi* (Jenkins et al., 2001). The structures of the Michaelis complexes of PME from *E. chrysanthemi* with methylated hexagalacturonates, suggest the following residues are involved in the reaction mechanism: Asp 199, Asp 178 and Gln 177 (Fig. 8). Arg 267, conserved amongst all PMEs, is not a direct participant in catalysis (Fries et al., 2007).

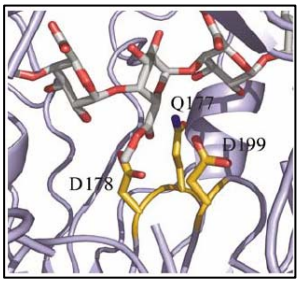

Figure 8. **Stereo-view of the active site residues in the Michaelis complex** (Fries et al., 2007)**.**

In analogy with the proposed mechanism of action of PME from carrot and from *E. chrysantemi* (Johansson et al., 2002; Fries et al., 2007), a mechanism of catalysis of PME-1 from tomato, have been described: in particular Asp153, polarized by the proximity with Arg221, performs a nucleophilic attack on the carboxymethyl group of the substrate. The tetrahedral anionic intermediate formed is stabilized by the interaction with two conserved Gln residues (Gln109 and Gln131). Afterwards, Asp132 likely acts as a proton donor in the cleavage step where methanol is released. The resulting carboxylate group of Asp132 then behaves as a base and receives a proton from an incoming water molecule (W227), thus restoring the active site of the enzyme (Fig. 9).

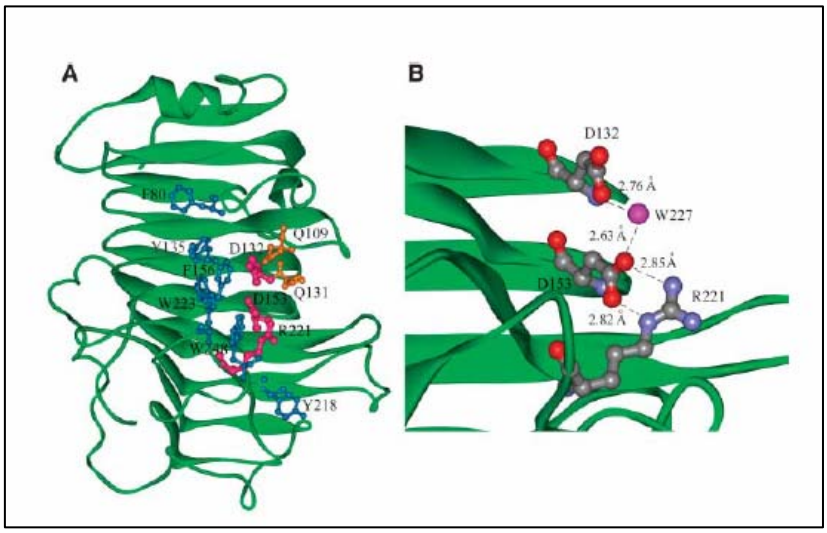

Figure 9. **Close-Up View of the Tomato PME Active Site**. **(A)** Structure of tomato PME in which residues involved in catalysis (violet), in stabilization of the catalytic intermediate (orange), and in substrate binding (blue) are shown in ball and stick representation. **(B)** Further close-up view representation of amino acid residues and a water molecule (blue ball) putatively involved in catalysis; H-bond pattern is highlighted (Di Matteo et al., 2005).

1.3.2.4 Mode of action of pectin methylesterase

After their secretion into the cell wall, mature PMEs could exhibit three different modes of action: (I) a single-chain mechanism where the enzyme converts all substrate sites on the polymeric chain, (II) a multiple-chain mechanism where the enzyme catalyses only one reaction and then dissociates from the substrate and, (III) a multiple-attack mechanism where the enzyme catalyses a number of reaction cycles before the enzyme-polysaccharide complex dissociates. Plant and bacterial PMEs produce products with contiguous regions of galacturonic acid and both a single-chain and multiple-attack mechanism have been proposed (Dongowski G and Bock W, 1984; Kohn R et al., 1985; Christensen et al., 1998). In contrast, fungal PMEs attack more randomly and a multiple-chain mechanism has been proposed for those enzymes (Limberg et al., 2000; van Alebeek et al., 2003; Duvetter T et al., 2006).

When PMEs act randomly on pectic polymer, the demethylesterification releases protons that promote the action of endopolygalacturonases (Moustacas et al., 1991) and contribute to cell

wall loosening (Fig 10). When PMEs act linearly on methylated pectin, PMEs give rise to blocks of free carboxyl groups that could interact with Ca^{2+}, creating the so called junction zones. Because the action of endopolygalacturonases in such a gel is limited, this action pattern of PMEs contributes to cell wall stiffening (Fig. 10).

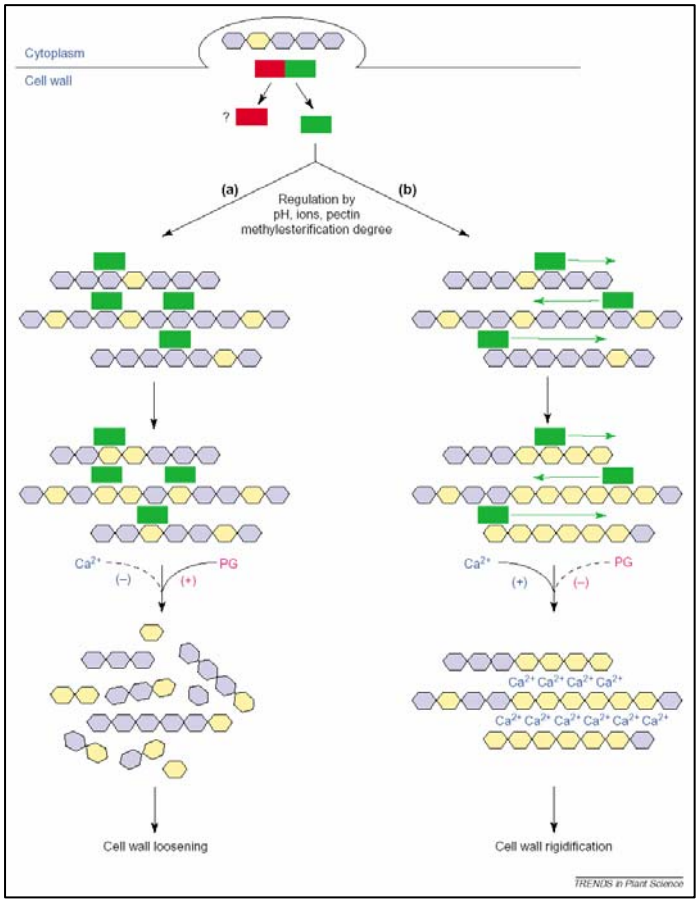

Figure 10. Modes of action of pectin methylesterases (PMEs). Mature PMEs (green) can act randomly (a), promoting the action of pH-dependent cell wall hydrolases such as endopolygalacturonases (PG) and contributing to cell wall loosening, or can act linearly (b), giving rise to blocks of free carboxyl groups that interact with bivalent ions (Ca^{2+}), so rigidifying the cell wall. Methylesterified galacturonic acids are represented in blue and demethylesterified galacturonic acids in yellow (Micheli et al., 2000)

Because acidic PMEs were thought to be essentially confined to fungi, the simplest hypothesis is that random demethylesterification is produced by acidic fungal PMEs, whereas linear demethylesterification is determined by alkaline plant and bacterial PMEs. However, more recent studies have shown that PME activity also depends on pH and on the initial degree of methylesterification of the pectins. Some isoforms can act randomly at acidic pH but linearly at alkaline pH. At a given pH, some isoforms are more effective than others on highly methylesterified pectins (Catoire et al., 1998; Denes et al., 2000).

1.3.2.5. Multiple roles of PMEs in plants

The diversity of the putative roles of PMEs in plants can be illustrated by the diversity of their expression patterns. In both Arabidopsis and Populus, as revealed by microarray analyses, PME isoforms cluster into several distinct groups, highlighting their putative redundancy of function, and organ or stress-specific expression patterns.

1.3.2.6. Role of PMEs in plant growth.

Various experiments have demonstrated that PMEs are involved, directly and indirectly, in diverse physiological processes associated with both vegetative and reproductive plant development. It has been shown that PMEs play roles in cell wall extension and stiffening (Moustacas et al., 1991; Jenkins et al., 2001), microsporogenesis and pollen tube growth (Wakeley et al., 1998; Futamura et al., 2000; Bosch et al., 2005), cellular separation (Wen et al., 1999), seed germination (Ren and Kermode, 2000), root development (Pilling et al., 2004), leaf growth (Hasunuma et al., 2004), hypocotyls elongation (Bordenave and Goldberg, 1993), fruit ripening and loss of tissue integrity (Brummell and Harpster, 2001).

Cellular adhesion and tissue elongation: during the separation of the border cells of the root cap of pea PME activity increase and is correlated with an increase of acid pectic and decrease of cell wall pH (Stephenson and Hawes, 1994). Transgenic plants expression of the PME gene *rcpme1* in pea root caps influences cell-shape, root growth, and border cell separation (Wen et al., 1999). Transgenic potato plants over-expressing a *Petunia inflata* PME, showed increased elongation rates (Pilling et al., 2000). The same authors have obtained an inverse phenotype with the silencing of PME (Pest2) gene in potato plants.

Microsporogenesis and pollen tube growth: recent analysis of pollen-specific transcriptome of *Arabidopsis* indicated that several PMEs are specifically expressed in floral buds, and pollen (Pina et al., 2005). In Arabidopsis, it has been shown that QUARTET1 (QRT1, encoded by AT5G55590), which is expressed in pollen and surrounding anther tissues, has a role in pollen tetrad separation during floral development and has PME activity when expressed in *E. coli* (Francis et al., 2006). QRT3, one of 66 putative PGases identified in Arabidopsis, might act in tandem with QRT1, leading to the degradation of demethylesterified polygalacturonic acid in pollen mother cell primary walls. Thus, pectin degradation might involve a precise interplay between highly specific PME-PMEI-PGase isoforms that might be temporally or spatially regulated. Disruption of the *Arabidopsis* gene encoding VANGUARD1 (VGD1), demonstrated to be a functional PME, causes a slight reduction in pollen PME activity and retarded pollen tube growth within the style transmitting tract (Jiang et al., 2005). The mutant phenotype has lower levels of

pollen fertility than wild-type and, hence, smaller siliques with fewer seeds. Similar effects, albeit weaker, have been observed in AtPPME1 (AT1G69940) mutants (Tian et al., 2006). Among PME genes expressed in pollen in Arabidopsis (Francis et al., 2006), some are able to complement the phenotype of VGD1, whereas others are not (Jiang et al., 2005). In tobacco different authors have suggested that the degree of pectin esterification of the apex might control oscillatory pollen tube growth (Bosch et al., 2005; Bosch and Hepler, 2005).

Wood development: emerging roles for PMEs in vegetative development include their putative involvement in wood development. In Arabidopsis, five different PME encoding genes are highly expressed in the xylem. Several PME isoforms have been observed at specific stages of xylogenesis, implying that specific isoforms may have different functions at different stages during the course of xylem cell differentiation (Micheli et al., 2000). Another emerging role of PME is played by the extensive pectin modifications that occur during secondary wall deposition in xylem cells also mediated by pectate lyases and polygalacturonases (PGases) (Hertzberg et al., 2001). Furthermore the presence of homogalacturonan (HGA) and its de-esterification are likely to be essential for xylem lignification.

1.3.2.7. PMEs and tomato fruit ripening

The role of PME in fruit ripening has been intensively examined in tomato in an attempt to relate changes in PME activity to modifications in the cell wall structure of the pericarp (Brummell and Harpster, 2001).

Tomato PMEs belong to small gene family consisting of at least four genes, some of which show high level of identity (Ray et al., 1988; Harriman et al., 1991; Hall et al., 1994). Tomato PMEs characterized so far are type I and are typically represented by multiple isoforms (Pressey R and Avants JK, 1972; Delincee, 1976; Tucker et al., 1982; Warrilow et al., 1994). Three immunologically related isoforms are specific to fruit, plus several other isoforms found in all tissues including fruit (Gaffe et al., 1994). PME protein and activity, present throughout fruit development, increase from the early stages of green fruit to red ripe fruit (Harriman et al., 1991; Tieman et al., 1992). *PME* mRNA shows a different pattern of accumulation, increasing to a maximum in mature green fruit and declining as ripening progresses (Ray et al., 1988; Harriman et al., 1991).

Transgenic tomato plants, silenced with the insertion of antisense cDNA of a fruit-specific *PME*2 were generated (Tieman et al., 1992; Hall et al., 1993). Although *PME*2 mRNA and immunodetectable protein were reduced to undetectable or trace levels in fruit, PME activity was present at almost 10% of wild type. In leaf and root PME activity was not reduced by introduction

of this *PME*2 transgene, although no mRNA or immunodetectable protein homologous to the *PME*2 gene were detected (Hall et al., 1993). The coding region of *PME*2 hybridizes with the more highly expressed *PME*1 (Hall et al., 1994), thus mRNA of neither gene was detected in fruit of antisense plants. This suggests that the antisense *PME*2 transgene suppressed mRNA accumulation of *PME*2 and homologous genes including *PME*1, and that the residual activity in fruit and activity in other tissues was due to the presence of more divergent *PME* gene products. The degree of pectin methylesterification in transgenic antisense PME fruits was higher than controls by 15–40% throughout ripening (Tieman et al., 1992; Hall et al., 1993), however the fruit otherwise ripened normally (Tieman et al., 1992). On the contrary, in over-ripe fruit PME-silencing, caused an almost complete loss of tissue integrity (Tieman and Handa, 1994).

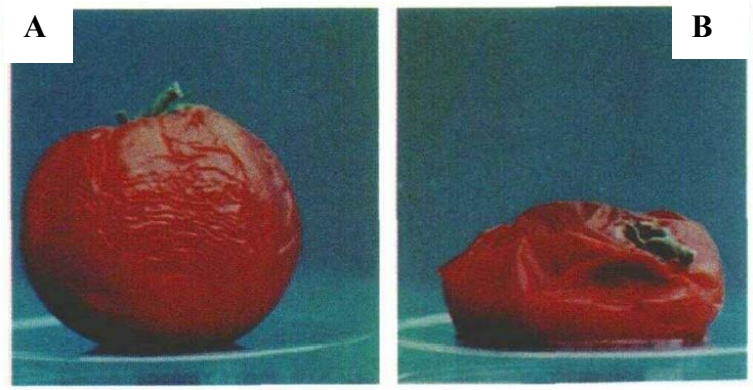

Figure 11. Phenotypes of detached transgenic PME (**A**) wild-type Rutgers and (**B**) transgenic PME-silencing fruits after 7 weeks storage (Tieman and Handa, 1994).

Increased pectin methylesterification resulted in reduced polyuronide depolymerization in red ripe fruit, and decreased the amount of chelator-soluble pectin during ripening by 20–30% (Tieman and Handa, 1994). The changed ionic and physical conditions in the wall may also have affected the activity of other cell wall modifying enzymes, including PG (Chun and Huber, 1998). Raw juice prepared from antisense PME fruit showed an almost 20% increase in soluble solids content (Tieman et al., 1992). Processed juice showed significantly high total and soluble solids, serum viscosity, paste viscosity and reduced serum separation (Thakur et al., 1996). This was associated with a large increase in polyuronide molecular weight relative to controls, larger than the difference in ripening fruit, presumably due to the high degree of pectin methyl-esterification protecting pectin from PG-mediated hydrolysis during fruit homogenization (Thakur et al., 1996). PME activity thus plays little role in fruit softening during ripening, but substantially affects tissue integrity during senescence and fruit processing characteristics.

1.3.2.8. PMEs and plant defence

Because cell wall constitutes a physical barrier between the environment and the internal contents of plant cells, its modifications are often associated with plant defence responses (Vorwerk et al., 2004). Arabidopsis microarray database has revealed that the expression levels of about 75% of predicted PME sequences vary in response to biotic and abiotic stresses. For example, some PME transcripts are regulated by cold , wounding, ethylene, OGAs and phloem-feeding insects (Lee and Lee, 2003; De Paepe et al., 2004; Moscatiello et al., 2006; Thompson and Goggin, 2006).

PME and microbial pathogens: PME activity is necessary for complete degradation of pectin by PGs and PLs, since these enzymes are not able to cleave highly methyl-esterified pectin. The disruption of *pmea* gene in the bacterium *Erwinia chrysantemi*, reduces strongly its virulence on *Saintpaulia ionanta* (Boccara and Chatain, 1989; Beaulieu et al., 1993). Decreases and increases in PME activities observed in antisense or overexpressing plant lines, and associated changes in the degree of methylesterification (DM) of cell wall pectins, have been correlated with changes in the susceptibility of plants to pathogens and abiotic stresses (Marty et al., 1997; Dorokhov et al., 2006a; Lionetti et al., 2007). For example, the potato resistance to soft-root *Erwinias,* was related to cell wall pectin esterification (McMillan et al., 1993a).

Many pectin-derived compounds have been reported to be involved in plant defence. Following PME processing, polygalacturonic acid glycosidic bonds can be cleaved by glycoside hydrolases, such as polygalacturonases, allowing the subsequent formation of eliciting active oligogalacturonides (OGs). The induction of plant defences by OGs has been widely studied, and its efficacy has been shown to depend upon the degree of OGs polymerization and methylesterification (Vorwerk et al., 2004; Moscatiello et al., 2006). The mode of PME action itself might modulate the susceptibility of a plant to stress. Indeed, significant differences in HGA methylesterification patterns have been found between stem rust fungus-resistant (block-wise distribution of methylesters) and susceptible (nonblock-wise distribution) lines of wheat (Wietholter et al., 2003).

PME and virus: The binding of functional plant PMEs to the movement proteins (MPs) of Taboma virus is required for cell-to-cell diffusion of the viruses via plasmodesmata (Chen et al., 2000). However, although it is known that (i) PMEs are associated with cell wall-embedded plasmodesmata, (ii) MPs colocalize with plasmodesmata and (iii) PME-like proteins bind to MPs in cell wall extracts, the mechanism allowing PMEs to facilitate viral movement remains unclear. From inoculated non-vascular tissues, virions are loaded into the phloem in a PME-independent manner and subsequently spread systematically from source to sink organs (Chen and Citovsky, 2003). Phloem unloading is partly PME-dependent and systemic infection by viruses in tobacco can be delayed by antisense mRNA reductions in PME expression and activity (Chen and Citovsky,

2003). Unfortunately, a plant protection strategy based on this approach might only delay infection but not fully suppress it. These results indicate that cell wall PMEs are only one of the targets for virus-induced infection. It has been shown that co-agroinjection of functional proPME (type I proteins) cDNA and a viral vector stimulates plant virus defence via virus-induced gene silencing mechanisms that repress virus reproduction in tobacco (Dorokhov et al., 2006a). The roles of PME in viral infections are still unclear, but tight regulation of different tissue-specific isoforms, and the balance between PME and MP levels, is likely to be involved. The abolition of the pro-PME anti-viral effect following overexpression of the Tobacco Mosaic Virus MP gene indicates that the PME:MP ratio is important (Dorokhov et al., 2006a).

PME and plant-herbivore interaction: Methanol production has been observed in plant-herbivore interactions (Penuelas et al., 2005; von Dahl et al., 2006b). Rapid and sustained increases in methanol emissions have been observed from tobacco after wounding, and are enhanced in the presence of caterpillar oral secretions, owing to up-regulation of the activity and expression of PMEs (von Dahl et al., 2006a). PME genes have also been found to be specifically regulated by aphids in phloem tissues of celery (Divol et al., 2005), indicating that PME-induced methanol production might be more generally involved in plant-stress signalling.

1.3.2.9. PME activity regulation

In addition to the translational control, PME activity is regulated by different post-translational mechanisms. It was postulated that PME activity in the cell wall is regulated by H^+ concentration in a cyclic manner during cell growth (Ricard and Noat, 1986). The enzyme optimal activity occurs at pH close to neutrality and is reduced by the local decrease of pH generated by protons released as a consequence of the reaction. In turn, the pH decrease activates glycosidases and glycosyl-transferases, involved in cell wall extension and building up. The consequent dilution of negative charges and increase of local pH result in reactivation of PME, starting a new cycle (Giovane et al., 2004). In addition, a mechanism of regulation on PME activity is played by specific PME inhibitors (PMEIs).

1.3.3. Pectin methylesterase inhibitors

The first PMEI was isolated from the sap extract of potato tuber (Ricard and Noat, 1986). It was extremely thermostable, and its molecular mass was in the range of 158–232 kDa. The purified inhibitor contained no detectable protein, whereas the presence of uronic acid and neutral sugars was detected. The inhibitory molecule was suggested to have a pectic configuration since it was inactivated by the PG and PNL. The inhibitor was active against PME from potato and from different plant species and exhibited an uncompetitive mode of action, whereas it did not affect bacterial and fungal PMEs. An inhibitory PME activity was also found in banana fruit (*Musa sapientum L.*) (Wu et al., 2002) in particular in rubbery fruits. The molecule was active against its own banana PME and the pea pod (*Pisum sativum*) PME, and was extremely thermostable. The chemical nature of this inhibitor was not elucidated. A highly thermostable inhibitory activity was found in intact jelly fig (*Ficus awkeotsang*) achenes. This inhibitor, fractionated by gel filtration and concanavalin A Sepharose chromatography, was found to consist of polypeptides with molecular mass ranging from 3.5 to 4.5 kDa (Jiang et al., 2002).

1.3.3.1. Proteinaceous inhibitors of PME (PMEIs)

Since now three proteinaceous inhibitors of PME have been identified and characterized. The first, AcPMEI (accession number P83326), was discovered in fully ripe kiwi fruit (*Actinidia chinensis*) during studies focused on PME characterisation (Balestrieri et al., 1990). Protein micro heterogeneities were detected at five positions of the amino acid sequence (Ala/Ser56, Tyr/Phe78, Ser/Asn117, Asn/ Asp123, and Val/Ile142), indicating that several isoforms of the protein were present in the fruit (Camardella et al., 2000). The presence of three cDNA sequences in *Actinidia deliciosa*, other kiwi specie, (AB091088, AB091089 and AB091090) confirmed this hypothesis (Irifune et al., 2004).

Two others genes (AtPMEI-1/At1g48020 and AtPMEI-2/At3g17220), encoding for PMEI sequences have been more recently identified in Arabidopsis (Wolf et al., 2003; Raiola et al., 2004). The intronless AtPMEI-1 and AtPMEI-2 genes share 64% identity at the nucleotide level. The encoded AtPMEI-1 and AtPMEI-2 share about 38% identity at the amino acid level with AcPMEI, and 45% amino acid identity, respectively, with each other. Removal of the predicted N-terminal signal peptide generates mature AtPMEI-1 and AtPME2 proteins of 151 amino acids (16.266 Da, predicted pI =7.7) and 148 amino acids (15.615 Da, pI = 9.0) respectively (Camardella et al., 2000; Raiola et al., 2004). PMEIs show a conserved C-terminal hydrophobic region (CxIxLVISN) and five conserved Cys residues, the first four of which have been shown to be engaged in disulfide bridges. The fifth Cys residue has a free thiol group. AcPMEI is not glycosilated while AtPMEI-1

shows one N-glycosylation and AtPMEI-2 shows two N-glycosylations (Fig. 12) (Raiola et al., 2004).

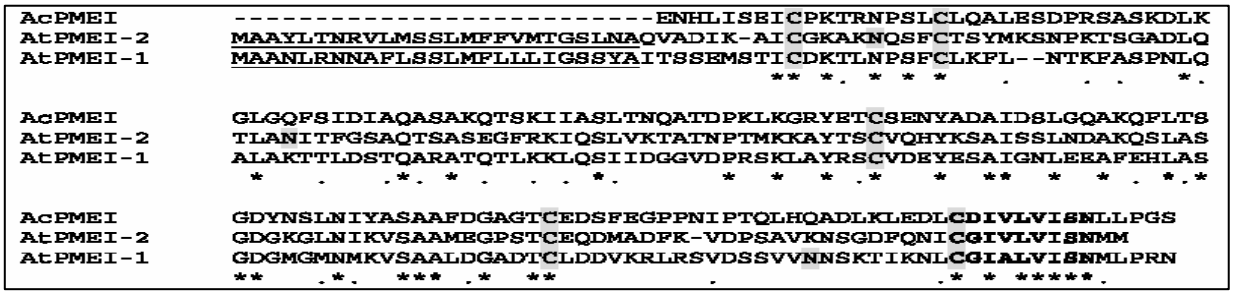

Figure 12. Amino acid sequence alignment of AtPMEI-1 and AtPMEI-2 with AcPMEI. Asterisks and dots indicate 100 and 66% amino acid identity, respectively. The five conserved Cys residues and the putative N-glycosylation sites are grey shadowed. Signal sequence of *Arabidopsis* proteins is underlined. The conserved C-terminal hydrophobic region is in bold (Raiola et al., 2004).

Search for homology in databank revealed similarity of PMEI with a sharp number of sequences. The identity level is not high, however, the position of the four Cys residues engaged in disulfide bridges is strictly conserved. We can distinguish two groups of related sequences, the first comprising cDNAs encoding proteins belonging to Pfam04041 (Fig. 13); members of this group include pectin methylesterase and invertase inhibitors, making difficult the functional characterization of the different inhibitors on the basis of their amino acidic sequence.

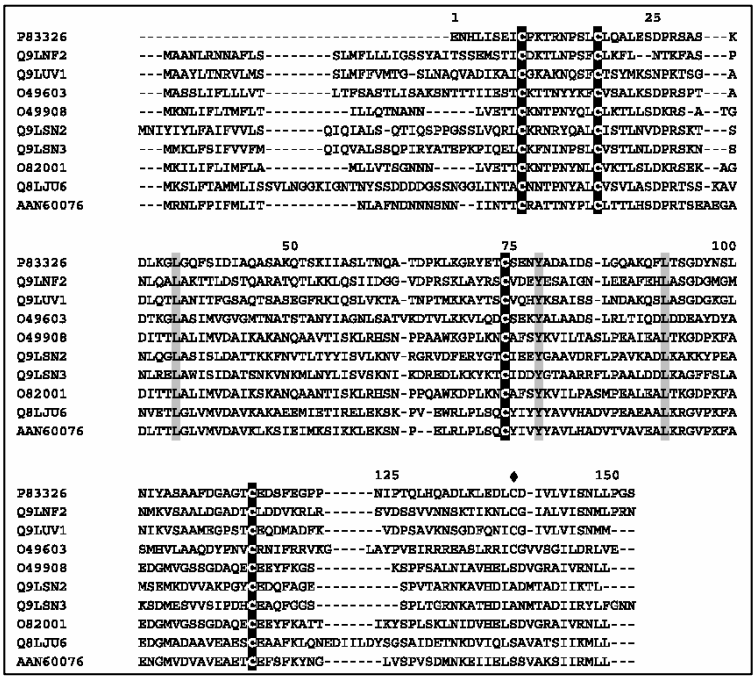

Figure 13. PMEIrp alignment Alignment of kiwi fruit PMEI (P83326), AtPMEI-1 (Q9LNF2), AtPMEI2 (Q9LUV1) with the apoplasmic (O49908) and vacuolar (AAN60076) INH isoforms from N. tabacum, with INH from Lycopersicon esculentum (O82001), with INH-like protein from Ipomoea batatas (Q8LJU6), and with INH-like proteins (Q9LSN2, Q9LSN3), INH homolog (O49603). Conserved Cys residues are black-shadowed. Other conserved residues are grey-shadowed (Giovane et al., 2004).

The second group contains the N-terminal pro-domains, PME precursors which are removed in mature PMEs (a representative alignment is shown in Fig.14). These sequences are quite variable; however, they maintain the conservation of the four Cys residues (Fig. 14). Secondary structure predictions on the basis of the deduced amino acid sequence indicate in the pro-domain region a prevalence of a-helix structure, in contrast with the mature protein, which is rich in β-sheets (Gaffe et al., 1997). The amino acid sequence and the predicted structure similarity of the PME pro-domain with the PMEIs are in favour of the hypothesis that a genome rearrangement occurred during evolution producing the physical separation of the pro-domain, initially linked to the catalytic domain, leading to a distinct protein with PME inhibitory activity (Giovane et al., 2004).

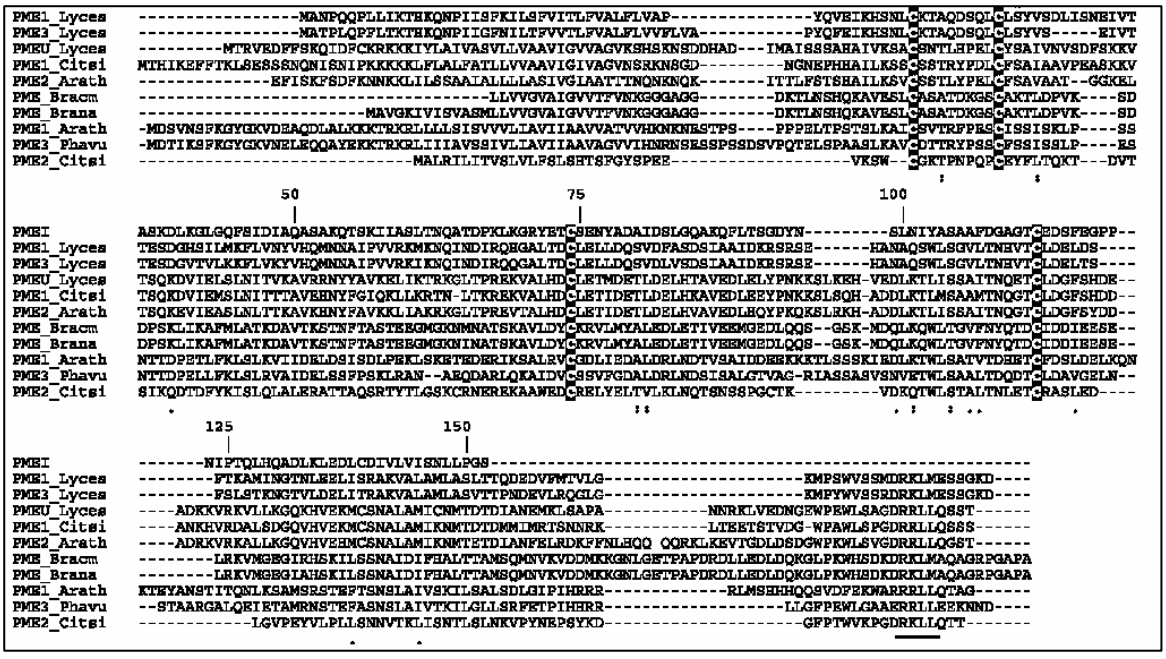

Figure 14. Sequence alignment of PMEI with PME pro-peptides sequence numbering refers to PMEI. Four Cys residues conserved in all sequences are black-shadowed. Strongly similar residues (:) and weakly similar residues (.) are indicated. The conserved R(R/K)L(L/M) sequence, which is close to the cleavage site of PME precursor, is underlined (Giovane et al., 2004).

PMEIs are typically active against plant PMEs, however they typically do not inhibit fungal and bacterial PMEs (Balestrieri et al., 1990; Raiola et al., 2004). The inhibition occurs through the formation of a reversible 1:1 stoichiometric complex. The stability of the complex between AcPMEI and PME-1 from tomato is strongly influenced by pH (Di Matteo et al., 2005), indicating that PME activity can be modulated by pH either directly or by modulation of the affinity between the enzyme and its inhibitor. Kinetic parameters of PMEIs/PME interaction have been investigated

through the analysis of Surface Plasmon Resonance (SPR). A dissociation constant value of 53 nM was calculated at pH 7 for the interaction between AcPMEI and PME-1 from tomato, the value decreases 10 times at pH 6 (Mattei et al., 2002). Therefore, the affinity of the two proteins is higher at a pH close to that of the apoplastic environment. SPR analysis of tomato PME-1 and AtPMEIs interactions showed, at pH in the range 5.5/8.5, the absence of dissociation for AtPMEI-2, and a K_D of 5.5 nM for AtPMEI-1 at pH 8.5 while no dissociation occurred at lower pH values (Raiola et al., 2004).The dissociation of the kiwi PME/PMEI complex at pH values ranging from 3.5 to 8.0 is undetectable, and that complete dissociation occurs only at pH 10.0. The dissociation kinetics observed at pH 9.5 is similar to that observed for tomato PME at pH 7.0. Size exclusion chromatography confirmed these results indicated that both free and immobilised kiwi PME are able to form a complex with PMEI, which is stable in a large pH range than that reported for tomato PME-1 (Ciardiello et al., 2008).

The inhibition mode of AcPMEI on tomato and carrot PME was competitive, indicating that the inhibitor interact on substrate binding site preventing substrate to enter in active cleft (D'Avino et al., 2003; Ly-Nguyen et al., 2004; Di Matteo et al., 2005). However, AcPMEI is able to inhibit banana or strawberry PME with non competitive mode (Ly-Nguyen et al., 2004).

1.3.3.2. Three-dimensional structure of PMEIs alone and in complex with PME

To date, the three-dimensional structure of AtPMEI-1 and AcPMEI in complex with tomato PME-1 have been solved (Hothorn et al., 2004b; Di Matteo et al., 2005). Inhibitors are almost all helical, with four long α-helices aligned in an antiparallel manner in a classical up-and-down four-helical bundle (Fig. 15).

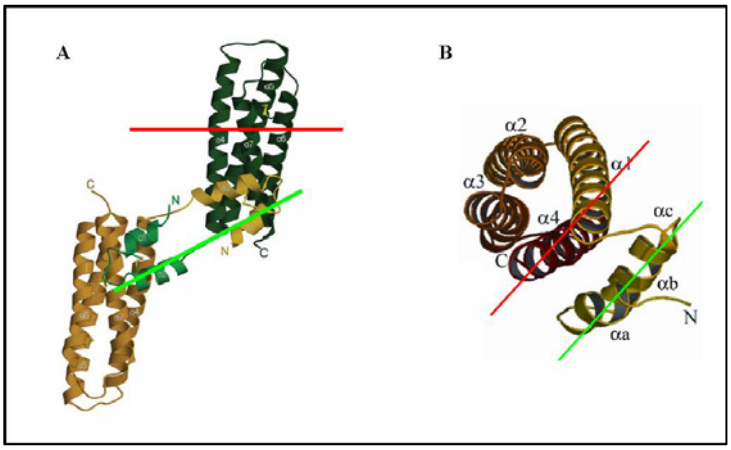

Figure 15. AtPMEI1 3D structure. (**A**) Ribbon representation of the AtPMEI1 dimer with the respective molecules shown in green and yellow. (**B**) ribbon representation of the AcPMEI monomer. Red line show core plan orientation while green line show N-terminal extension orientation (Hothorn et al., 2004b).

The interior of the bundle is stabilized by hydrophobic interactions and by a disulphide bridge which connects helices α2 and α3. Even if the two inhibitors are quite similar in the bundle, significant differences are located in the N-terminal extension. It is puzzling that the N-terminal region of AcPMEI folds back and packs with the bundle through hydrophobic interaction, whereas the N-terminal extension of At-PMEI1, which crystallizes in a dimeric form (Fig 15), packs against the bundle of another molecule (Hothorn et al., 2004b). Interestingly Pro28 residue of AtPMEI1, which is located in the linker between the N-terminal region and the four-helix bundle and is responsible for the orientation of the N-terminal region (Hothorn et al., 2004b), is replaced by a Lys in AcPMEI, suggesting that the different topology of the two inhibitors is due to the presence of different residues at the same position (Di Matteo et al., 2005).

1.3.3.3. PME-PMEI complex

Tomato PME-1 and AcPMEI form a stoichiometric 1:1 complex in which the inhibitor covers the shallow cleft of the enzyme where the putative active site is located. The four-helix bundle of PMEI packs roughly perpendicular to the parallel β-helix of PME, and the three helices α2, α3, and α4, but not α1, interact with the enzyme in proximity of the putative active site (Fig. 16).

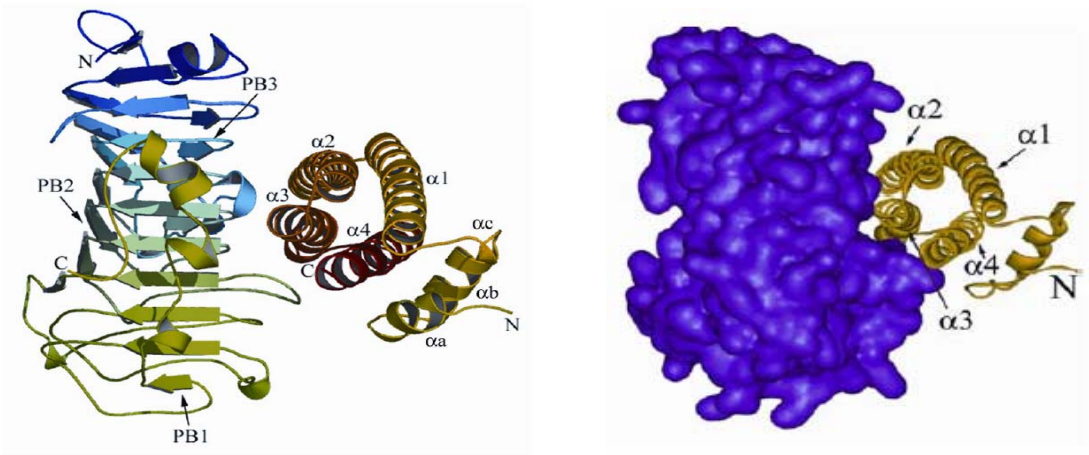

Figure 16. Structure of the PME-PMEI complex. Ribbon representation illustrating the relative positions of PMEI and PME in the complex. The enzyme is shown in green–blue on the left side. The inhibitor is represented in yellow–red on the right side; the α-helices of the four-helix bundle are indicated as α1 to α4, whereas helices of the N-terminal region are named αa, αb, and αc (Di Matteo et al., 2005).

The relative position of α2 and α3 helices is maintained by a disulphide bridge between Cys74 and Cys114. The N-terminal region of PMEI is poorly involved in the formation of the complex and

may play a role in the structural stability of the inhibitor. Detailed analysis of residues involved in forming the complex reveals that the putative catalytic residues (Asp132, Asp153, and Arg221) do not establish contacts with the inhibitor, neither do Gln109 and Gln131, which are thought to stabilize the anionic intermediate formed after the first nucleophilic attack. Instead, three aromatic residues (Phe80, Tyr135, and Trp223), likely responsible for substrate binding, interact with the inhibitor. Remarkably, Phe80 is one of the residues mostly involved in the interaction. This residue establishes 17 contacts with four different residues of the inhibitor (Thr73, Glu76, Asn77, and Thr113) and a water-mediated hydrogen bond. Trp223 of PME forms three contacts with its interacting counterpart, whereas Tyr135 forms only one contact; moreover, each of them forms a water mediated hydrogen bond. Upon formation of the complex with the inhibitor, Trp223 buries almost half of its solvent-exposed surface, and this explains the decrease of fluorescence observed in PME upon addition of the inhibitor (D'Avino et al., 2003). In summary, the inhibitor covers the active site cleft preventing the access of the substrate, and prevents the interactions of Phe80, Tyr135, and Trp223 with the substrate. These observations are consistent with the observed competitive mode of inhibition. The structure of the PME-PMEI complex provides a possible explanation for the lack of inhibition of PMEIs on PMEs from the bacterium *E. crysanthemi* and the fungus *Aspergillus aculeatus* (Raiola et al., 2004; Giovane et al., 2004). In *E. crysanthemi*, the putative binding site cleft is much deeper than in plant-derived PMEs (Figure 7/B). It is likely that the external loops of the bacterial enzyme create a steric hindrance that prevents the interaction with the inhibitor. On the other hand, the amino acid sequence alignment among PME from tomato, carrot, and *A. aculeatus* (Swiss-Prot code Q12535) reveals that almost all of the residues important for the interaction of tomato PME with the inhibitor are conserved in plant PMEs but not in the fungal enzyme, thus providing a reason for the observed lack of interaction (Di Matteo et al., 2005).

1.3.3.4. PMEIs expression and physiological role

Similar to PME, PMEIs appear to be ubiquitously express in higher plants. Quantitative Real-time PCR has shown that *AtPMEI1/2* genes are highly expressed in flowers, followed by root tissue for AtPMEI1 and by sink leaves for AtPMEI2. In general, AtPMEI2 showed a broader expression range than AtPMEI1. The analysis of *AtPMEI*s::GUS transformants confirmed the results obtained by real-time PCR, showing no expression in most tissues for *AtPMEI1*, and low, but variable expression for AtPMEI2, whereas for both isoforms the high expression in flowers could be largely attributed to the anthers and pollen.

Whereas AtPMEI1 expression appeared to be exclusively confined to anthers and pollen (Fig. 17), GUS activity in *AtPMEI2*::GUS lines was also detected at the base and the conducting tissues of the sepals (Fig.17).

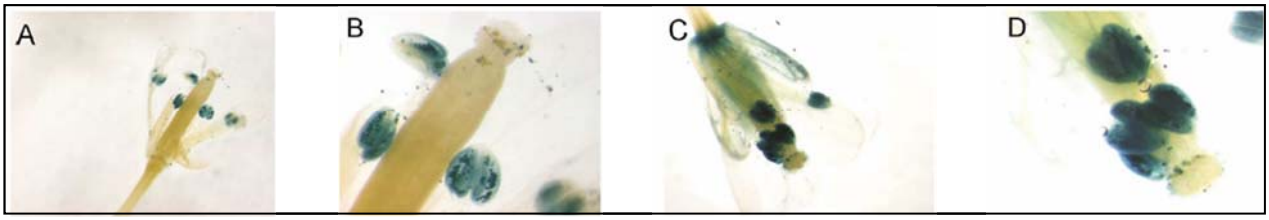

Figure 17. **Analysis of flower-specific expression of AtPMEI1 and 2, using promoter::GUS fusions.** (**A**) and (**B**) AtPMEI1, pollen specific expression. (**C** and **D**) AtPMEI2 highest expression in pollen (Wolf et al., 2003).

In pollen tubes, several pectin methylesterases (PMEs), are co-expressed with different PMEIs. This raises the possibility that interactions between PMEs and PMEIs play a key role in the regulation of cell-wall stability at the pollen tube tip. Ectopic expression of AtPPME1 (pollen-specific PME isoform; (Tian et al., 2006) in *Nicothiana. benthamiana* leaves, resulted in a significant increase in total PME activity, which was completely inhibited by recombinant AtPMEI2; these results support the notion that the pollen-expressed inhibitors AtPMEI1 and AtPMEI2 are regulators of the pollen-expressed PME isoform AtPPME1, and also inhibit pollen-expressed tobacco PME isoforms (Rockel et al., 2008). As during pollen formation and, in particular, during pollen tube growth the process of PME-mediated pectin deesterification appears to be under tight control, both spatially and temporally, an interaction of PME with PMEI proteins may be part of this regulation (Wolf et al., 2003).

Constitutive expression of *AtPMEI-1* and *AtPMEI-2* in Arabidopsis plants have been recently performed. The transgenic expression of the two inhibitors decreases the plant PME activity and alters the level of pectin methylesterification of the wall. Seedlings vertically grown on solid medium, showed a significant increase in root length in transgenic lines with respect to wild-type (Lionetti et al., 2007). The transformed plants show an altered growth response and a lower susceptibility to *B. cinerea* (Lionetti et al., 2007). The reduced symptoms caused by the fungus on transgenic plants can be related to its impaired ability to grow on methylesterified pectins (McMillan et al., 1993b; Marty et al., 1997).

1.3.4. PME and PMEI biotechnological applications

Most of the vegetable transformation processes that are routinely employed in the food industry, aim at the maintenance of firmness and texture of fruit and vegetable derived products, (Corredig et al., 2001; Bourne, 2002). The technologies employed are largely reliable, however, some problems concerning the quality of the product are not yet solved. Two problems in particular have been identified: the lack of firmness in canned vegetable during the storage and the cloud-loss of vegetable juices (Castaldo et al., 1996; Castaldo et al., 1997). Firmness and texture changes of fruit and vegetable products during technological process and subsequent storage depend on the alterations of cell wall components, in particular the pectic substances (Krall and McFeeters, 1998). Modification of pectin during processing is due to the action of endogenous pectin degrading enzymes, such as PME and PG. The synergic action of the two enzymes, yields short demethylated pectin chains, leading to softening of fruit and vegetable products and decrease of viscosity (C.Versteeg et al., 1980; Wicker et al., 2002). The fruit and vegetable juices can be considered biphasic systems, made up by a dispersing phase, called serum, in which the hydrosoluble components are dissolved, and a dispersed phase, called cloud, consisting of particles (R.Baker, 1977). During the juice extraction step, PME de esterifies the pectin. The low methylesterified pectin may interact with calcium ions forming insoluble pectates, which co-precipitate with the pulp-particles, thus causing cloud loss (Krall and McFeeters, 1998). The juice stability also depends on the charge and hydration of pulp particles in the suspension, both affected by the action of PME (Beresovsky et al., 1995; M.Chii et al., 2001). Therefore, PME is responsible for particle precipitation and cloud loss of fruit juice. In order to prevent this phenomenon, PME must be inactivated. This is usually achieved by thermal treatments (pasteurisation or High Temperature Short Time (HTST) treatment). Cloud loss of thermically treated juices often still occurs, suggesting the existence of extremely thermostable PME isoforms which survive the thermal treatment. This is a serious problem for the food industry. The PMEI purified from kiwi fruit has a potential utilisation in PME inactivation. PMEI can be use as adjuvant in the manufacturing of vegetable derived products. In fact, Castaldo et al.(Castaldo et al., 1991) found that the addition of PMEI to non-pasteurised orange juice prevented cloud loss after 9 months of storage at 5° C. The PMEI-treated juices showed the same aspect as the pasteurised juices throughout the observation period. The PME inactivation by PMEI could allow a thermal treatment of juices at temperatures lower than those needed for inactivation of highly thermostable PMEs. Such milder thermal treatment could result in better flavour quality and higher vitamin content, thus producing high quality products.

Kiwi PMEI coupled to CNBr-activated Sepharose, has been utilized for the purification of PMEs from tomato, carrot, apple, banana, and strawberry (Ly-Nguyen et al., 2002a; Ly-Nguyen et al., 2002b). The affinity chromatography on PMEI-Sepharose has also been used to detect low levels of PME in industrial plant derived products. This activity, even if present in trace amounts, which cannot be detected by usual determination methods, may produce undesirable effects after prolonged storage of the fruit juice. The residual PME is concentrated by binding to the affinity chromatography medium, and eluted in a small volume by increasing the pH of the buffer, allowing detection of low level of PME by conventional assay methods (Sorensen et al., 2004).

1.4. Invertase

In higher plants, sucrose is the major transport form of carbohydrates. Sucrose is exported from the source tissues (leaves) and transported via the phloem to the different sink tissues (roots, stem, reproductive organs and vegetative storage organs). Cells in the target tissue may take up sucrose symplastically or apoplastically. The only known enzymatic pathways of sucrose cleavage in plants are catalyzed by invertases and sucrose synthases (SuSy) (Fig. 18).

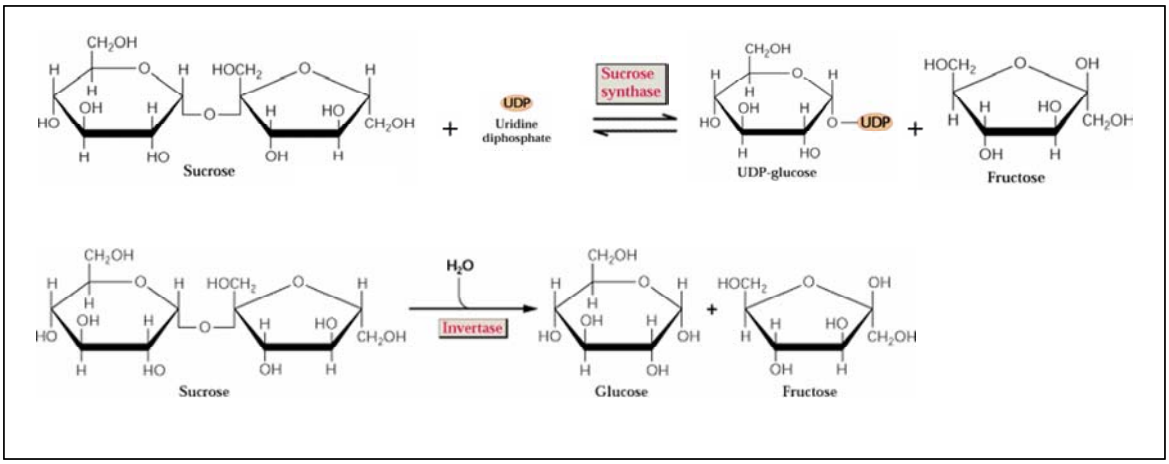

Figure 18. Sucrose cleavage in plants by invertase and sucrose synthases

Both of these pathways typically degrade sucrose in *vivo* but the products of their reactions differ in important ways (Tymowska-Lalanne and Kreis, 1998). Under physiological conditions, the hydrolysis of sucrose by invertase is irreversible, whereas the cleavage catalysed by sucrose synthases is reversible. However in plant cell SuSy is mainly involved in sucrose degradation (Geigenberger and Stitt, 1993)

Based on their pH optima, invertases can be divided into acid (pH 4.5-5.0) and alkaline (pH 7.0-7.8). Spatially they occur as extra- and intracellular and bound and soluble forms. It is generally accepted that tree types of plant invertase exist in higher plant: (1) the acid-insoluble invertases, ionically bound to the cell-wall (CWI); the acid-soluble invertases, localised in the vacuole (VI); and (3) the alkaline-soluble invertases, thought to be cytoplasmic (CI).

1.4.1 Cytosolic invertases

The presence of alkaline invertases, have been reported for a number of plants. The intracellular location of this type of invertase is suggested by its recovery in the soluble fraction, and its pH optimum between 7.0 and 7.8 (Roitsch, 2004). CIs are not glycosylated and are extremely unstable (Sturm, 1999). The protein sequences of plant CIs are highly homologous to

each other but not the acid invertases. Not clear function during plant development has been assigned to CIs, but they are assumed to channel cytoplasmic sucrose into catabolic reactions (Sturm and Tang, 1999). Neutral and alkaline invertases from *Daucus carota* are inhibited competitively by fructose and non-competitively by glucose. The inhibition by their reaction products is an important regulation process, which adapts the hydrolysis of cytosolic sucrose to the utilization of glucose and fructose in cytosolic sucrose metabolism (Lee and Sturm, 1996).

1.4.2. Acid invertases

Acid invertases have been purified from several plant species (Unger et al., 1992). The enzymes have a *K*m for sucrose in the low-millimolar range. Activity is inhibited by heavy metal ions such as Hg^{2+} and Ag^{+}. Acid invertases are also inhibited by their reaction products, with glucose acting as a non-competitive inhibitor and fructose as a competitive inhibitor. The mature polypeptides are *N*-glycosylated and their molecular masses range between 55 and 70 kDa. Analysis of some of the purified proteins on denaturing SDS gels under reducing conditions revealed the presence of proteolytic fragmentation. A 70-kDa monomeric form of vacuolar invertase of mung bean hypocotyls was found to be split into a 30-kD N-terminal and a 38-kD C-terminal fragment (Arai et al., 1991). Likewise, the 68-kDa monomer of isoform I of vacuolar invertase from carrot was fragmented into N- and C-terminal polypeptides of 43 and 25 kDa, respectively (Unger et al., 1992b; Unger et al., 1994). Under native conditions, these fragments appear to be tightly associated and, in complex, possess enzyme activity. Fragmentation does not appear to be an artefact of the protein purification, but instead seems to be under developmental control. For example, the full length proteins predominate in very young hypocotyls of bean and seedlings of carrot, whereas with increasing hypocotyls and seedling age the fragments are more abundant. Whether the fragmentation has a physiological function is not clear.

As illustrated in the Figure 19, cell wall and vacuolar invertases are synthesised as pre-pro-proteins, with a long leader sequence which is cleaved off during transport and protein maturation. The leader sequence can be divided into two segments: a signal peptide, required for entry into the endoplasmic reticulum (ER) and, thus, into the secretory pathway (Blobel, 1980). The leader sequence, which is characteristic of all known vacuolar forms, may play a role in the regulation of enzyme activity and/or in the folding and stability of the polypeptide, or it may contain information for vacuolar targeting. It is known that several short amino acid domains, N-terminal propeptide, C-terminal extension or an exposed region, act as vacuolar sorting signals in plants of the mature protein (Matsouka, 1991; Bednarek and Raikhel, 1992; Chrispeels and Raikhel, 1992). In contrast to the cell wall enzyme, the sequences of the vacuolar invertase contain an additional C-terminal

extension. These sequence might be involved in the vacuolar targeting of the protein(Bednarek and Raikhel, 1992).

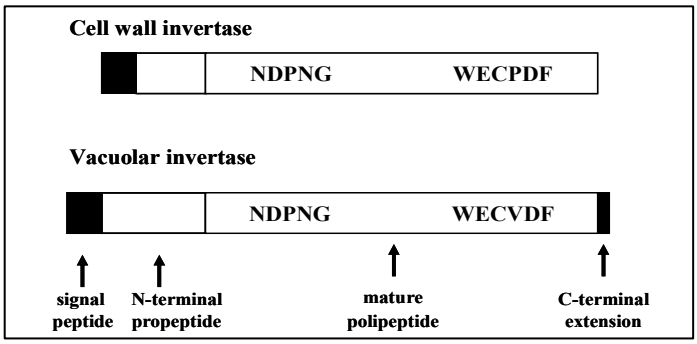

Figure 19. Schematic comparison of cell wall invertase and vacuolar invertase. The amino acid sequence NDPNG is a hallmark of plant acid invertases. The sequence WECXDF indicates a highly conserved peptide domain consisting of a Cys residue and a few neighbouring amino (Tymowska-Lalanne and Kreis, 1998).

The pH optimum of CWI is slightly more acidic (pH 3.5-5.0) than of VI (pH 5.0-5.5) (Roitsch, 2004). The different pH optimum of the two isoforms is determined by an amino acid exchange in the conserved WEC-P/V-D box (Fig. 19), which is characteristic for all acid invertases (Goetz and Roitsch, 1999). CWIs carry a proline residue at the fourth position where VIs have a valine residue (Roitsch, 2004). By a proline to valine exchange in the extracellular invertase CIN1 from *Chenopodium rubrum*, the pH optimum of the heterologous expressed CIN1 was shifted from 3.75 to 4.4. Additionally, the cleavage rate of raffinose was lowered compared to the wild type CIN1 protein (Goetz and Roitsch, 1999). Another conserved sequence motif is the NDPNG motif (Fig.19) close to the N-terminus of the mature polypeptide found in invertases from plant, bacteria and yeast. It forms an important part of the catalytic domain of acid invertases (Sturm and Tang, 1999).

A classification based on overall amino-acid sequence similarities (http://afmb.cnrs-mrs.fr/CAZY/; (Henrissat, 1991)) regroups cell-wall and vacuolar invertases, fructosyl transferases and fructan exohydrolases (FEHs) from plants together with β-fructosidases and FEHs from microbial origin, within the family 32 of the glycosyl hydrolases (GH 32). While neutral/alkaline invertases belong to GH 100 family 100 (GH 100(Ji X et al., 2005)).

1.4.3. Cell wall invertase three-dimensional structure

Recently the protein structure of a cell wall invertase from Arabidopsis (AtcwINV1) has been solved (Fig. 20) (Verhaest et al., 2006). The structure comprises an N-terminal fivefold β-propeller domain followed by a C-terminal domain formed by two β-sheets. The active site is

positioned in the fivefold β-propeller domain containing the nucleophile Asp23 and the acid/base catalyst Glu203 of the double-displacement enzymatic reaction.

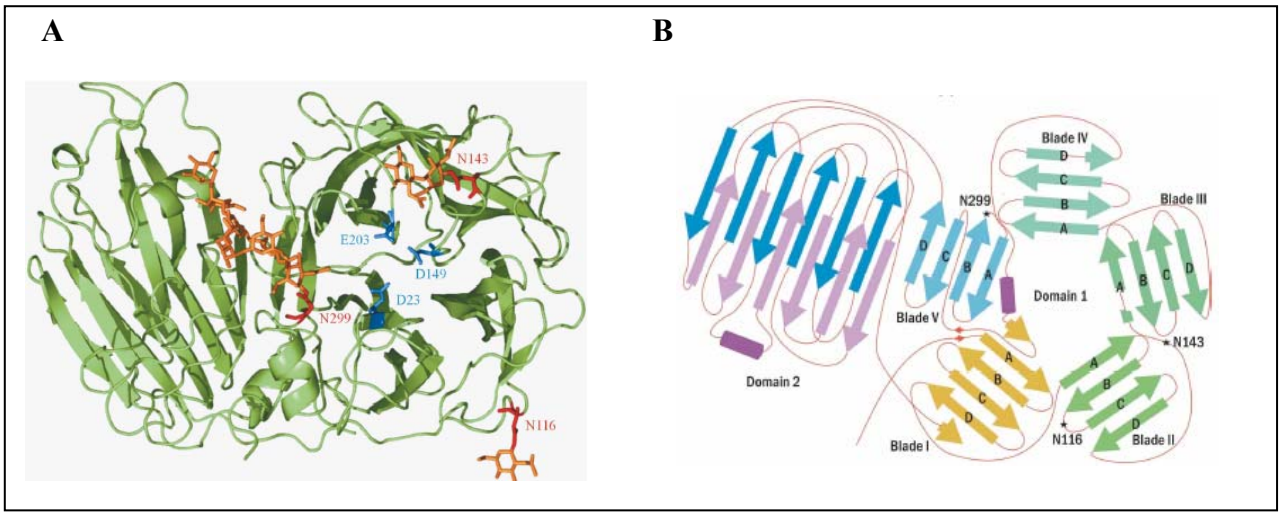

Figure20. ***Arabidopsis thaliana*** **invertase. (A)** overall three dimensional structure of Arabidopsis cell wall invertase. In red are indicated glycosylation sites, in orange are indicated the glycosylation chains. (**B**) Schematic diagram of the topology of invertase. β-Strands are depicted by arrows and a-helices by cylinders. Asterisks represent the glycosylation sites (Verhaest et al., 2006).

The reaction scheme for invertase can be summarized as follows. Sucrose binds to the active site, where its glycosidic oxygen is protonated by Glu203. Subsequently, a nucleophilic attack is performed by the carboxylate of Asp23, forming a covalent fructose–enzyme intermediate. Finally, this intermediate is hydrolyzed, releasing fructose and the free enzyme (Fig. 21).

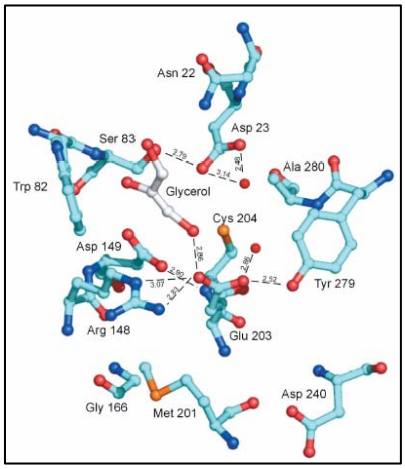

Figure 21. Invertase active site. The key residues of the active site and one glycerol molecule are displayed. Bonding interactions are shown as dashed lines, while the spheres represent water molecules (Verhaest et al., 2006).

Site-directed mutagenesis-based data on AtcwINV1 demonstrate an important role for the Asp-239 residue in both binding and hydrolysis of sucrose. In general, GH32 family enzymes containing an Asp-239, have sucrose as a preferential donor, whereas enzymes lacking this residue use fructans as

their donor substrate. Asp-239 is proposed as a reliable determinant for the identification of non characterized members within the group of cell wall invertases/FEHs (Le Roy et al., 2007).

1.4.4. Acid invertases and plant development

Investigation of plant invertase activity revealed that often the acid isoforms of invertase are active in different tissues, organs and at different stages of plant development. It might be possible that each tissue in plant expres a unique set of genes encoding the different isoforms (Cheng et al., 1996).

Biochemical and physiological studies suggest that cell-wall invertases play a key role for apoplastic floem unloading. The released hexoses can be taken up by hexoses transporters, which have been shown to be expressed in tissues close to high CWI activity.

VIs regulate the ratio and levels of hexoses and sucrose, stored temporarily or permanently, in vacuoles (Sturm and Tang, 1999). VIs are especially active in growing zones and expanding tissues like root tips, internodes and developing leaves. In these tissues they enhance cell enlargement via the increase in osmotic potential (Weschke et al., 2003) and probably play also a role in phloem unloading.

To study the functions of acid invertases in carrot, the antisense technique was used to generate transgenic with reduced enzyme levels (Tang et al., 1999). Phenotypic alterations appeared at very early stages of development. In somatic embryos expressing antisense mRNA for a cell wall invertase, the cotyledons failed to separate. In contrast, embryos expressing antisense mRNA for a vacuolar invertase had quite large cotyledons but stunted hypocotyls and roots. When control plantlets had two to three leaves and one primary root, shoots of transgenic plantlets expressing antisense mRNA for either cell wall invertase or vacuolar invertase were not separated into individual leaves but consisted of several stunted, interconnected green structures. Plants in soil expressing antisense mRNA for cell wall invertase showed the development of extra leaves and a delayed and reduced tap root development. Plants expressing antisense mRNA for vacuolar invertase also had more leaves but the tap root developed normally though smaller.

The data suggest that cell wall and vacuolar invertases have multiple functions. In the early stages, both invertases appears to play a role in plant development, most likely via control of sugar composition and metabolic fluxes. Later, with the reduction of cell wall invertase or vacuolar invertase activity, both isoenzymes appear to have important functions in sucrose partitioning (Tang et al., 1999).

1.4.5. Vacuolar invertases in tomato fruit ripening

Hexose-accumulating tomato fruits (*S. lycopersicum*.) undergo a developmental metabolic transition with respect to sugar metabolism and sugar uptake (Ruan and Patrick, 1995). The early stage of tomato fruit development is characterized by symplastic sucrose uptake. The initial step in sucrose metabolism occurs primarily via sucrose synthase, leading to a transient accumulation of starch. During the following stage of ripening there is a transition in uptake pathway from symplastic to apoplastic, whereby sucrose is hydrolysed by apoplastic acid invertases to hexoses, which are transported into the cytosol via energy-dependent plasmalemma hexose transporters (Ruan and Patrick, 1995; Ruan et al., 1997; Brown et al., 1997).

The reduction of a tomato vacuolar invertase (TIV-1) by an antisense approach (Klann et al., 1996) or gene suppression (Ohyama et al., 1995) led to the conversion of hexose-storing into sucrose storing fruit, and to a reduction in fruit size. Although the change in sugar composition does not affect the amount of sugar accumulated per fruit. This fruits appear to acquire less water during development and exhibit a corresponding reduction in expansion (Klann et al., 1996).

Fruit from *L. pimpinellifolium* have higher invertase activities, greater hexose content and lower sucrose accumulation than *L. esculentum* fruit (Husain et al., 2001). Genetic analysis in *L. pimpinellifolium* has shown that the locus conferring high hexose content, coincides with the region containing vacuolar invertase (Tanksley et al., 1996; Grandillo and Tanksley, 1996). Vacuolar invertase mRNA from *L. pimpinellifolium* LA 722 fruit was present earlier in development than that from *L. esculentum* fruit (Elliott et al., 1993). This indicates that invertase may be important in the observed high sugar content of the former fruit.

1.4.6. Expression pattern and regulation of acid invertases

Most plant species contain several invertase isoforms. In the genome of *A. thaliana* six CWI and two VI isoforms have been annotated, which differ remarkably in their expression pattern. Analysis of isoform specific steady-state transcript levels, suggested independent modes of regulation and showed markedly different organ- and development-stage-specific expression patterns (Sturm et al., 1995). Similar results were obtained in a study of the expression of genes for one vacuolar and four cell wall invertase isoforms from tomato (Godt and Roitsch, 1997). Interestingly, both carrot (Lorenz et al., 1995) and tomato (Godt and Roitsch, 1997) contain a flower-specific gene for an acid invertase. Together, these findings suggest that plants have evolved a small family of acid invertase genes that are expressed independently at specific stages and tissues during plant development. Fast transcriptional up-and down-regulation of invertase isoforms has been described under various conditions and seems to be a general regulatory mechanism of these

proteins (Sturm and Chrispeels, 1990; Zhang et al., 1996; Ehneÿ et al., 1997; Zeng et al., 1999). In potato, a posttranscriptional regulation via exon-skipping of a CWI gene has been described (Bournay et al., 1996). The intron-exon gene organization of the invertase genes is conserved between monocots and dicots (Roitsch, 2004). With the exception of the gene for the main form of carrot cell wall invertase (Ramloch-Lorenz et al., 1993), all of the other genes contain an invertase gene carrying a small mini-exon of nine nucleotides, which encodes for a conserved β-motif NDPNG and represents one of the smallest exons described in plants (Simpson et al., 2000). In potato, the mini exon of one of the genes was susceptible to alternative splicing (Bournay et al., 1996). No aberrant posttranscriptional processing was observed during normal invertase gene expression in potato. In contrast, RNA processing was perturbed by cold stress, resulting in the deletion of the mini exon from some transcripts. It is not known whether the aberrant splicing of the invertase gene has a physiological role (Sturm, 1999).

Increase in acid invertase activity in response to hormones such as auxins, gibberellic acid (Wu et al., 1993), or cytokinins (Ehness et al., 1997) was observed in several plant species. It is not clear whether these effects are due to direct regulation of invertase genes by plant hormones or via stimulated cell proliferation creating new sinks for sucrose. In cultured cells of *C. rubrum*, the increase in cell wall invertase mRNA by cytokinin was correlated with an increase in transcripts for a glucose transporters (Ehness et al., 1997), most likely resulting in a higher carbohydrate supply of hormone stimulated cells.

Genes for acid invertases have also been found to be regulated by wounding. Expression of a gene for carrot cell wall invertase was markedly altered by mechanical wounding of tap roots (Sturm and Chrispeels, 1990). Induction of gene expression was not systemic but was restricted to the wound site. A correlation between increased acid invertase activity and infection of plants with various pathogens has been reported several times (Sturm and Chrispeels, 1990). In carrot tap roots, the response to infection with the bacterial pathogen *Erwinia carotovora* was extremely fast and transient (Sturm and Chrispeels, 1990). Induction of gene expression by pathogen infection appears not to be systemic, but restricted to the site of infection (Benhamou et al., 1991).

1.5. Regulation of invertases by proteinaceous inhibitors

In addition to the translational control, invertase activity is regulated by posttranslational inactivation through invertase inhibitor proteins. Invertase inhibitors have been described in various plant species, especially in storage organs of crop plants (Greiner et al., 1999; Balibrea Lara et al., 2004). The first description of invertase inhibitors came from potato tubers (Pressey, 1966). Later the presence of this class of inhibitor was also described in the storage tissues of sweet potato, red

potato and sugar beet (Pressey, 1968) and in the endosperm of maize kernels(Jaynes and Nelson, 1971). The invertase inhibitors are non-glycosylated proteins, 15 - 23 kDa in molecular weight, showing an high stability against treatment with heat and acidic conditions (Rausch and Greiner, 2004).

The first sequence data of the inhibitor protein came form the purification and N-terminal sequencing of inhibitors in tomato (Pressey, 1994) and tobacco (Weil et al., 1994). The first invertase inhibitor cDNA was cloned by Greiner et al. (Greiner et al., 1998) via tryptic digest of purified inhibitor protein obtained from tobacco suspension-cultured cells, peptide sequencing, and cDNA library screening. The deduced protein sequence confirmed the N-terminal sequence of the mature protein and predicted a classical signal peptide. From the same suspension-cultured cell cDNA library, a related cDNA clone was isolated (Greiner et al., 1999). As the second clone was later assigned to the vacuolar compartment, the two inhibitors have been named: NtCIF, the apoplasmic isoform (cell wall inhibitor of α-fructosidase;), and NtVIF, the vacuolar isoform. While NtCIF protein showed a broad range of inhibition against different plant CWI and VI preparations, NtVIF protein was rather specific for VI. Recently two inhibitors (AtC/VIFs) from *Arabidopsis thaliana* were indentified (Link et al., 2004). AtC/VIF1 showed specific inhibition of VI activity, whereas AtC/VIF2 inhibited both, CWI and VI. It is noteworthy that all invertase inhibitor characterised so far, did not inhibit fungal invertases (Pressey, 1994; Rausch and Greiner, 2004).

Interestingly, the substrate sucrose appeared to protect CWI against inhibition. Surprisingly this strong substrate protection was only observed for the specific combination of CWI and NtCIF isolated from tobacco suspension cultured cells (Weil et al., 1994). The inhibition of CWI was dependent on the pH, being strongest at pH 4.5 (close to the CWI activity optimum). In vitro effects of Mg^{+2}, Zn^{+2}, suggested that divalent cations promoted CWI inhibition (Weil et al., 1994). The formation of tight protein–protein complexes was later confirmed by native cathodic gel electrophoresis (Krausgrill et al., 1998a). Additionally, the complex formation between NtCIF and NtCWI is markedly slower than the binding of NtCIF to a VI preparation from tomato fruit (Sander et al., 1996).

Kinetic analysis obtained by the study of the interaction between a potato invertase with the endogenous inhibitor indicate that the protein-protein interaction is complex. The inhibitor appeared to bind to invertase in more than one step: initially the interaction was rapid, relatively weak readily reversible and non competitive with the substrate at pH 4.7(Bracho and Whitaker, 1990a). While non competitive inhibition was observed in tomato fruits between a vacuolar invertase and a not well characterized inhibitor (Pressey, 1994).

1.5.1. Molecular structure of NtCIF

As described above, invertase inhibitors belong to the same structural family of pectin methylesterase inhibitors (Pfam 04043). The protein sequence homology of this family is not very high. The two identified invertase inhibitors from tobacco shows only 47% amino acid identity and the two from *A. thaliana*, only 29% amino acid identity. However, all members possess 4 cysteine residues at conserved positions, which are important for the formation of two disulfide bridges (Camardella et al., 2000; Raiola et al., 2004). To date only the three dimensional structure of NtCIF has been determined (Hothorn et al., 2004a). NtCIF showed a four-helix bundle structure and an uncommon N-terminal extension. The structure is stabilized by a disulfide bridge and it was shown, that the N-terminal extension of NtCIF is important for overall protein structure and activity (Hothorn et al., 2004a).

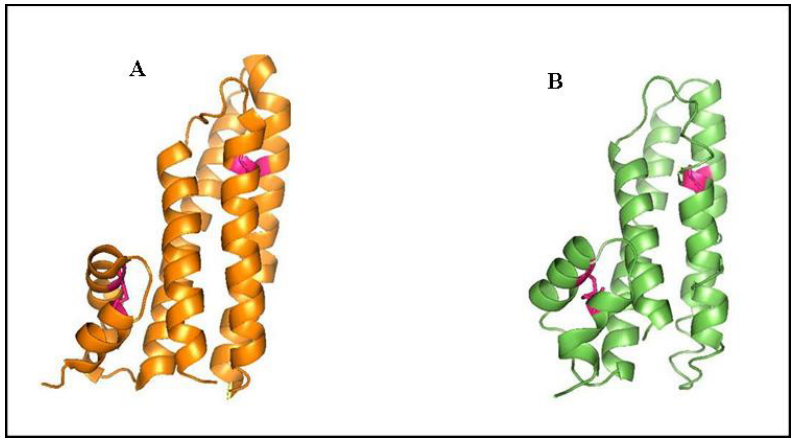

Figure22: NtCIF and AcPMEI 3D structure. Ribbon representation of (**A**) NtCIF and **(B**). AcPMEI disulfide briddges are in pink (Hothorn et al., 2004b; Di Matteo et al., 2005).

PMEI and Nt-CIF exhibit an almost identical fold (Fig. 22) but recognize different target enzymes. The structural view of the PME-PMEI, the sequence comparison among the PMEIs and Nt-CIF and structural over imposition between PMEI and Nt-CIF, provide possible explanation of the specificity of interaction. The subset of residues of the kiwi inhibitor, Asn101, Asp109, Thr113 (located on α3), and Asn147 (located on α4), which form intermolecular H-bonds with the enzyme, are conserved only in PMEIs (Fig. 23). In addition, an amino acid insertion that produces a distortion of the α2 helix of Nt-CIF is close to residues corresponding to Asp82 and Ser83 in α2 of PMEI, which are involved in H-bonds with PME.

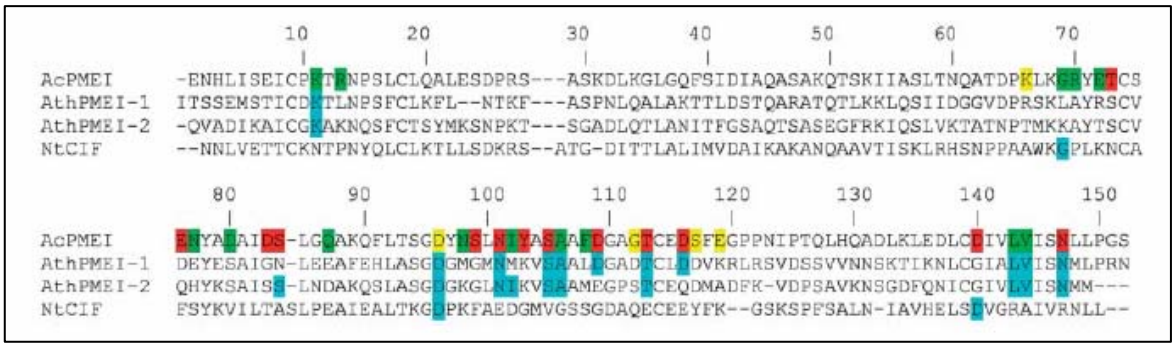

Figure 23: **Sequence Comparison of PMEIs form Kiwi, PMEIs from Arabidopsis, and Invertase Inhibitor from Tobacco**. Residues of the kiwi inhibitor involved in H-bonds (violet), Van der Waals contacts (green), and water-mediated H-bonds (yellow) with tomato PME are shown. Conserved residues are in blue (Di Matteo et al., 2005).

It was speculated that the lack of residues important for the formation of the complex as well as the distortion of α2 helix of Nt-CIF compared with that of PMEI are responsible for the lack of interaction between Nt-CIF and PME (Di Matteo et al., 2005).

1.5.2. Expression pattern and physiological functions of invertase inhibitors

High amounts of NtCIF are found in suspension culture cells of tobacco, where during the culture it is expressed in correlation with CWI, but due to the protective effect of sucrose on CWI inactivation, it probably only becomes active when sucrose in the medium is depleted (Krausgrill et al., 1998b). In tobacco, NtCIF is most strongly expressed in floral tissues, but it is also detected in source and senescent leaves. NtCIF shows an increased expression in response to abscissic acid and poly ethylen glycol treatment, which simulate senescence and drought stress (Rausch and Greiner, 2004). The expression analysis of the inhibitors AtC/VIF1 and AtC/VIF2 from *A. thaliana*, revealed that expression of AtC/VIF1 was restricted to specific organs (vascular tissues of flowers, roots and senescent leaves), AtC/VIF2, however, was weakly expressed throughout plant development. Promoter::GUS transformants confirmed pronounced differences of tissue/cell type-specific expression between both isoforms (Link et al., 2004).

In the early development of maize kernels, a cell wall invertase inhibitor (ZmINV- INH1) is expressed in the area surrounding the embryo, where it can interact with apoplastic invertases (Bate et al., 2004). Since the embryo at that phase develops much slower than the surrounding endosperm, the authors propose that the presence of ZmINV-INH1 ensures that the embryo is exposed to lower hexose concentrations than the endosperm. Analysis of *A. thaliana* plants with reduced expression of AtC/VIF1 and AtC/VIF2 showed no obvious phenotypic difference in growth and only a minor increase in soluble invertase activity in the case of AtC/VIF1 (Link et al., 2004), most likely due to the presence of multiple inhibitor isoforms with redundant functions. All these results indicate that

even if the presence of invertase inhibitors in tissues, correlate with the presence of invertases, precise physiological role of the inhibitors in *planta* have to be provided.

1.6. Biotechnological approaches using invertase and invertase inhibitors

Acid invertases are interesting targets for biotechnological approaches aiming to improve the performance of crop plants. Since the overexpression of invertases on a whole plant level led to adverse effects (Von Schaewen et al., 1990; Sonnewald et al., 1991); a specific increase of apoplastic invertase activity during the development of potato tubers (Sonnewald et al., 1997) leads to an increase in tuber size, albeit a total reduction in tuber number seed yield increasing. (Heyer et al., 2004). The alteration of invertase activity via overexpression of heterologous genes might have negative effects and, due to the high stability of the formed proteins, difficult to control. Another option to prolong invertase activity is the down-regulation of invertase inhibitors.

The suppression of NtCIF expression led to an increase in seed weight and oil content, the number of seeds per flower and the seed size was not altered (Rausch and Greiner, 2004). An extension of this approach onto seed crops like maize, soybean and rapeseed, which all are described to express invertase inhibitors during seed development, is a promising target for the enhancement of these crops.

Transgenic plant technologies can be used to study the effect of changing the timing and amount of acid invertases gene expression on hexose accumulation in ripening tomato fruit. It was hypothesized that the genetic engineering of tomato cultivars to increase invertases gene expression earlier in fruit development will result in a higher fruit soluble solid content.

1.7. Aim of the work

PME and invertase inhibitors form a large plant structural family named invertase/pectin methylesterase inhibitor family which members are selectively targeted toward structurally and functionally unrelated enzymes. Nevertheless the very similar four-helix bundle fold members of this family exhibit limited amino acid conservation making impossible a functional prediction by sequence comparison. For this reason a functional genomic approach need to be applied to biochemically characterise each member.

Tomato can be considered a model plant for modern and basic plant science for its easy genome manipulation, available genomic information and to study plant-pathogen interaction.

The aim of this thesis is to functionally characterised and define the physiological role of members of INH/PMEI protein family in tomato. In this thesis two inhibitors i.e. SolyCIF end SolyPMEI have been identified in tomato, expressed in *Pichia pastoris* purified and biochemically characterised as well as characterise the natural partners of interaction.

Due to the importance of these inhibitors as posttranslational mechanism to regulate invertase and pectin methylesterase activity for the biology of the plant, this study can open new perspectives for plant biotechnology applications have been purified and characterised by affinity fishing.

2. Materials and methods

2.1. Microbiological techniques

2.1.1.*Escherichia coli* and *Pichia pastoris*

For cloning procedures the *E. coli* strain DH5α (Stratagene) was used. Genotype *sup*E44 *hsd*R17 *rec*A1 and A1 *gyr*A96 *thi*-1 *rel*A1. For the expression of recombinant proteins the strain Rosetta-gami (Novagen) was used. The strain carries an additional plasmid (pRARE, Chloramphenicol resistance), coding for six tRNAs seldom used in *E. coli*, and therefore supports the expression of eukaryotic genes. Mutations in the thioredoxin (trxB) and glutathione (gor) reductase enzymes promote the formation of disulfide bonds in the *E. coli* cytoplasm.

For the expression of recombinant proteins *P. pastoris* X33 (Invitrogene) was used. Media and plates were prepared according to the Pichia Expression Kit Manual provided by Invitrogen (Invitrogen, 2002).

2.1.2. Media and antibiotics

Bacteria were either grown in LB-medium for cloning purposes or in TB-medium for bacterial overexpression (both prepared according to Sambrook 1989 (Sambrook et al., 1989)). Selection was carried out with the following concentrations of the antibiotics: Ampicillin 100 µg/ml, Chloramphenicol 34 µg/ml, Kanamycin 50 µg/ml, Spectinomycin 100 µg/ml, Tetracyclin 12.5 µg/ml, Zeocin 50 µg/ml (low salt LB (5gNaCl/l)). SOC-medium: 20% tryptone; 0.5 % yeast extract; 0.5 % NaCl; 0.186 % KCl; 2.03 % MgCl2; 3.96 % glucose-monohydrate; pH 7.0. YPD-medium: 1%Yeast Extract; 2%Peptone; 2%Dextrose

2.1.3. Preparation of electro-compentent *E. coli*, *P pastoris* and *Agrobacterium tumefaciens* cells and transformation by electroporation

50 ml of low salt LB containing the appropriate antibiotics was inoculated with 5 ml of an over night bacterial culture and incubated until OD_{600nm} reached 1. Then the culture was cooled. and cells were collected by centrifugation. The pellet was washed fourth with 50 ml of dd-H_2O, then resuspended in 1 ml 10% glycerol, frozen in 25 µl aliquots in liquid nitrogen and stored at -80. The electro-competent cells were transformed by electroporation with a GenePulserII (BioRad) set to 200 W, 1.8 kV, 25 µF and incubated in 1 ml SOC-medium for *E* or YPD-medium for *P. pastoris,* for 1 h at 37°C before plating variable volumes on selective LB/YPD-plates. Agrobacteria were transformed as described for *E. coli*, except that after transformation the cells were incubated for 2 h at 28. in SOC-medium and allowed to grow on selective plates for 3 days at 28°C.

2.1.4. Agrobacterium-mediated transformation of *Nicotiana tabacum* leaves

Agrobacterium tumefaciens cells (strain GV3101) were grown overnight in 5 mL of LB medium supplemented with kanamycin (50 µg/mL), rifampicin (25 µg/mL) and gentamycin (50 µg/mL) until the stationary phase. Successively, a scale up culture was performed on 25 mL in LB supplemented with previous antibiotics, buffered with 100mM MES pH 5.5 and in presence of 50 µM acetosyringone, for 20 h. After centrifugation at 5000 *g* for 10 min at room temperature, the cells were suspended in volume to obtain a final OD_{600} of 1.0 with infiltration buffer (Musharige-skoog/2, 500 µM MES pH5.5 and acetosyringone 600 µM) and incubated in dark for at least 3 h. Subsequently, the cell suspensions were infiltrated into the lower epidermis of 8- to 12-week-old *N. tabacum* SR1 (Cv Petit Havana) leaves with a needleless 5-ml syringe.

2.2. Molecular biology techniques

2.2.1. Agarose gels

For separation of purified DNA, 0.8 to 1.5% agarose gels were prepared in 1xTAE-buffer with 1 µg/ml Ethidium bromide (Sambrook et al., 1989). DNA samples were prepared by adding a suitable volume of 5x loading buffer (50% glycerol, 5x TAE buffer, 1% Orange G (w/v)). As molecular weight markers, either SmartLadder (Eurogentec) or the 2-log ladder (NEB) were used.

2.2.2. PCR techniques

For most PCR applications Taq Polymerase from Invitrogen was used with the supplied buffers. A standard sample consisted of 1 µl template (various concentrations of cDNA or plasmid), 1 µl dNTPs (10mM each), 2 µl of each primer (10 pmol/µl), 5 µl 5x PCR-buffer, 1.5 µl MgCl2 (50 mM), 0.2 µl Taq (5 U/µl) and was adjusted to 50 µl with water. PCR was carried out with in a Biorad- cycler with the following program:

Initial denaturation	95°C	5 min	1 cycle
Denaturation	95°C	45 sec	35 cycles
Annealing	48 - 60 °C	45 sec	
Extension	72°C	0.5-3 min	
Final extension	72°C	5-10 min	1 cycle

The extension time and the annealing temperature were adjusted according to the length of the amplified product and the used primers respectively.

For cloning of larger PCR products, the proofreading Pwo DNA Polymerase (Invitrogen) was used according to the manufacturer's instructions.

2.2.3. Oligonucleotides

All oligonucleotides were purchased from Invitrogen (Groningen, Netherlands) The lyophilized primers were dissolved in H_2O DEPC at a concentration of 100 pmol/ µl. In the following list, the oligonucleotides are sorted according to the experiments they were used for. The primer name and the primer sequence in 5' to 3' direction are given.

pSolyPMEI 3' RACE	
GFP fw	GATTTGATAGATGAGATTTGCTCG
Nested fw	GCTCGAAAACAGATGTGAAG
poly-T rv	TTCTAGAATTCAGCGGCCGCTTTTTTTTTTTTTTTT
cloning and expression in *E. coli*	
pSolyPMEI fw	ATGGCACACTCATACAACTTCGCC
pSolyPMEI rw	TCTAGATTACAATAAATTTCTTACAATGGCTCTACCAACATC
Expression in P.pastoris (pPICZα)	
EcoRI-SolyCIF fw	GAATTCAATAATAATCTAGTAGAGACAACATGCAAG
XbaI-SolyCIF rv	TCTAGATTACAATAAATTTCTTACAATGGCTCTACCAACATC
EcoRI-pSolyPMEI fw	GAATTCGATTTGATAGATGAGATTTGCTC
XbaI-pSolyPMEI rv	TCTAGATAGAAGGTTCACGTATAGCAGCAG
N101Y fw	ACGGTTTGAGTGCTTATGCTTCTGCTGCTATAC
N101Y rv	GTATAGCAGCAGAAGCATAAGCACTCAAACCGT
N101Q fw	ACGGTTTGAGTGCTCAAGCTTCTGCTGCTATAC
N101Q rv	GTATAGCAGCAGAAGCTTGAGCACTCAAACCGT
N101S fw	ACGGTTTGAGTGCTAGTGCTTCTGCTGCTATAC
N101S rv	GTATAGCAGCAGAAGCACTAGCACTCAAACCGT
Overexpression of SolyCIF-GFP (pREV-1)	
SacI-35S fw	TTTGAGCTCAGCTTGCATGCCTCCAGGTC
SmaI-35S rv	CGATCCCGGGGATCCGCGGCCGCGAATTCTCTAGAGTCCCCCGT
SmaI-Nos fw	GCCCCGGGGGTACCAAGCTTCTGCAGGATCGTTCAAACATTTGGC
ApaI-Nos rv	TTTGGGCCCCATCTAGTAACATAG
AvrII-GFP fw	TTTCCTAGGAGTAAAGGAGAAGAACT
KpnI-GFP rv	AAAGGTACCTTATTTGTATAGTTCATCCAT
SolyCIF-BamHI fw	CGTAGGATCCATGAAAATTTTGATTTTCC
SolyCIF-KpnI-stop-AvrII rv	GCATGGTACCTTACCTAGGCAATAAATTTC
real time RT-PCR	
ACT4 RT fw	GGGATGATATGGAGAAGATA
ACT4 RT rv	AGTACAGCCTGAATAGCAAC
SolyCIF RT fw	AAGTATGCCAGAAGCAATAG
SolyCIF RT rv	GCTCTACCAACATCAGAAAG
pSolyPMEI fw	CATGTAATCTCGTTAGCACA
pSolyPMEI rv	AGAAGGTTCACGTATAGCAG

Table 2. oligonucleotides sequence in 5' to 3' direction

2.2.4. Isolation and determination concentration of total RNA

For cDNA synthesis, total RNA was isolated using the Tri Reagent (Sigma) according to the manufacturer's instructions. Concentration of RNA was determined photometrically at 260nm ("=25 µl x µg-1 x cm-1), using appropriate dilutions of the RNA sample (usually 1:200). The OD at 230nm and 280nm was used to estimate contamination with polysaccharides or proteins, respectively (Good quality RNA should have an OD260nm/OD280nm ratio of 1.8 to 2.0 and an OD260nm/OD230nm ratio greater than 1.8).

2.2.5. Real-time RT-PCR

S. lycopersicum cv Moneymaker plants were grown on soil in a green-house. Suitable amounts of various plant organs were collected after about 14 weeks of growth, frozen in liquid nitrogen, and homogenized with a mortar and pestle. Total RNA was extracted from red tomato fruits. For quantitative RT-PCR analysis, RNA was treated with Turbo-DNase I, and first strand cDNA was synthesized using ImProm-II reverse transcriptase, inline with the manufacturer's instructions. Real-time PCR analysis was performed using an iCycler (Biorad) as indicated by the manufacturer. cDNA (3 μL, corresponding to 120 ng of total RNA) was amplified in 30 μL of reaction mixture containing 1X Real Time SYBR Green JumpStart Taq ready Mix and 0.4 mM of each primer. The following primers were used: *SolyCIF* or SolyPMEI sense and antisens; *ACT4* sens and *ACT4* antisens. The expression levels of the gene of interest were determined relative to the expression of actin (*ACT4*) reference genes, using a modified version of the Pfaffl method (Pfaffl, 2001). Briefly, average cycle threshold (aC_T) was calculated for each gene from three replicates, corrected for the efficiency of PCR (E), as follows: $aC_T \times \log2(1+E)$, to obtain C_T. ΔC_T between *SolyCIF* and *ACT4* was then calculated for each sample, and the expression levels of each transcript were calculated as $2^{-\Delta CT}$ and expressed in arbitrary units. Amplification efficiency of *SolyCIF/SolyPMEI* and *ACT4* with the primers specified above was determined using serial dilutions of cDNA samples and was found to be comparable; E was 0.97 to 0.98, with a highly linear pattern of amplification (Pearson correlation coefficient $r > 0.95$).

2.2.6. 3'-RACE technique

For the determination of the full length sequence of partially known SolyPMEI cDNAs, polyT primer was used. Total RNA was isolated using the Tri Reagent (Sigma).

The amplification of the full length sequence of partially known cDNAs, for the determination of the 3'-end of the SolyPMEI was performed using a sense gene-specific primer (GSP) and polyT reverse primer. In order to increase the specificity of the reaction, a nested PCR was carried out using the first PCR as template. The PCR products were subcloned, and several clones from independent PCR reactions were sequenced.

2.2.7. Isolation of plant genomic DNA

To 100 mg of grinded tomato leaves material, 550 μl of extraction buffer (200mM Tris-HCl, 400mM LiCl, 25mM EDTA, 1%SDS, pH 9) and 550 μl of PCI (phenol:chloroform:isoamyl alcohol 25:24:1 (v:v:v)) were added and vortexed for 20 sec. After centrifugation (5 min, 15,000 g, 4 .), the

supernatant was again vortexed with 550 µl of PCI and centrifuged. DNA was precipitated by adding one volume of isopropanol to the supernatant and, after 15 min incubation at RT, collected by centrifugation (10 min, 15,000 g, 4). After removing the supernatant, the pellet
was air dried and resuspended in 500 µl TNE (10mM Tris-HCl, 100mM NaCl, 1mM EDTA, pH 8) plus 20 µg RNaseA (from a 10 mg/ml stock) and incubated for 10 min at 37 . to allow RNA digestion. RNase was removed by shaking out with 550 µl PCI and centrifuging as before. The supernatant (approx. 475 µl) was precipitated with 750 µl isopropanol and centrifuged (10 min, 15,000 g, 4.). The pellet was washed once with 70% ethanol and, after drying, resuspended in 50 µl TE-buffer (10mM Tris, 1mM EDTA, pH 8).

2.3. Cloning procedures

2.3.1. Gel extraction and PCR purification

For the purification of DNA fragments from agarose gels or the clean-up of PCR products the NucleoSpin Extract II Kit (Macherey-Nagel) was used according to the manufacturers instructions.

2.3.2. Cloning using restriction digestion

All restriction enzymes were purchased from New England Biolabs (NEB) and used with the supplied buffers. For analytical digestions 1 µg and for preparative digestion 5 to 20 µg of plasmid DNA were used. Incubation was performed for 2 to 16 h at recommend temperature. Usually 3U of enzyme were added per µg of DNA. Ligation of digested DNA fragments was carried out using T4-DNA Ligase (Promega) according to the manufacturer's instructions.
For subcloning of PCR fragments, the TOPO TA Cloning Kit (Invitrogen) was used according to the manufacturer's instructions.

2.3.3. Cloning and expression of SolyPMEI

cDNA from red tomato fruit was amplified, using SolyPMEI fw and rw primers. After purification the amplicon was ligated in the expression vector pET 101**.** The *Escherichia coli* strain Rosetta-gami1 (DE3) (Novagen, Madison, WI, USA) was used as host for protein expression. Overnight cultures (37°C) were raised from single colonies. After 1:500 dilutions with Luria-Bertani medium, bacteria were grown to a density of 0.6, induced by adding IPTG to 0.2mM, and further grown for 24 h at 17°C. Thereafter, cells were pelleted for 15 min at 10 000 g and extracted with lysis buffer (1/20 volume of initial culture volume: 50 mM Na_2HPO_4/NaH_2PO_4, pH 7.0, 500 mM NaCl, 1% Triton X-100, 1 mg/ml lysozyme).

2.3.4. Cloning and expression of SolyPMEI and SolyCIF in *Pichia pastoris*

cDNA from red tomato fruit was amplified by performing RT-PCR, using the following primers: EcoRI-SolyCIF fv and XbaI-SolyCIF rw and EcoRI-SolyPMEI fv and XbaI-SolyPMEI rw ,for 30 PCR cycles at an annealing temperature of 42°C. PCR product was cloned in TOPO-TA and sequenced by Genome Express (Meylan, France). The pPICZαA-derived *P. pastoris* expression plasmid with the cDNA insert encoding SolyCIF was constructed using standard procedures (Sambrook et al., 1989). The insert was purified using the Qiaquick® (Qiagen) purification kit and ligated into the XbaI/EcoRI pPICZαA plasmid, which was digested with BglII to linearize the DNA for integration into *P. pastoris* genome. The linearized DNA was used for electroporation into *P. pastoris* strain X-33 using a Multiporator® (Eppendorf) at 1500 V for 5 ms. Transformants were selected on YPD plates containing 100 µg/mL zeocin®.

2.3.5. Site-directed mutagenesis of SolyPMEI

Mutations were introduced into the pPICZα SolyPMEI plasmid using the QuickChange XL site-directed mutagenesis kit (Stratagene Europe, Amsterdam Zuidoost, The Netherlands). Two overlapping complementary oligonucleotides containing the corresponding nucleotide changes were designed for each mutation (Table 2). Each primer (125 ng) was annealed to pPICZα SolyPMEI (50 ng) and both strands of the plasmid were amplified using 1 U Pfu polymerase in a linear extension reaction carried out by PCR under the following conditions: 30 s denaturation at 95°C, and 16 cycles of 30 s denaturation at 95°C, 1 min annealing at 55°C, and 07 min extension at 68 °C. PCR cycling was performed in a Mastercycler gradient 5331 system (Eppendorf). Reaction mixtures were cooled on ice for 2 min and treated with DpnI restriction enzyme for 1 h at 37° C, to hydrolyze the methylated parental plasmid strands. DpnI-treated DNA (1 ll) was used to transform XL1-Bleu Supercompetent cells (Stratagene). Transformants were selected on LB medium plates containing 50 µg /ml zeocin and the mutations were confirmed by DNA sequencing by Genome Express (Grenoble, France).

2.4. Biochemical techniques

2.4.1. SDS-PAGE

SDS-Polyacrylamide gel electrophoresis (SDS-PAGE) was done according to Sambrook et al. (1989), using resolving gels containing 12 to 15% polyacrylamide and stacking gels with 5 %. Gels were either directly stained with Coomassie Brilliant Blue or silver staining or used for Western blotting. Samples for SDS-PAGE were denatured by addition of a 4x concentrated SDS-

sample buffer containing a reducing agent (DTT) and boiling for 5 min at 95°C. For the conservation of disulfide bridges, the non-reducing buffer was used.

2.4.2. Coomassie staining

Gels were stained in 0.25% Coomassie Brilliant Blue G250, 45% methanol, 10% acetic acid, destained with 45% ethanol, 10% acetic acid.

2.4.3. Silver staining

For silver staining, protein gels were fixed in 50% methanol, 10% acetic acid, 0.05% formaldehyde (37%) for at least 1 h, washed twice for 25 min in 50% methanol. The gel was sensitized for 1 to 2 min in 0.02% sodium thiosulfate ($Na_2S_2O_3x5H_2O$), followed by rinsing the gel in water twice. The gel was stained for 20 min in staining solution (0.2% AgNO3, 0.075% formaldehyde (37 %)), rinsed three times in water and developed until bands were visible with developing solution (6% Na Na_2C_3, 0.0004% $Na_2S_2O_3x5H_2O$, 0.05% formaldehyde). Development was stopped by incubating the gel in 12% acetic acid.

2.4.4. Periodic acid-Schiff staining

SDS-PAGE was stained for carbohydrate with periodic acid-Schiff (PAS) stain using a SIGMA glycoprotein staining kitR according to the manufacturer's protocol.

2.4.5. Western Blot

After SDS-PAGE, the resolving gel was incubated in transfer buffer (48mM Tris-base, 39mM glycine, 20% methanol (v/v), 0.0375 % SDS) for 10 min. The protein transfer was performed on a nitrocellulose filter (Hybond ECL C-EXTRA Amersham) in Trans Buffer) on a constant voltage (100V) for 1 hour at 4°C. After transfer, the filter was saturated in 100mL of Blocking Buffer (PBS, 0.2% Tween 20, 3% BSA) at room temperature, on an orbital shaker, for 2 hours. The nitrocellulose was washed in Washing Buffer (PBS, 0.2% Tween 20) and incubated at room temperature for 2 hours with specific polyclonal antibodies from rabbit in Washing Buffer with 0.5% BSA. The antibody anti SolyPMEI was used in 1:5000 dilution. Removed from the incubation buffer, the filter was washed and incubated at room temperature in agitation for 2 hours with the secondary antibody (anti rabbit Ig horseradish peroxidase linked whole antibody, (Amersham) diluted 1:5000 in Washing Buffer with 0.5% BSA). The Amersham kit "Western blotting analysis system" was used for development.

2.4.6. Molecular mass determination and N-terminal sequencing

Automated repetitive Edman degradation was performed on a model 494 Procise^{TM} Protein Sequencer (Applied Biosystems Division). N-terminal amino acid sequencing of the invertase band (pattern) from SDS-PAGE was performed after performing electro-transfer onto a polyvinylidene difluoride membrane as described previously (Matsudaira, 1987). Native anionic gels were prepared in 10% (w/v) polyacrylamide gel in the absence of DTT and SDS, and run in the presence of two different buffers. Top buffer was composed of Tris-Gly buffer 5mM at pH 8.9 and bottom buffer of Tris-HCl 10mM at pH 8.1.

2.4.7. Circular dichroism

CD spectroscopy was performed at 20 °C on a J-710 spectropolarimeter (Jasco, Tokyo, Japan) equipped with the Neslab RTE-110 temperature controlled liquid system (Neslab Instruments, Portsmouth, NH, USA) and calibrated with a standard solution of (1)-10-camphosulfonic acid. Photomultiplier high voltage did not exceed 600 V in the spectral region measured. Each spectrum was averaged five times and smoothed with Spectropolarimeter System Software version 1.00 (Jasco). All measurements were performed under nitrogen flow. The percentages of secondary structures were estimated according to the Yang's method (Yang, 1986).

2.4.8. Protein alkylation

The purified protein was alkylated with iodoacetamide under denaturing conditions, with and without previous reduction. The protein (50 mg) was dissolved in 250 mL of 0.1 m Tris/HClpH 8.0, 10 mm EDTA, 8 m guanidine hydrochloride. Dithiothreitol was added at a final concentration of 0.05 m and incubation was carried out at 37 8C for 30 min under nitrogen (this step was omitted in the sample alkylated without previous reduction). Iodoacetamide was added at a final concentration of 0.12 mM and the reaction proceeded at room temperature for 15 min. The reaction was stopped by addition of 0.2 m β-mercaptoethanol, and the sample was desalted by gel filtration on a pre-packed PD-10 column (Pharmacia, Uppsala, Sweden). For amino-acid analysis, vapor phase hydrolysis was carried out with 6 m HCl containing 1% 2-mercaptoethanol and 1% phenol at 150 8C for 1 h. The analyses were performed as reported (Verde et al., 1989).

2.4.9. Mass spectrometry

For this analysis, 3 mg of total proteins isolated red tomato fruit was run on a Superdex75 preparative column (HR26/ 60) in the same buffer as above at a flow rate of 2 mL min21, and fractions of 3 mL were collected and analyzed by immunoblot to select the fraction containing the

inhibitor. The selected fractions were analyzed by SDS-PAGE and stained with Coomassie Brilliant Blue. After staining the protein bands were excised from the gel, reduced, alkylated, and digested with trypsin according to Hellman et al. (1995). Tryptic peptides were analyzed by LCMS/ MS (LC-ESI-quadrupole iontrap MS 1100 Series; Agilent Technologies) equipped with a column Zorbax SB-C18 5-mm 150 3 0.5 mm. Protein identification was performed by searching the Mass Spectrometry Protein Sequence DataBase (Imperial College London) using the Mascot search engine, which uses a probability-based scoring system. The following parameters were used for database searches: peptide and MS/MS mass tolerance of 1.5 D; peptide charge of 11, 12, or 13; trypsin as digesting enzyme with one missed cleavage allowed; and carbamidomethylation of Cys as a fixed modification.

2.5. Protein purification

2.5.1. Purification of recombinant from *Pichia pastoris*

For the purification of the recombinant SolyCIF/SolyPMEI/N101Y proteins, the Pichia pastoris strain X-33 carrying the pPICZα vector was used. A single colony was used to inoculate 100 ml BMGY-medium with 100 µg/ml Zeocin and was grown overnight at 30°C. To induce expression from the alcohol oxidase promoter, the culture was centrifuged (5 min, 1300 g), resuspended in 1.5 l BMMY medium in a 5 l Erlenmeyer flask and grown overnight at 30°C under vigorous shaking.

To harvest the SolyCIF/SolyPMEI/N101Y proteins secreted into the medium, the culture was centrifuged (30 min, 4,000 g, 4°C.) and the medium precipitated by adding 430 g of ammonium sulfate per liter medium (70% saturation) under constant stirring at 4°C. The precipitated protein was collected by centrifugation (30 min, 9,800 g, 4.), resuspended in 50 ml of Na acetate buffer (20mM Na acetate, pH 4.5) and residual ammonium sulfate was removed by dialysis against 10 l of Na acetate buffer. The dialised proteins were that applied to a MonoS column, and eluted with a linear gradient ranging from 0 to 0.5 M NaCl in the equilibration buffer, using an FPLC system (Pharmacia). The fractions containing activity were pooled, concentrated to 2 mL using a Centriplus YM-3 centrifugal device (with a 3000 Da cut-off) and subjected to gel filtration on a Hiload 16/10 Superdex 75 column (Pharmacia) by eluting them in 20 mM Na-acetate buffer at pH 4.6 containing 250 mM NaCl.

2.5.2. Affinity purification of SolyN101YPMEI antibodies

Due to the presence of multiple immuno-signals in Western blots with plant extracts from tomato fruits the SolyN101Y PMEI-antiserum was affinity purified against recombinant N101Y protein 2 mg of the recombinant protein dialyzed in coupling buffer (0.1M $NaHCO_3$, 0.5M NaCl pH 8.3), was incubated with 0.5 g of CNBr-activated Sepharose 4B (pre-swollen in 100 ml 1mM HCl and equilibrated in coupling buffer) for 1 h at ambient temperature. The matrix was poured into a

column (Econo-Pac, Bio-Rad) and the buffer was allowed to drain by gravity flow. The column was first washed with 50 ml of coupling buffer and residual amine binding sites were blocked by incubation in 10 ml 100mM Tris-HCl, pH 8 for 2 h at ambient temperature. For washing, the column was incubated with 10 ml 100mM sodium acetate, 500mM NaCl, pH 4.5 and 10 ml 100mM Tris-HCl, 500mM NaCl, pH 8 and this procedure was repeated three times. Finally the affinity matrix was incubated in 1xPBS (20mM Tris, 150mM NaCl, pH 7.4).

The following steps were carried out at 4°C. For binding of the antibodies, 500 µl of 10xPBS (200mM Tris, 1.5M NaCl, pH 7.4) were added to 5 ml of the final bleed and incubated with the CNBr-coupled SolyN101Y PMEI protein overnight. Then the unbound antibodies were washed-out from the column. After washing with 50 ml of 1xPBS, bound antibodies were eluted with 0.2M glycine, 1mM EGTA, pH 2.0, first as 500 µl. The eluted antibodies were immediately neutralized by addition of 1/10 volume of 1M Tris, pH 8.5 containing 0.02% NaN_3. The protein content of the fractions was tested and the fractions with the highest protein content were combined. The purified serum was tested using different dilutions. A dilution of 1:5000 to 1:1000 was found suitable for Western blotting.

2.5.3. CNBr-SolyN101YPMEI affinity-chromatography

PME-1 from tomato fruit purified to homogeneity (gently provided by Dr Laura Camardella, CNR Naples) was loaded onto the SolyN101YPMEI column equilibrated with 20 mM Na acetate pH 4.5.Flow-through was collected and the column was washed with 60 ml acetate buffer. The PME-1 was eluted from the column by elution buffer 20mM Tris-HCl pH8.3, 2M NaCl.

2.5.4. Partial purification and immuno affinity column of SolyPMEI

All these steps were performed at 4°C. One kg of pericarp tissues from ripe tomato was homogenized in 1L of cold Na acetate 2M NaCl at pH 4.5 with a household blender and stirred for 2h and centrifuged. Proteins supernatant were precipitated with ammonium sulphate at final concentration of 80%. Proteins were centrifuged at 12000g for 30 min, pellet resuspended and dialysed against PBS. A partial separation of protein was performed on DEAE column.

Tomato PME/SolyPMEI complex was purified by affinity chromatography using a SolyN101YPMEI antibody covalently immobilized on CN-Br-Sepharose resin (Sigma) as described above. The tomato protein extract was added to the resin and gently mixed for 12h at 4°C. After that, matrix was pelleted by gravity and the flow-through was collected. The column was washed with PBS buffer at a flow rate of 1 mL/min. For the first column, the complex enzyme/inhibitor was dissociated from antibodies by elution with buffer A (0.1 M Glycine pH 2.0). Fractions were collected into 100 µL 1 M K buffer pH 8.3. The enzyme then was dissociated from SolyPMEIrp by

elution with buffer B (20 mM Tris-HCl pH 8.3 containing 2 M NaCl) and fractions were collected into 5 µL 2 M NaAc buffer pH 4.5. The column was washed with PBS. SolyPMEIrp was dissociated from antibodies with buffer A and fractions were collected into 100 µL 1 M K buffer pH 8.3.

2.5.5. Purification of invertase from tomato (TIV-1)

SolyCIF-sepharose affinity column was prepared by covalently coupling purified recombinant SolyCIF on an NHS-activated Sepharose^{TM} 4 Fast Flow column according with the manufacturer's instructions. Green and red tomato fruits were homogenized separately in 10 mM Na-acetate buffer at pH 4.6 (buffer A) containing 1M NaCl, stirred at 4°C for 2h and centrifuged at 20,000 g for 30 min. Proteins in the supernatant were precipitated with ammonium sulfate up to 80% saturation. The precipitated proteins containing most of the invertase activity were suspended in buffer A, loaded onto a SolyCIF affinity column and, after extensive washing with buffer A containing 0.1M NaCl, eluted with 50 mM potassium phosphate buffer pH 7.5. The resulting fractions were collected. For subsequent purification of invertase to homogeneity, fractions showing invertase activity were pooled, loaded onto to a Hiload 16/60 Superdex 75 column (Pharmacia) and eluted with 20 mM Na acetate at pH 4.6 containing 150 mM NaCl at a flow rate of 0.5.mL min^{-1} and 2-mL fractions of were collected.

2.6. Protein assay

2.6.1. Protein concentrations

Protein concentrations were determined by performing amino acid analysis. The inhibitor and invertase samples containing 1 nmole of Nor-leucine as the internal standard were dried in a SpeedVac Savant apparatus in pyrolyzed glass tubes and hydrolyzed under a vacuum in a vial containing 6 M HCl, 1% phenol and 0.5% 2-mercaptoethanol , for 20 h at 110°C . Samples were analyzed using a Thermo-Finnigan Surveyor LC System equipped with a ChromQuest data System (Thermo Scientific) and a Prometeus 300 Plus System post column ninhydrine derivatization (Rigas Labs).

2.6.2. Invertase activity determination and inhibition assay

Invertase activity was monitored during the purification procedure using the dinitrosalicylicacid (DNS) assay (Brutus et al., 2004). An aliquot of the enzyme extract or pure enzyme (20 µL) was mixed with 50 µL of sucrose (0.5M) in 50mM phosphate buffer at pH 4.6 (total reaction volume: 200 µL) at 46°C for 15 min. The reaction was ended by adding 300-µL DNS

reagent and boiled for 5 min. The reaction products were cooled and centrifuged for 5 min at 12 000g, and 200 µL were transferred onto a microtitre plate. One unit of invertase activity was defined as the amount of protein releasing 1 µmol of reducing sugar.min^{-1}. To calculate the catalytic constants, the invertase activity was assayed by measuring the amount of glucose produced by hydrolysing sucrose for 30 min at 37°C using the glucose oxidase-peroxidase method (Scognamiglio et al., 2003). An invertase sample was then added to 50 µL of 0.2 M sodium acetate buffer at pH 4.9; a final volume of 100 µL was obtained by adding water. The reaction was started by adding 50 µL of sucrose stock solutions giving final concentrations ranging from 2 to 150 mM sucrose in 150 µL reaction volume. After a 30-min incubation at 37°C, 15 µL of the incubation mixture were added to 50 µL of 0.5 M potassium phosphate buffer at pH 7.0, to stop the reaction. The amount of glucose produced was measured by adding 1 mL of the glucose oxidase-peroxidase reagent system Glu-cinet. The reaction was also carried out in control assays on a standard mixture containing 55 nmoles of glucose in 65 µL of the potassium phosphate buffer. Absorbance was measured at 510 nm against a blank (65 µL of the same buffer and 1 mL of the reagent system). Km and Vmax of invertase were determined from the curves giving the invertase activity on sucrose (2-150 mM), using two enzyme concentrations differing by a factor of two (10 µl and 5 µl of 0.1 µM invertase).

Inhibition was assayed in the presence of 100 mM sucrose after pre-incubating fixed amounts of invertase (10 µl of 0.1 µM enzyme, final concentration 6.7 nM) for 15 min at pH 4.9 at a temperature of 37°C with mixtures containing 1mM, 1.7 mM, 2.3 mM, 3 mM, 4 mM, 5 mM, and 6.7 mM inhibitor.

2.6.3. PME activity determination and inhibition assay

PME activity was quantified by the radial gel diffusion assay as described by Downie (Downie et al., 1998) with some modifications. 1% (w/v) agarose was added to 0.1% (w/v) pectin from citrus fruit (81% esterified) (Sigma), and were dissolved in 12.5 mM citric acid 50 mM Na_2HPO_4 buffer pH 6.3. They were heated until the agarose had dissolved. 25 mL of the solution was immediately transferred into Petri dishes and allowed to polymerize at room temperature. Wells were punched in the gel with a 4 mm diameter cork borer and the gel plug removed by aspiration. 20 µL of sample was pipetted into each well which was been labelled. Wells were reserving for controls as standard dilution. The whole incubated at 30°C over night in closed containers lined. After incubation, the gels were stained with 0.02% (w/v) Ruthenium Red dye (Sigma) for 45 min. The dye was then poured off, the gels were rinsed with water and the diameters of the stained zones, resulting from the hydrolysis of esterified pectin in the gel, were measured and compared.

2.7. Bioinformatic analysis

2.7.1. Sequence alignments and phylogenetic tree

Nucleotide and amino acid sequences were identified on NCBI (http://www.ncbi.nlm.nih.gov/entrez/query.fcgi) and on Solanaceae Cornell University data bank (www.sgn.cornell.edu). (NB: Amino acidic sequence, corresponding to *SGN-U317539*, published on Cornell university web site present a different sequence that published here. These differences are due to nucleotidic insertion and deletions during the sequence treatment by ESTScan software). Thus our analysis confirm the presence of these bases, demonstrating the Cornell mistakes. The signal peptide, putative cleavage site and putative glycosylation sites were predicted using SignalP 3.0 server, NetNGlyc 1.0 Server (http://www.cbs.dtu.dk/services/NetNGlyc/) and DictyOGlyc server, respectively (http://www.cbs.dtu.dk/index/shtml/). All alignment was performed with Bioedit (Hall, 1999). Dendogram was inferred using the Neighbor-Joining method (Saitou and Nei, 1987). The optimal tree with the sum of branch length = 403.2 is shown (Fig1.). All positions containing gaps and missing data were eliminated from the dataset (Complete deletion option). There were a total of 115 positions in the final dataset.

2.7.2. Modeling analysis

Comparative modeling was performed on a Silicon Graphics O2 workstation, using Homology (Greer, 1990) and MODELER (Sali and Blundell, 1993) software programs in the InsightII molecular modeling system from Accelrys Inc. The structural model for vacuolar invertase from tomato (P29000) was drawn up using the *Arabidopsis thaliana* cell-wall enzyme (PDB code 2AC1) as a structural template. The structural model for pSsolyPMEI from tomato was drawn up using the AcPMEI enzyme (PDB code P83426) as a structural template. Sequence alignment of the proteins, was minimized using MODELER. The protocol included careful refinement of the loop regions. A set of 6 models was generated. Analysis of the structural violations of the probability density function (PDF) was performed on each model structure. The ϕ and φ angles of the residues were assessed from the Ramachandran plot obtained using the Swiss-PdbViewer program.

2.7.3. GFP imaging

The GFP-dependent fluorescence was monitored by 48h after infection in cells of the lower epidermis. Pieces of leaf were randomly cut from the infected area and mounted in water for microscopic observations. Materials were analysed using a Leica DM IRE epifluorescence microscope equipped with a digital cooled camera (DFC350FX R2; Leica, http://www.leica.com). GFP fluorescence was excited with a 488-nm laser line, and emitted fluorescence was collected at 543nm. The Leica Confocal Software and Adobe Photoshop 5.0 were used for postacquisition image processing.

3. Results and Discussion

3.1. Identification of putative SolyINH/PMEI members in *Solanum lycopersicum*

The NCBI/BLAST databank (http://www.ncbi.nlm.nih.gov/blast/Blast.cgiand) and the Solanaceae Cornell University (http://www.sgn.cornell.edu/) database search for Solanaceae genes encoding invertase or pectin methylesterase inhibitors identified a number of sequences with level of amino acid identity above 70% with NtCIF and NtVIF and 30% with respect to AcPMEI and AtPMEIs. The dendrogram generated with these sequences including all the functionally characterized INH and PMEI identified two independent main groups (Fig.24).

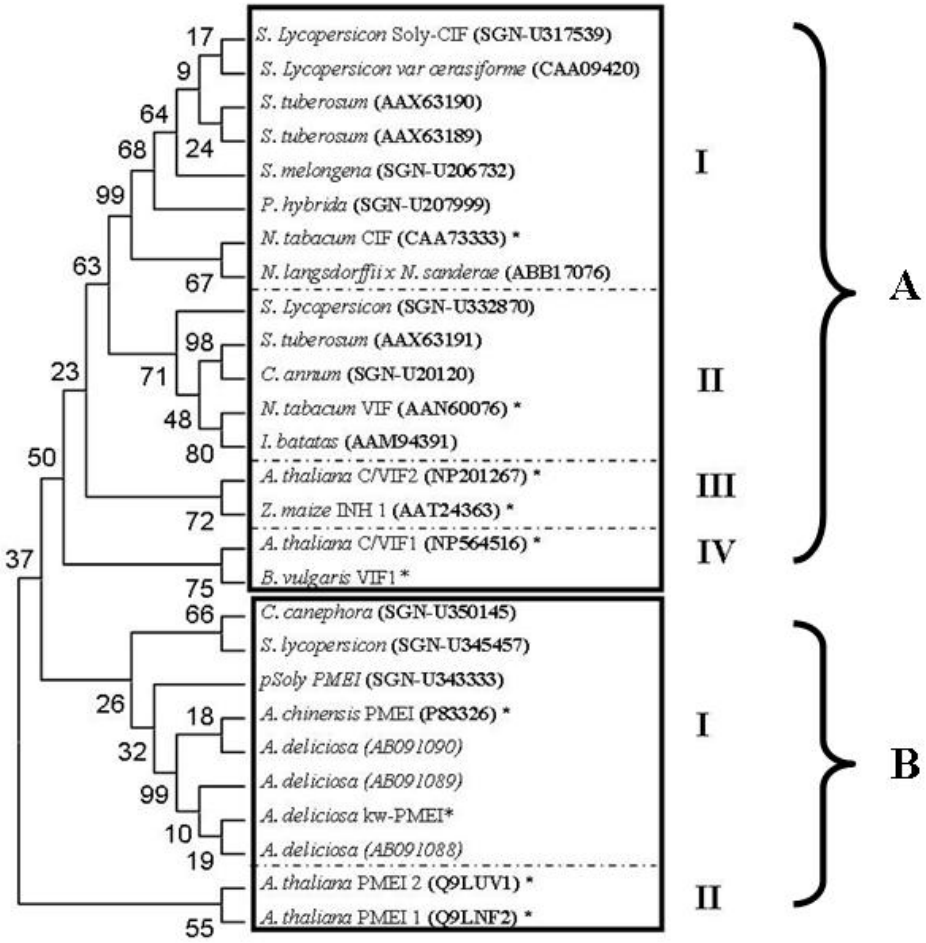

Figure 24. Dendrogram of 28 protein sequences belonging to the PMEI-INH family. Dendrogram as generated using the MEGA 4.0 program (Tamura et al., 2007) (See *Materials & Methods* section). The percentages of the replicate trees in which the associated taxa were clustered together in the bootstrap test (1000 replicates) are shown next to the branches (Felsenstein, 1985). Sequences of *Beta vulgaris* VIF and kw-PMEI were borrowed from Eufinger 2006 and Mei *et al*. 2007 (Eufinger, 2006; Mei et al., 2007). The two groups as well as the subgroups are indicated.

The group A including the invertase inhibitors consists of four independent subgroups. Subgroups I and II, to which the Solanaceae sequences belong, include NtCIF and NtVIF, respectively, which indicates that the primary protein sequences of the various members are sufficiently well conserved to be able to predict whether they have a vacuolar or cell wall localization.

Due to their different taxonomic origins, functional invertase inhibitors from *A. thaliana*, *B. vulgaris* and *Z. mays* cluster into two distinct additional subgroups III and IV.

The group B including the pectin methylesterase inhibitors consists of two independent subgroups. Subgroup I, to which belongs the Solanaceae sequences and PMEI from kiwi and the subgroups II to which belong the functional characterised Arabidopsis PMEIs.

Based on this dendrogram the sequence (SGN-U317539), belonging to group A, subgroup I of apoplastic invertase inhibitor, here after called *SolyCIF*, and the second sequence (SGN-U343333) belonging to group B, subgroup I of pectin methylesterase inhibitor, hereafter called *SolyPMEI*, were selected for the functional characterization.

3.2. Pectin Methylesterase Inhibitor from tomato *Solanum lycopercicum* (SolyPMEI)

3.2.1. Identification, complete gene sequencing and expression of the SolyPMEI

The SGN-U343333 EST fragment (Clone ID: E274293) identified from Cornell University data bank (*www.sgn.cornell.edu*) was incomplete. The complete sequence of the putative *PMEI* gene (*SolyPMEI*) has been identified and amplified from cDNA of tomato red fruits, by using the 3'- RACE approach. The nucleotidic sequence of *SolyPMEI* was in agreement with the SGN-U343333 partial sequence, except for a difference in position 454 responsible for the modification of Arg127 residue in Lys.

SolyPMEI shows 38% and 30% amino acid identity with AcPMEI and AtPMEIs respectively (Fig. 25). Removal of the predicted N-terminal signal peptide generates a mature protein of 124 amino acids with a molecular mass of 18335 Da and predicted alkaline p*I* = 8.0 (typical of proteins bound to the cell wall). Two potential N-glycosylation sites at position 69 and 101 were found to be present in the protein sequence. In comparison with functional PMEIs the four conserved Cys residues known to be engaged in disulfide bridges, in functional PMEI characterised so far, are present in SolyPMEI, while a fifth Cys conserved in functional PMEI is substituted by a Ile residue in SolyPMEI, was in a different position respectively at others inhibitors (Fig. 25).

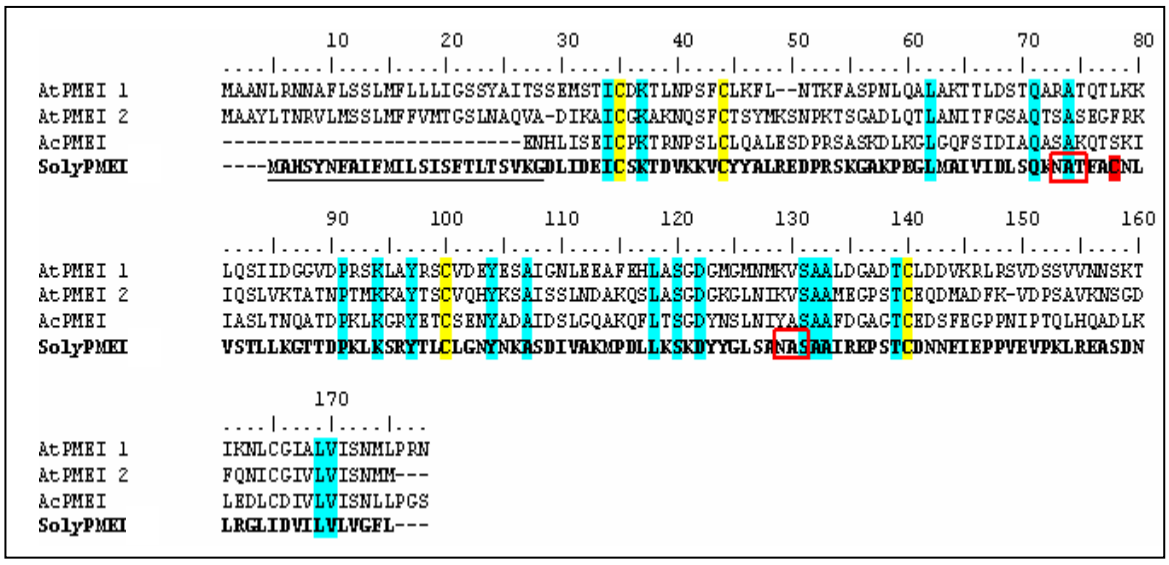

Figure 25. Multiple alignment of SolyPMEI and known PMEIs. The SolyPMEI represented in bold was aligned with *Arabidopsis thaliana* PMEIs (AtPMEI-1: At1g48020 and AtPMEI-2: At3g17220) and kiwi fruit PMEI (AcPMEI: P83326) Conserved Cysteine residues are indicated in yellow. The free Cysteine residue is in red. Other conserved residues are blue. Two N-glycosylation sites are surrounded in red. Peptide signal of SolyPMEIrp was underlined in black. Alignment was performed by Bioedit (Hall, 1999).

Structural modelling using as a template the solved 3D structure of kiwi PMEI, indicates that the SolyPMEI, as well as the characterised members of PMEI, folds in a up-and-down four helical bundle (Fig 26/B). Structural superimposition of AcPMEI and SolyPMEI also reveals the similarity of the overall folding topologies (Fig. 26/B)

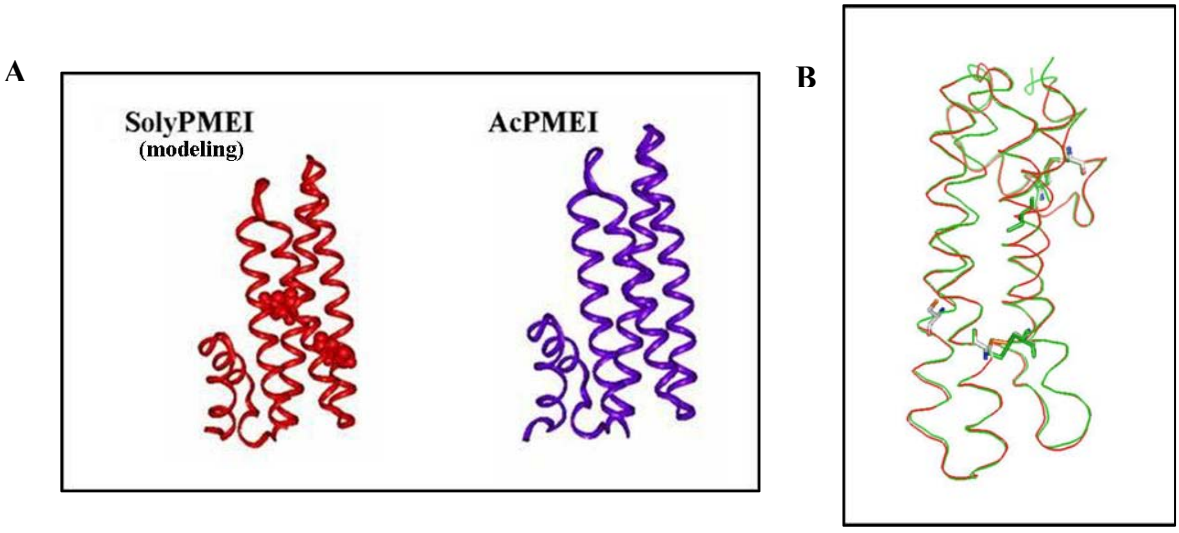

Figure 26. SolyPMEI structural modeling .(**A**) in red SolyPMEI model using as a template kiwi PMEI structure, putative glycosylation sites are shown, in violet 3D representation of AcPMEI. (**B**) Structural superimposition of AcPMEI (in green) and SolyPMEI (in red); disulfide bridge and free Cys residue are shown.

To analyse the expression of *SolyPMEI* mRNAs in different tissues, transcripts were quantitatively estimated by real-time PCR, using *Actin 4* for normalization. The results revealed a higher *SolyPMEI* transcript level in tomato red fruits, on the contrary, no transcripts were observed in green tomato indicating a role of this protein at late stage of ripening. Moreover a reduced mRNA expression was observed in flowers and pollen (Fig. 27).

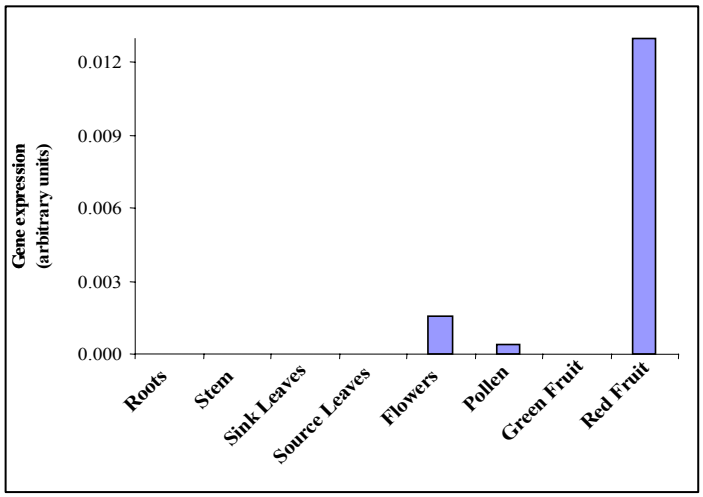

Figure 27. Real-time PCR of SolyPMEI mRNA. Quantitative expression analysis of SolyPMEI transcript in different plant organs by real time PCR.

The occurrence of *SolyPMEI* transcripts in flower and pollen tissues, typical of PMEIs so far characterised (Wolf et al., 2003; Raiola et al., 2004), suggests a developmental role of this inhibitor during flower formation and reproductive process. The distribution of PME activity was also analyzed in different tissues (Fig.28). In particular it has been observed that maximal activity was present in red fruits (Fig).

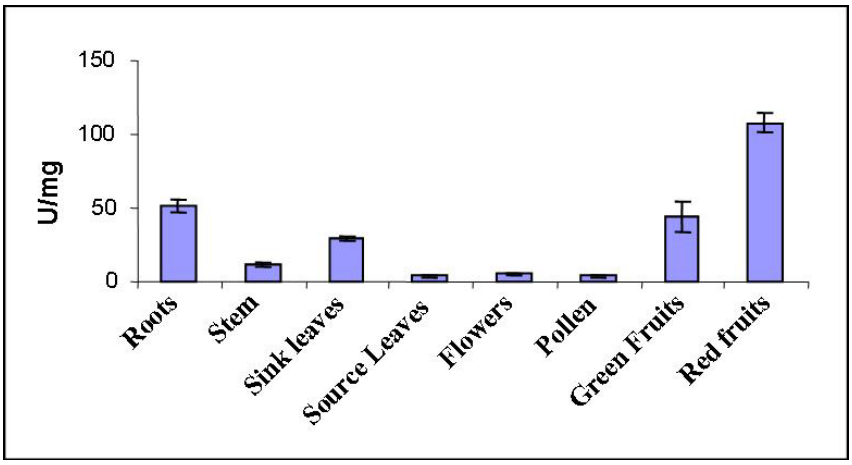

Figure 28. PME specific activity in different tomato tissues

It is noteworthy that higher expression of PMEI correlates with higher level of PME in red fruits indicating that expression of the inhibitor is induced to modulate the enzymatic activity during late phase of ripening.

3.2.2. Heterologous expression of recombinant SolyPMEI, purification and biochemical characterization

To characterise SolyPMEI, the region encoding the predicted mature protein was amplified by PCR using cDNA from tomato red fruit as a template. Firstly, *Escherichia coli* strain Rosetta-gami (DE3) was used as heterologous system for protein expression as described by Wolf (Wolf et al., 2003). Due to the presence of predicted disulfide bridge in the protein, the *E. coli* strain Rosetta-gami1 was chosen. Its deficiencies in thioredoxin reductase and glutathione reductase activities provide an oxidizing environment to facilitate disufide bridges formation.

However after induction with isopropylthiogalactoside (IPTG) the transformed bacteria stop to growth (Fig. 29), indicating that the protein was toxic and that this heterologous

system, as observed for other plant proteins (Johansson et al., 2002), was considered not useful to express SolyPMEI

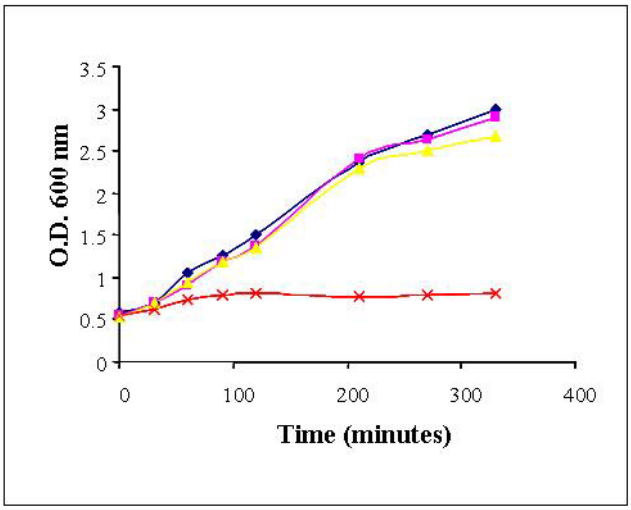

Figure 29. *E. coli* growth rate. The transformed bacteria stop to growth respect to the controls. (+) induced with IPTG; (-) not induced. —◆— : *E. coli* wild type (-); —■— *E. coli* transformed (-); —▲— *E. coli* wild type (+); —×— *E. coli* transformed (+).

Alternatively, the coding region of SolyPMEI gene was cloned and expressed in *Pichia pastoris*. The recombinant protein was expressed and efficiently secreted in the culture medium (10 mg/l). The protein was purified to homogeneity by using cation exchange chromatography as described in material and methods. In figure 30/A-B chromatogram and SDS-PAGE analysis of the eluted fractions is shown.

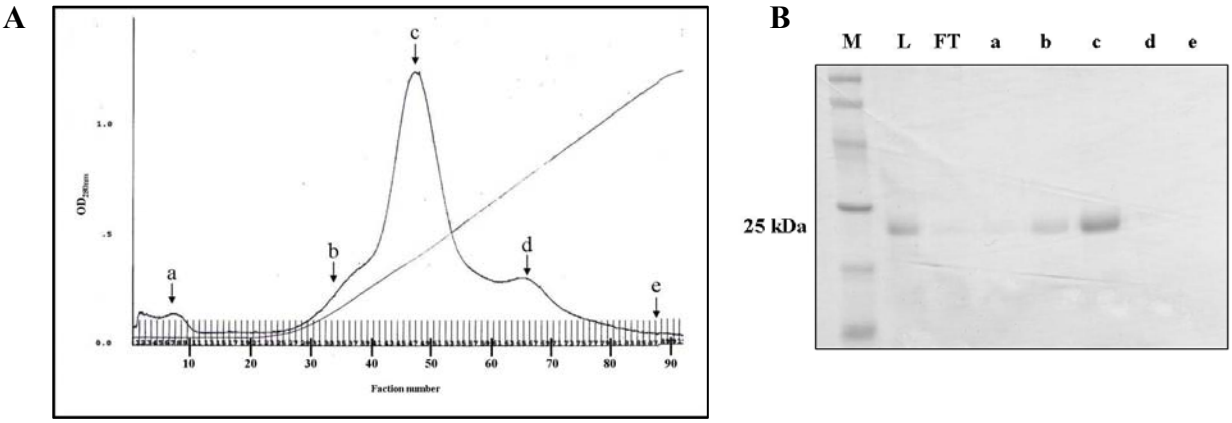

Figure 30. SolyPMEI purification: (**A**) cation exchange chromatography of recombinant protein on CM Sepharose. The fraction eluted with a gradient of 0 to 1M NaCl were loaded on SDS-PAGE.(**B**) SDS-PAGE of purified recombinant protein: (**M**) molecular mass; (**L**) loaded sample; (**FT**) flow through; (**a-b-c-d-e**) correspond to 7, 34, 46, 66, 87 eluted fractions indicated with arrows in the chromatogram. The gel was stained with Coomassie blue.

To confirm the protein identity, N-terminal sequencing was carried out. SolyPMEI had the N-terminal sequence EAEAEFDLDE, in agreement with the sequence expected, were the amino acid residues EAEA, EF and DLIDE corresponded to the peptide signal C-terminal sequence after peptidase digestion, the cloning vector restriction site and the NH_2-terminal sequence of the expressed SolyPMEI, respectively.

In order to determine whether SolyPMEI is a functional invertase/ pectin methylesterase inhibitor, we tested its ability to inhibit invertase or PME activity in crude protein extracts from red tomato fruits, Arabidopsis and tobacco leaves. SolyPMEI did not show PME (Fig.31) or invertase inhibitory activity (not shown).

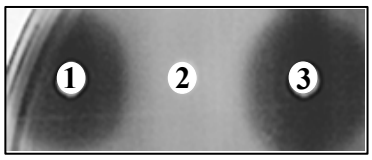

Figure 31. Agar diffusion assay : (**1**) tomato PME-1; (**2**) PME-1 + AtPMEI-1; (**3**) PME-1 + SolyPMEI

To exclude that the absence of inhibitory activity was due to structural alteration of the protein expressed in heterologous system, firstly the ability to correctly form disulfide bridges, was analysed. SDS-PAGE was performed in reducing and not reducing conditions. Figure 32 shows a shift of molecular mass of non-reduced proteins with respect to reduced form, indicating that the Cysteine residues are engaged in disulfide bridges, as in the case of all characterised INH/PMEIs family members.

Figure 32. SDS-PAGE performed in reducing and not reducing conditions. Lane 1 SolyPMEI in reducing conditions; lane 2 SolyPMEI in not reducing conditions.

In order to determine the arrangement of disulfide bridges, the protein was denatured and pyridylethylated without previous reduction, so that cysteinyl residues involved in disulfide bridges were not available for modification with the alkylating agent. Asp-N endoproteinase digestion was

carried out, and peptides containing the half-cystine residue were identified by difference with the digest obtained after alkylation under reducing conditions. The resulting peptide elution pattern under reducing conditions identified two disulfide bridges between Cys7 with Cys16, and Cys 72 with Cys 120, while Cys 50 bears a free thiol group.

The recombinant SolyPMEI, with a predicted molecular mass of 18.335 Da, shows an apparent molecular mass of 25.000 Da probably due to glycosylation. Periodic acid-Schiff staining revealed glycosylation predicted by bioinformatics analysis (Fig. 33/A). To determine the level of glycosylation, Endo N-glycosidase was used on native and denatured SolyPMEI. The digested proteins were run on SDS-PAGE(Fig. 33/B). Only one band about 18 kDa was present in lane 2, corresponding to the completely deglycosilated denaturised protein. In contrast, in lane 3, two bands are present, the first of about 22 kDa, corresponding to the partially deglycosylated protein, and the second of about 18 kDa corresponding to the fully deglycosylated form. In conclusion, the results indicates that both the predicted sites are glycosylated.

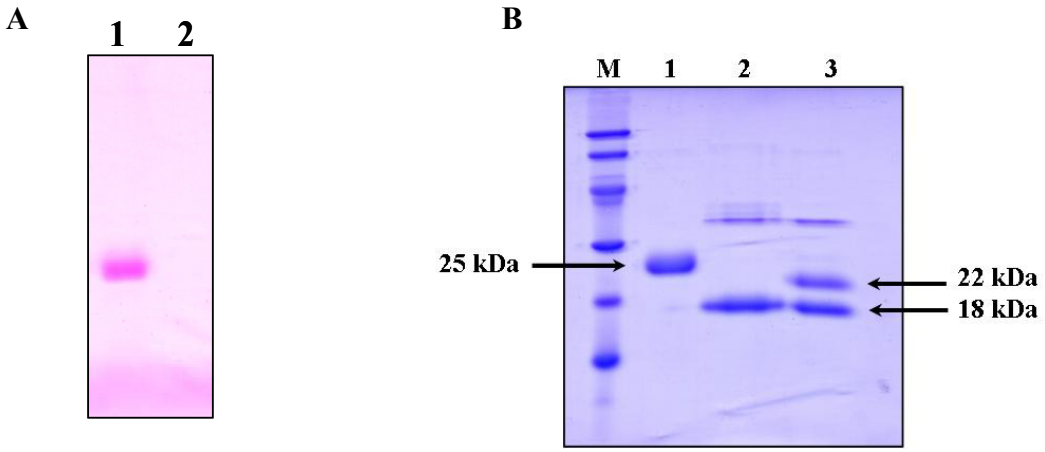

Figure 33. SolyPMEI glycosylation analysis. (A) Periodic acid-Schiff staining: (1) SolyPMEI; (2) negative control. **(B)** Endo N-glycosidase digestions: (1) molecular mass; (1) SolyPMEI; (2) SolyPMEI deglycosylated after denaturation at 100°C; (3) SolyPMEI deglycosylated without denaturation.

Structural modeling of SolyPMEI, based on the known 3D structure of complex PME-1/AcPMEI in which the SolyPMEI was substituted to the inhibitor from kiwi, indicated that one N101-glycosylation site was likely located at the interface of interaction between the enzyme and the inhibitor (Fig. 34).

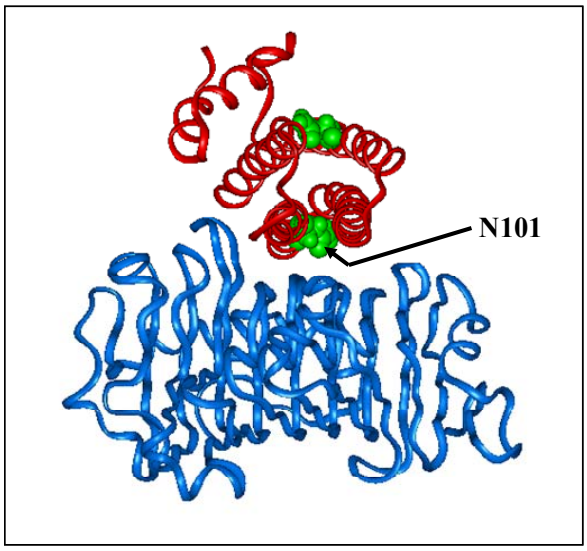

Figure 34. SolyPMEI model in complex with tomato PME-1. Modelling analysis, based on tomato PME-1/AcPMEI complex in which the SolyPMEI substituted the AcPMEI, PME-1 is shown in blue on the bottom. SolyPMEI is represented in red on the top. Asparagine residues involved in N-glycosylation are indicated in green. Arrow shows N-glycosylation site (N101) at the interface of interaction between the enzyme and the inhibitor.

The observed absence of inhibitory activity could be due to the Asn101 glycosylation possibly hampering the binding of the putative inhibitor with the PME inside the active cleft of the enzyme. For this reason N-glycosylation was eliminated by mutating Asn 101 residue, by site-directed mutagenesis. In particular Asn101 was substituted with: 1) Tyr (N101Y), the residue present at the same position in AcPMEI; 2) Gln (N101Q), a residue showing the same positive charge of Asn and 3) Ser (N101S), residue with a minimum steric encumber. The mutated proteins were expressed in Pichia heterologous system and purified to homogeneity.

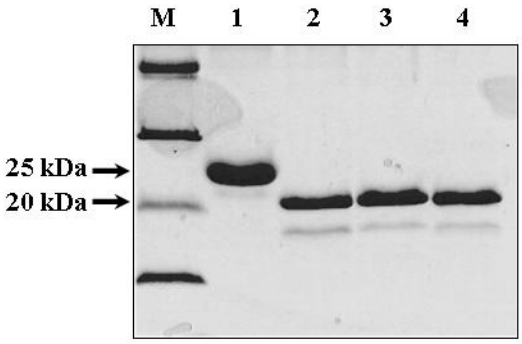

Figure 35. Asn101 site-directed mutagenesis: (M) Molecular weight; (1) SolyPMEI wild type, (2) N101Y, (3) N101Q, (4) N101S.

In figure 35, SDS-PAGE analysis shows the reduction of molecular masses of mutants with respect to the wild type protein, due to the reduced glycosylation.
However, nevertheless the reduced glycosylation, no inhibitory activity was exhibited by SolyPMEI mutants.

To exclude that the partially glycosylated protein exhibited an incorrect folding, CD spectrum of N101Y mutant was performed.

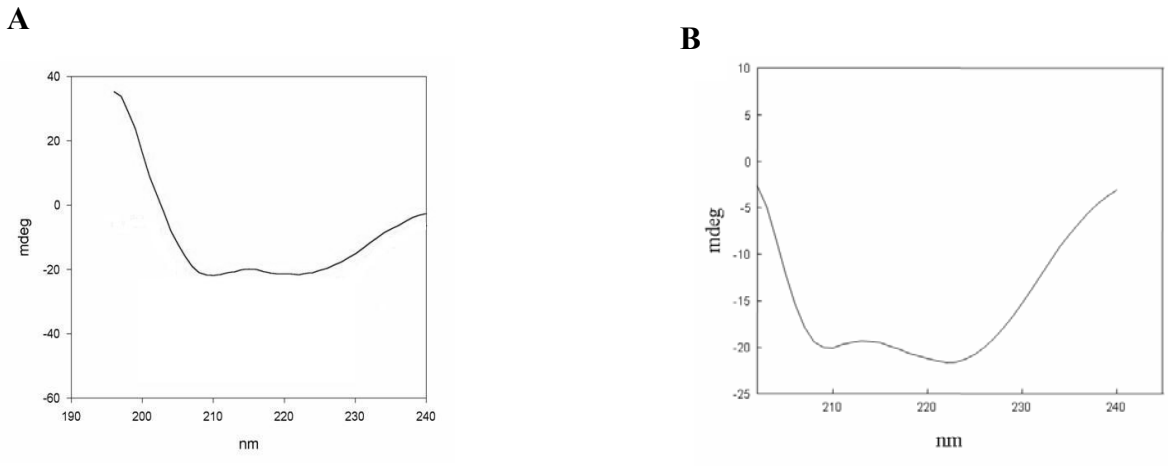

Figure 36. Circular Dichroism analysis. (A) SolyPMEI and **(B)** AcPMEI

As shown in figure 36/A the CD spectrum of SolyPMEI N101Y between 200 and 240 nm was characterized by two negative bands centered at 208 and 222 nm indicative of predominant α-helical secondary structures (Fig. 36/B), in particular, the estimated percentage of secondary structure was: 56% α-helix; 0% β-sheet; 22% β-turn; 22% random coil in agreement with similar value exhibited by functional AcPMEI (Camardella et al., 2000) and indicating a correct organization of the secondary structure of the expressed N101Y mutant.

To verify the possible interaction of N101Y mutant to tomato PME-1, affinity fishing approach was used. The recombinant protein was covalently linked to CNBr-Sepharose resin. PME-1 purified to homogeneity from tomato fruit (gently provided by Dr Laura Camardella, CNR Naples), was loaded onto the column and PME activity was evaluated in flow through and in bounded fractions eluted with Tris-HCl pH 8.0 containing 2M NaCl. High PME activity was observed in flow through, no activity was present in fractions eluted after washing the columns with loading buffer and PME activity was observed in fractions eluted from the column with buffer containing NaCl (Fig. 37), indicating that SolyN101YPMEI protein binds tomato PME-1. On the other hand no protein bands were observed after analysis of the eluted fractions, positive for PME activity, with SDS-PAGE followed by silver staining indicating a very low quantity of PME retained by affinity column. To exclude aspecific

binding of PME-1 to the affinity column, PME-1 was loaded into a CNBr column used as a control and no enzymatic activity was eluted.

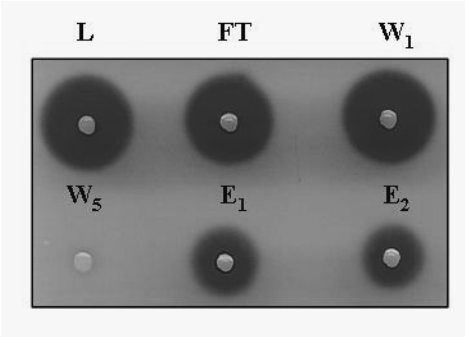

Figure 37. Gel diffusion assay of fraction eluted after affinity chromatography. (L) loaded; (FT) flow through; (W) washing; (E) eluted fractions.

3.2.3. Isolation from tomato red fruit of the natural SolyPMEI

To asses if the natural SolyPMEI exhibit the same biochemical characteristics of the recombinant protein, the immuno-affinity fishing approach was used to purify the SolyPMEI from tomato fruits. Polyclonal antibodies against N101Y mutant were generated from rabbit and purified onto a N101Y affinity chromatography. Western blot analysis was performed to estimate the level of the expression of the natural SolyPMEI in crude protein extracts of different tomato tissues. Consistently with the results obtained by real-time PCR, it has been shown that SolyPMEI is accumulated in flowers, pollen and mainly in red fruits (Fig. 38),

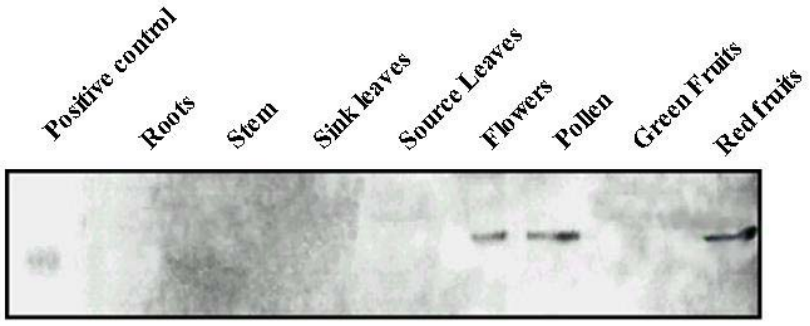

Figure 38. Western blot analysis on total protein extract from different tomato tissues with purified polyclonal antibodies generated against N101Y.

To purify the natural SolyPMEI from tomato fruit the purified antibodies were covalently linked to the CNBr-Sepharose resin. Due to the putative basic *pI* of SolyPMEI, proteins extracted from pericarp tissues of red fruits were previously loaded onto an anionic exchange column

(DEAE) and the flow through loaded onto a cationic column (Mono-S). The eluted fractions were pooled and loaded onto the Ab-SolyPMEI$_{N101Y}$ column. After washing with PBS buffer, specifically bounded proteins were eluted with 0.1 M glycine pH 2.0. Protein, eluted by affinity column, were separated by SDS-PAGE (Fig. 39). Two bands with an apparent molecular mass of 22000 and 35000 Da were eluted by the columns (Fig. 39). No protein bands were observed when the same samples were loaded onto Br-CN columns used as control (not shown). The analysis of the N-terminal sequence performed on the two bands isolated from the gel indicated that the 22000 Da band corresponded to the SolyPMEI and that the 35000 Da band corresponded to the tomato PME-1. To exclude the direct binding of PME-1 to SolyPMEI antibodies, PME-1 from tomato purified to homogeneity, was loaded into the affinity column and no interaction was observed (data not shown).

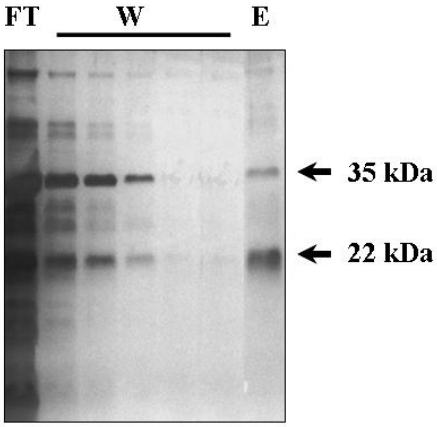

Figure 39. SDS-PAGE analysis of fractions elueted from after immuno-affinity chromatography.
(FT) Flow-through (**E**) Eluted fraction.

The isolation of both SolyPMEI and PME-1 by immuno-affinity chromatography indicates that SolyPMEIs was engaged in the formation of a stable complex with endogenous PME-1 in tomato fruit.

To dissociate PME from the complex and then to purify the SolyPMEI in free form, two elution steps with different buffers were performed after the binding of the complex to the affinity column. A first elution buffer at pH 8.3 2M NaCl was loaded to dissociate PME, and a second elution buffer at pH 2.0 was successively loaded onto the column to elute the SolyPMEI from the affinity column (Fig. 40). SDS-PAGEs shown in figure 40/A-B indicate the elution of both PME and SolyPMEI in free form.

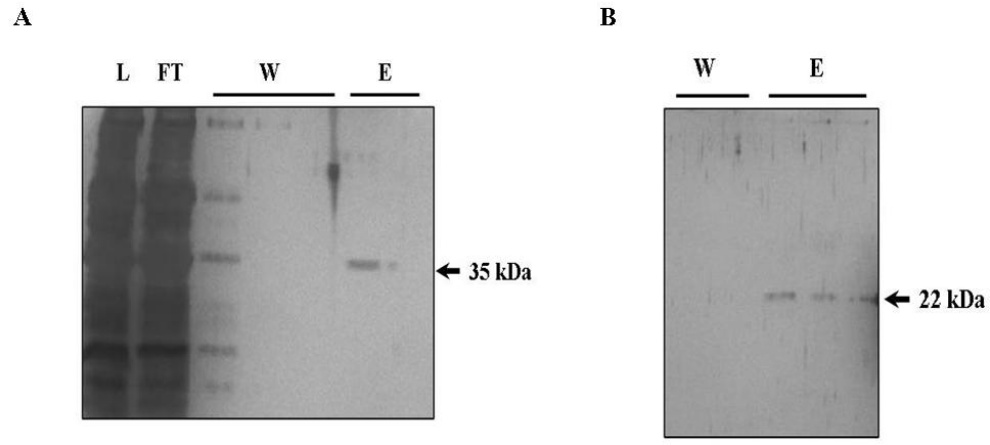

Figure 40. SDS-PAGE analysis after immuno affinity column. (A) PME-1 elution at pH 8.3, 2M NaCl. **(B)** SolyPMEI elution at pH 2.0. (L) Loaded ; (FT) Flow-through ; (W) Washing (E) Eluted fraction.

However the eluted proteins did not show PME or PMEI activity, probably due do drastic elution conditions used.

In order to purify an active PME/SolyPMEI complex, total proteins extracted from tomato red fruit were then separated by gel-filtration chromatography (Fig. 42/A) and subjected to SDS-PAGE followed by western-blot analysis using purified SolyPMEI polyclonal antibodies. SolyPMEI, expressed in *P. pastoris* and purified to homogeneity, eluted in fractions with a molecular mass of about 15 to 25 kDa (i.e. 26-27), consistently with its molecular mass (Fig. 42/C). Instead, SolyPMEI from tomato fruit eluted in the fractions 21-22, which contain proteins with an estimated molecular mass of about 50 to 60 kDa (Fig. 42/B); no PME activity was associated to the presence of the immunodetected bands. Moreover, PME activity was eluted in fractions 24 and 25, which contained proteins with a molecular mass of about 30 to 40 kDa indicating that the enzyme is also present in excess as an unbound active form. No immunoreacting bands were detected in fractions 26-27 indicating the absence of PMEI as unbound form. Fractions ctrypsin, and analyzed by liquid chromatography-tandem mass spectrometry (LC-MS/MS). PME-1 (P14280), PME2/1 (P09607), PME3 (Q96576) and PMEU-1 (Q43143) were recognised in SolyPMEI containing fractions, indicating that SolyPMEI, interacts with different PMEs, according with the large spectrum of recognition played by the characterised inhibitors.

The chromatographic behaviour of SolyPMEI isolated from tomato fruits and the absence of detectable PME activity indicates that the SolyPMEI in tomato fruits is engaged in the formation of a complex with endogenous PMEs and that the binding of the inhibitor abolish the enzymatic activity.

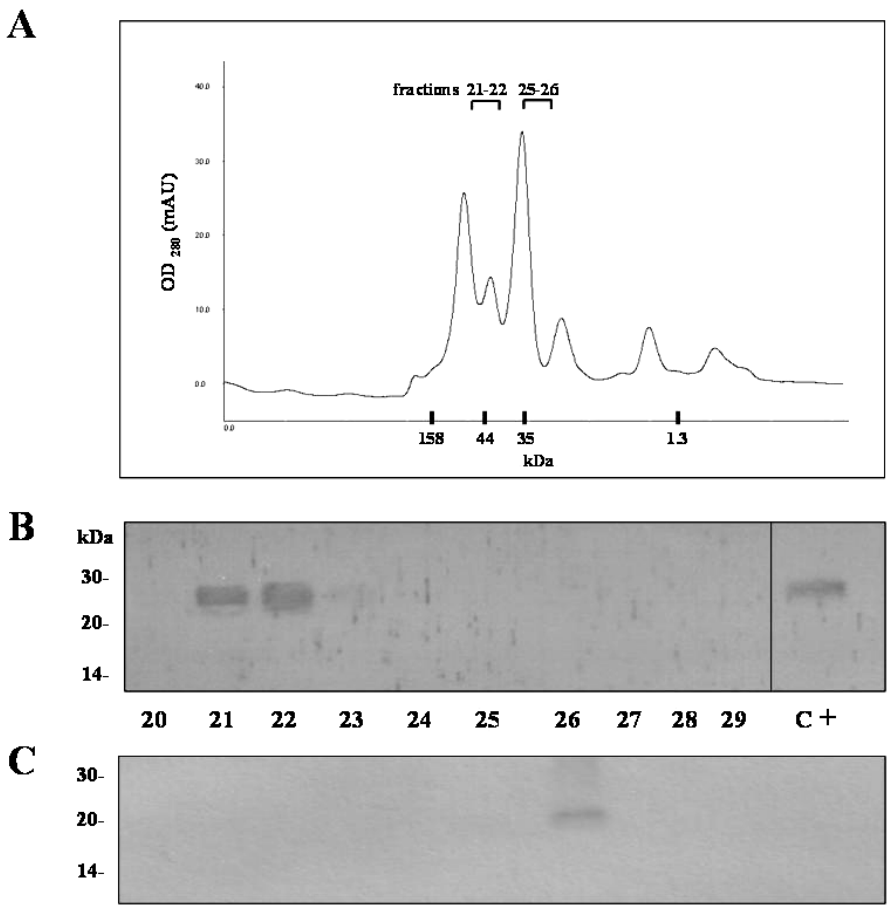

Figure 42. Gel filtration. (A) gel-filtration chromatography of tomato red fruit extract; (**B)** Immunodetection of SolyPMEI in tomato fruit extracts after gel filtration, (**C)** Immunodetection of recombinant SolyPMEI$_{N101Y}$ expressed in Pichia; **C +:** positive control; 20-29 elution fractions.

3.3.Invertase inhibitor from *Solanum Lycopercum* (SolyCIF)

3.3.1. Identification, expression and subcellular localization of the SolyCIF

The *SolyCIF* gene has been amplified from c-DNA of tomato red fruits, cloned in TOPO TA vector and sequenced. Despite *SolyCIF* sequence was in complete agreement with the *SGN-U317539* sequence, differences in positions 1201 and 1222 were observed in comparison with the AJ010943 sequence. These differences are responsible for two amino acid modifications, Thr103Pro and Ile110Leu in SolyCIF and AJ010943 respectively (Fig. 43). These Thr and Ile are conserved in tobacco cell wall INH (CIF).

SolyCIF shows 84% and 61% amino acid identity with Nt-CIF and Nt-VIF, respectively. Removal of the predicted N-terminal signal peptide generates a mature protein consisting of 153 amino acids with a molecular weight of 16.632 Da and a predicted alkaline p*I*=8.06, which is characteristic of cell wall bound proteins. In addition to the four conserved Cys residues, which have been found to be engaged in disulfide bridges in functional INH and PMEI, SolyCIF shows a well conserved N-terminal alpha-helical hairpin extension which is crucial to the structural integrity of the protein and a well conserved C-terminus domain which is thought to contribute to the interface stabilization of the protein (Hothorn et al., 2004a). No potential N-glycosylation or O-glycosylation sites were found to be present in the protein sequence.

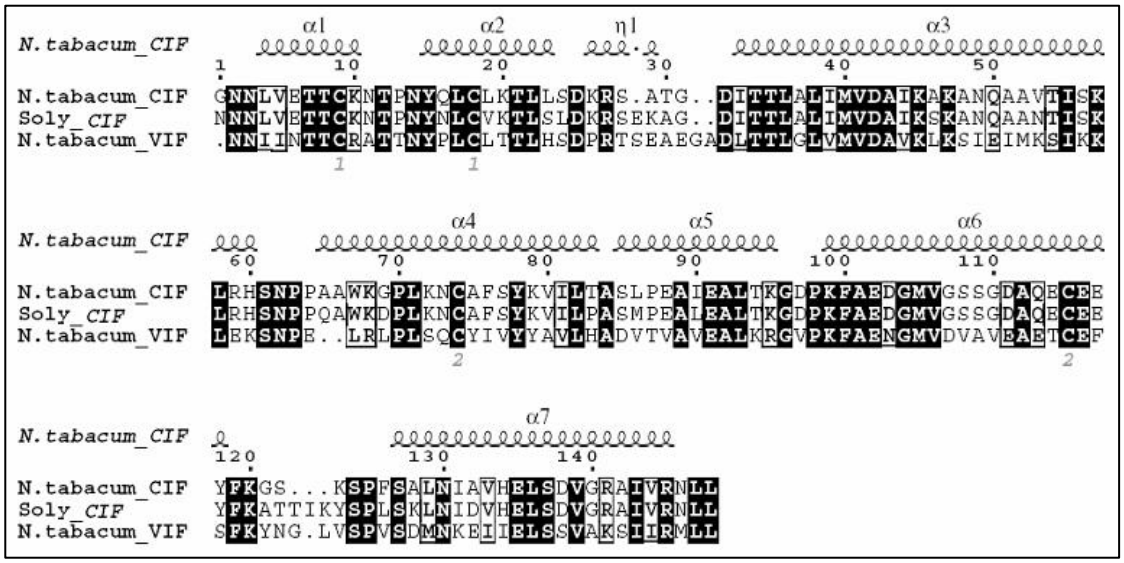

Figure 43. Amino acid sequence alignment of SolyCIF and other invertase inhibitors. Alignment is performed by Clustal X. Secondary structure is assigned by the alignment analysis program ESPript according to DSSP. Numbers 1 and 2, at the bottom of the sequence block, indicate disulfide bridges connecting the four conserved Cys residues.

To study the *SolyCIF* gene organization, a 1411 bp PCR fragment was amplified from genomic DNA and sequenced. Figure 44 shows the gene encoding the inhibitor, which includes two exons and one intron. In particular, the 895-bp intron shows GT-AT splice sites and is located after nucleotide 303 in the opening reading frame. Interestingly, in all the members of the INHs/PMEIs family characterized so far, introns have been found to exist only in genes which belong to the INHs subfamily. This feature could constitute a useful tool for discriminating between INH and PMEI.

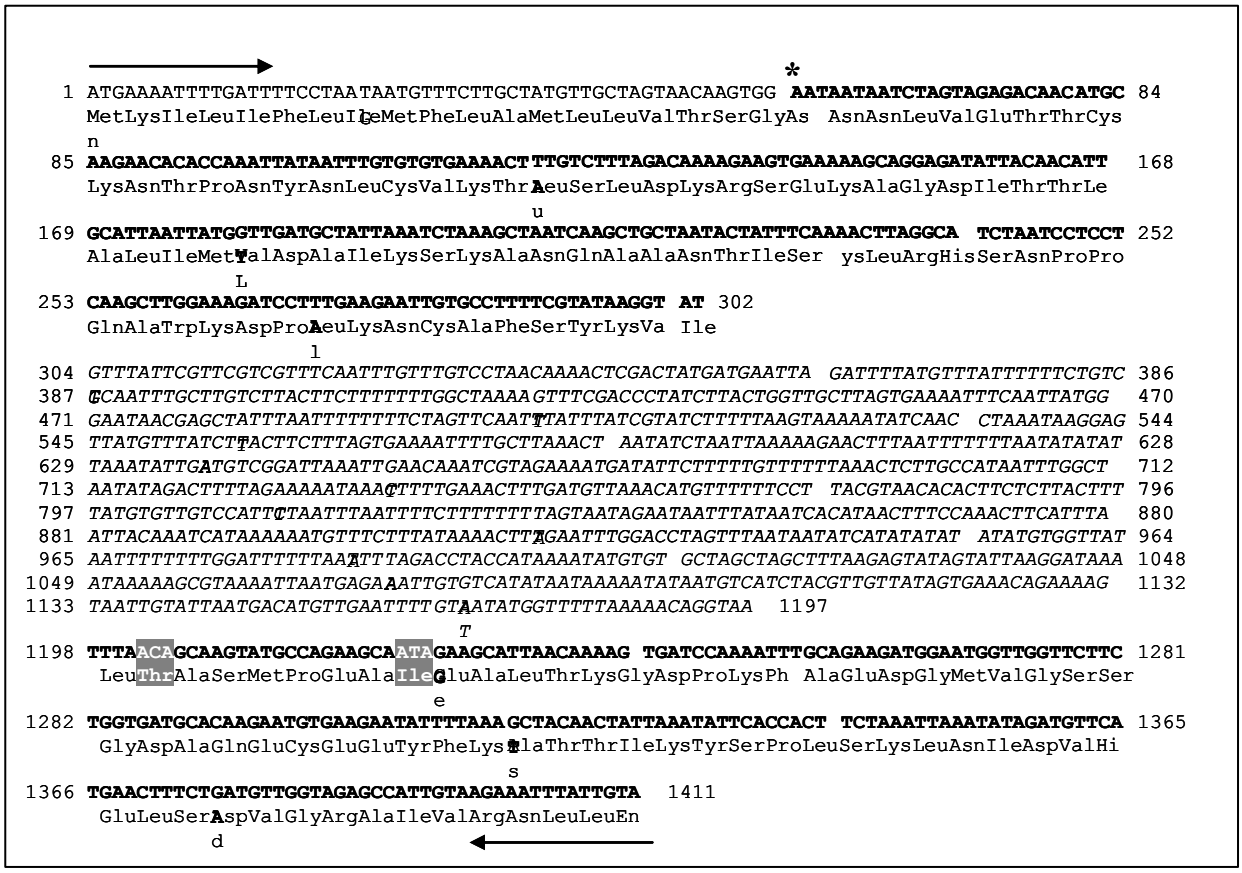

Figure 44. Nucleotide and deduced amino acid sequences of the SolyCIF gene. Coding sequence cloned in *Pichia pastoris* is in bold. Primer used to sequence genomic DNA are symbolized by arrows. Intron is in italic, case and the putative peptide signal cleavage site marked with asterisk. Positions of nucleotidic and amino acidic differences between thise sequence and AJ010943 are boxed.

To analyze the pattern of expression of *SolyCIF* in various tissues, the transcripts were assessed quantitatively by performing real time PCR, using *Actin 4* for the normalization procedure (Fig. 45). The results show that the highest *SolyCIF* transcript levels were present in flowers and source leaves, which suggests that this inhibitor may be involved in flower formation and development and in source-sink relations. In addition a high, although lesser transcript level was observed in green fruits, indicating that the inhibitor may contribute to channelling the flux of carbohydrate in the initial stages of fruit ripening. Lower but significant levels of *SolyCIF* transcripts were also observed in red fruits and other plant organs.

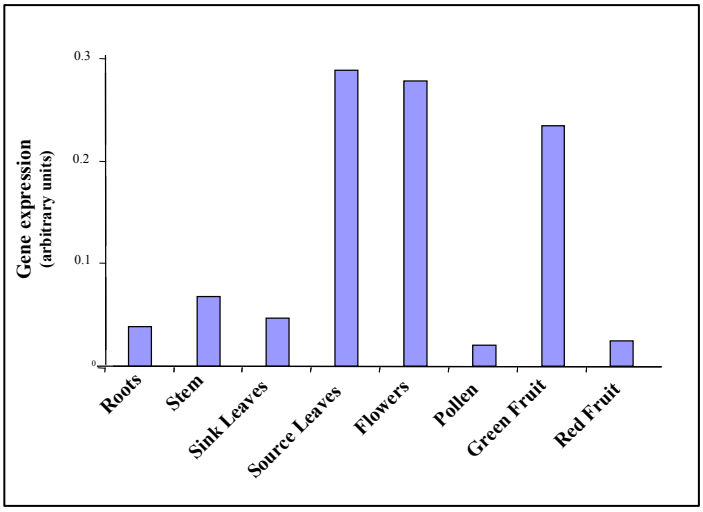

Figure 45. Real-time PCR of SolyCIF mRNA and invertase activity. Quantitative expression analisis of SolyCIF transcript in different plant organs by real time PCR.

To assess the apoplastic localization of SolyCIF predicted by bioinformatic analysis, tobacco leaves were inoculated with Agrobacterium containing the full length SolyCIF protein fused to GFP (SolyCIF-GFP). The polygalacturonase inhibiting protein from *Phaseolus vulgaris* (PvPGIP2), known to be secreted to the apoplast (De Lorenzo et al., 2001; Spadoni et al., 2006) and fused to GFP was also used. Tobacco leaves were inoculated with Agrobacterium strains containing either *SolyCIF-GFP* or *PvPGIP2-GFP* constructs; 48h later the abaxial epidermis was imaged by confocal scanning microscopy.

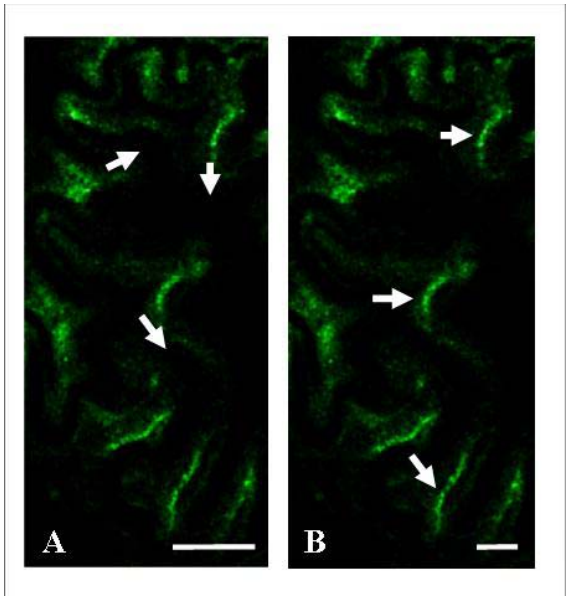

Figure 46 Localization of transiently expressed SolyCIF-GFP and PvPGIP2-GFP in tobacco leaves under the control of the CaMV 35S promoter. Low magnification confocal laser scanning micrographs of tobacco epidermal leaf cells 48h after agroinjection. Tobacco leaf cells expressing (A) PvPGIP2-GFP. (B) SolyCIF-GFP. Arrows indicate the apoplastic green fluorescence. Scale bars = 30μm

As shown in Fig. 46/A, PvPGIP2-GFP fluorescence was mainly detectable in the cell walls of the transformed leaf epidermal cells and no accumulation of GFP was observed in vacuole. A similar pattern has been observed with the *SolyCIF-GFP* construct (Fig. 46/B); also in this case apoplastic GFP fluorescence was observed in epidermal cells of tobacco transformed leaves.

3.3.2. Heterologous expression of recombinant SolyCIF, purification and functional characterization

In order to functionally characterize the inhibitor, the *SolyCIF* cDNA was cloned into the pPICZαA plasmid and expressed in *P. pastoris* as a recombinant protein. After an induction step with methanol, a major protein band with an apparent molecular mass of 20 kDa, which was not present in the supernatant of untransformed cells, was observed in the culture filtrate after SDS-PAGE analysis (Fig. 47). SolyCIF was purified to homogeneity as described in the Materials and methods section.

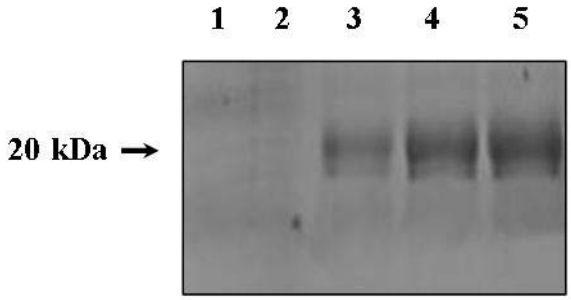

Figure 47. SDS-PAGE of *P. pastoris* culture filtrate: (1) molecular weight; (2) T_{48h} induction supernatant of untransformed cells; (3) T_{0h} induction supernatant of transformed cells; (4) T_{24h} induction supernatant of transformed cells; (5)T_{48h} induction supernatant of transformed cells; (6) T_{72h} induction supernatant of transformed cells.

The NH_2-terminal sequencing of SolyCIF led to the identification of 11 amino acid residues, EAEFNNNLVET. The sequence obtained was in complete agreement with that expected, where the amino acid residues EA, EF and NNNLVET corresponded to the peptide signal C-terminal sequence after peptidase signal digestion, the cloning vector restriction site and the NH_2-terminal sequence of expressed SolyCIF, respectively. The SolyCIF N-terminal sequence showed some amino acid variations with respect to the N-terminal of the invertase inhibitor purified by Pressey from tomato (N-terminal: -LVLVETKNKNTPNYNL-VKTL) (Pressey, 1994), which suggests the presence of multiple isoforms in *S. lycopersicum*. However, the possibility cannot be ruled out that amino acid micro heterogeneities may be due to allelic differences between inhibitors originating from different tomato cultivars.

Purified SolyCIF was analysed by SDS-PAGE using sample buffer with and without reductant. Under reducing conditions, the protein showed a single band with an apparent molecular mass of 20 kDa while, under non-reducing conditions, its mobility increased (Fig. 48), which indicates that the cysteine residues are engaged in intra-molecular disulfide bridges in the recombinant protein.

Figure 48. SDS-PAGE performed in reducing and not reducing conditions. (1) SolyCIF not reducing conditions; **(2)** SolyCIF in reducing conditions.

The presence of disulfide bridges was previously observed in the recombinant tobacco NtCIF and in pectin methylesterase inhibitors AcPMEI, AtPMEI-1 and AtPMEI-2. Crystallographic analysis of NtCIF, AcPMEI and AtPMEI-2 has shown that the two disulfide bridges connecting the α5 and α6 helixes in the four helix bundle as well as the α1 and α2 helixes in the N-terminal α-hairpin module contribute to the structural stabilization of the protein. (Hothorn et al., 2004a; Hothorn et al., 2004b; Di Matteo et al., 2005). The molecular mass of the recombinant protein (17,108 Da) determined by mass spectrometry indicates that the recombinant enzyme produced in *P. pastoris* is not glycosylated.

In order to determine whether SolyCIF is a functional invertase inhibitor, we tested its ability to reduce invertase activity in crude protein extracts from red tomato fruits. As shown in Figure 49, a decrease in the invertase activity levels was observed upon increasing the SolyCIF concentration.

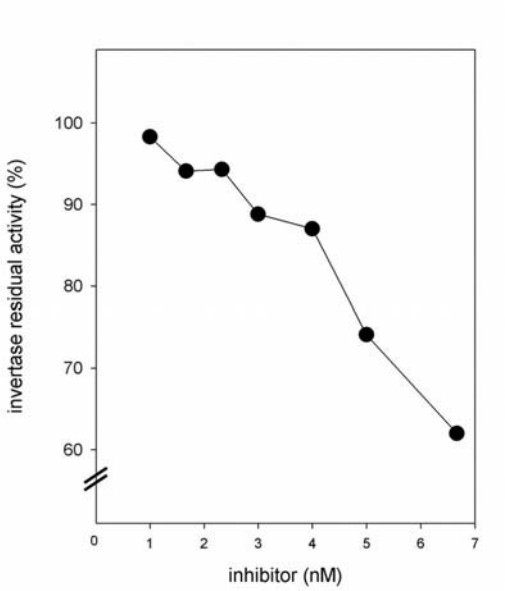

Figure 49. Inhibitory effect of recombinant SolyCIF on tomato vacuolar invertase. Residual invertase activity was measured at pH 4.9 and 37°C after 15 min pre-incubation of the inhibitor (1 to 6.7 nM) with 6.7 nM tomato invertase. Sucrose concentration in the assay was 100mM.

The inhibitory activity of SolyCIF on invertase shows quite a broad range of specificity in green tomato fruits, potato tubers, petunia flowers, *A. thaliana* and *N. tabacum* leaves, whereas it had no inhibitory effects on the invertases present in sugar beet roots and *S. cerevisiae* (Tab. 3). SolyCIF showed no inhibitory activity on purified tomato PME-1 (CAA01314).

Inv (origins)	***S. cerevisiae***	**Tomato solanacea**	**Potato solanacea**	**Petunia solanacea**	***N. tabacum* solanacea**	**Sugar beet *chenopodiacea***	***A. thaliana brassicacea***
Purity	**Commercial preparation**	**Crude extract**	**Crude extract**	**Crude extract**	**Crude extract**	**Crude extract**	**Crude extract**
Inhibition	**0**	**100**	**100**	**100**	**100**	**0**	**100**

Table 3. SolyCIF specificity

The inhibitory activity of recombinant SolyCIF persisted for several weeks when this inhibitor was stored in acetate buffer at pH 4.6 at a temperature of 4°C. In addition, SolyCIF showed a high level of thermal stability. No loss of activity was observed after heating the protein at 100°C for 45 min. These results are consistent with the high thermal stability previously described in Nt-CIF from tobacco, possibly due to the compact protein core formed by loop regions with a minimal length: these regions are folded into a four-helix bundle structure, which is stabilized by hydrophobic interactions and by the two disulfide bridges (Hothorn et al., 2004a).

3.3.3. Isolation of a vacuolar tomato invertase interacting with SolyCIF

To characterize the invertase interacting with SolyCIF, proteins extracted from green and red tomato fruits were separately loaded onto an INH-Sepharose affinity column and the proteins retained were successively eluted with 50 mM phosphate buffer at pH 7.5. Optimization of the elution conditions was based on preliminary studies by Pressey (Pressey, 1994) showing that the inhibitor and tomato invertase do not interact under alkaline conditions.

Fractions showing invertase activity were pooled, concentrated and loaded onto a Superdex 75 column. The invertase activity from both green and red fruits was eluted as a single peak in fractions with an estimated molecular mass ranging from 50 to 60 kDa. Under native conditions, PAGE analysis of active fractions from green (not shown) and red fruits showed that both fractions migrated in a single band, suggesting that the enzyme preparations were purified to homogeneity (Figure 50/A). However, under reducing conditions, SDS-PAGE analysis of the same fractions showed, instead of a band with a molecular mass of about 60 kDa corresponding to the full-length protein, the existence of different splitting products. In particular, fragments with molecular masses of 46.3 kDa, 27.7 kDa, 18.6 kDa and 16.8 kDa were present in both red and green fruits, while a 44-kDa band was observed only in the case of red fruits (Fig. 50/B). In addition another band with a molecular mass of 35 kDa was observed and subjected to Edman degradation procedures. However, its identification was not possible since the NH_2-terminal residue appeared to be blocked. This unknown protein was not found to occur when protein extracts were loaded onto the NHS-activated Sepharose^{TM} column used as control.

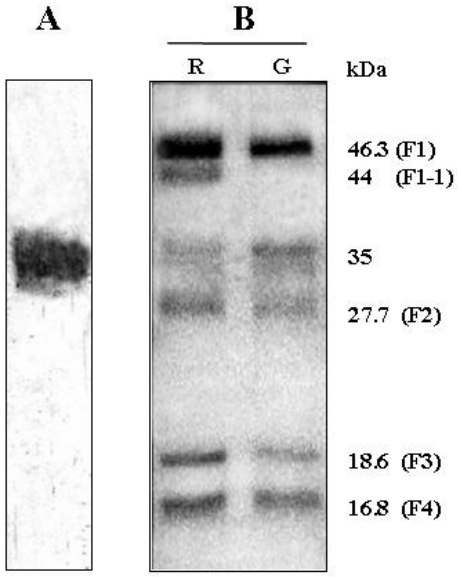

Figure 50. Electrophoresis analysis of TIV-1 purified with affinity chromatography: (**A**), PAGE of the purified native enzyme without SDS; (**B**) SDS-PAGE of TIV-1 purified from red (R) and green (G) fruits. Molecular mass of different fragments (F) are also indicated

All in all, these results indicate that the active enzyme consists of several splitting fragments which are tightly associated under native conditions. Fragmentation of vacuolar invertase from tomato fruit extracts was likewise previously reported by other authors (Konno et al., 1993; Bucheli and Devaud, 1994; Greiner et al., 2000). It is worth noting that the occurrence of splitting products has been reported to occur in vacuolar invertases in several other plant species (Sturm, 1999). Although the exact contribution of the proteolytic fragmentation process to the regulation of the enzymatic activity still remains to be elucidated, this process seems to be under developmental control (Unger et al., 1994; Sturm, 1999; Greiner et al., 2000). To characterize the purified invertase, the protein bands from the SDS-PAGE gel were transferred onto PVDF membrane for NH_2-terminal sequencing. The NH_2-terminal sequences and homology-based analysis assigned all the sequences determined to the tomato acid vacuolar invertase (TIV-1; Swiss-Prot accession P29000) (Fig. 51). Direct sequencing of the enzyme in solution also led to the presence of three different N-terminal sequences corresponding exactly to those obtained with the fragments**.** TIV-1, like other vacuolar acid invertases, is known to be synthesized as a preproprotein with a long leader sequence containing a signal peptide and an N-terminal extension that are trimmed off during transport and protein maturation (Elliott et al., 1993; Ohyama et al., 1995; Miron et al., 2002).

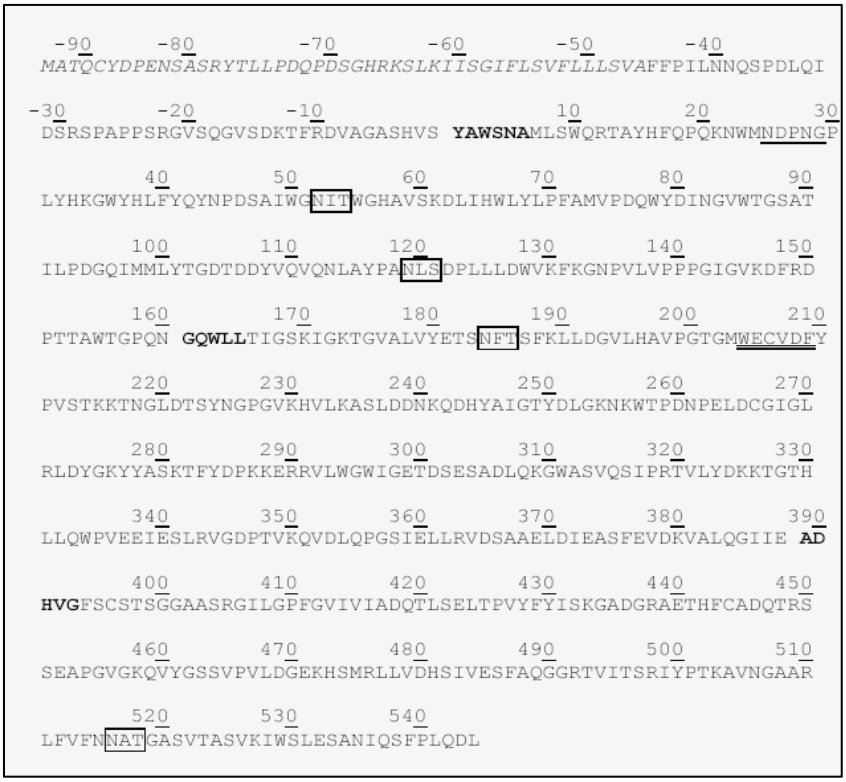

Figure 51. Analysis of the tomato vacuolar invertase fragments. Amino acid sequence of tomato invertase (Swiss-Prot code P29000). The three N-terminal sequences obtained by analysing the protein in solution are indicated in bold print. Putative N-glycosylation sites are shown (NetNGlyc in the ExPASy Proteomics Server). Single-underlined pentapeptide corresponds to the so-called F-motif and the double underlined sequence corresponds to the highly conserved peptide domain with a valine residue characterizing vacuolar invertase

Fragment	N-terminal Sequence	MW (Da) SDS_PAGE	MW (Da) Seq-deduced	Fragment Res. number
F1	YAWSNA	46.3*	43,788	1-388
F1.1	YAWSN	44.0	43,788	1-388
F2	GQWLL	27.7*	25,328	161-388
F3	YAWSN	18.6	18,478	1-160
F4	ADHVG	16.8	16,395	389-544

Table 4. N-terminal amino acid sequences of the five fragments. Apparent molecular masses determined by SDS-PAGE, sequence-deduced molecular masses and amino acidic positions of fragments in the sequence. Asterisks label the two fragments with substantially higher SDS-PAGE molecular masses than the sequence-deduced values. The two fragments were found to have the same N-glycosylation consensus sequence.

Three different motifs are present in the sequence. In common with other invertases, TIV-1 carries the pentapeptide NDPNG (βF-motif), which is located near the N terminus of the mature protein. Another motif is the sequence WECP/VDF, which indicates the existence of a highly conserved peptide domain consisting of a Cys residue and a few neighboring amino acids (Sturm and Chrispeels, 1990). Within the conserved WECP/VDF amino acid motif, all the VIs possess a valine residue, whereas all the CWIs are characterized by a proline residue. This conserved single amino acids substitution has been demonstrates to determine the different pH-optima and the substrate specificities of the two different classes of enzymes (Goetz and Roitsch, 1999). The sequence also includes a short C-terminal extension, which contains a hydrophobic amino acid stretch (F-P-L) thought to form the critical core of the vacuolar sorting signal (Unger et al., 1994). As shown in Fig. 51, four putative N-glycosylation sites are present in the invertase primary structure. Comparisons between the N-terminal sequences of the various bands and the apparent molecular masses determined by SDS-PAGE and with the molecular masses deduced by the amino acid sequences indicated that the fragments were produced in the mature protein by only two proteolytic cleavages (Tab. 4). In particular, the first cleavage site occurs between residues N160 and G161 and the second one between residues E388 and A389 (Fig.51). The difference of about 2 kDa observed between the apparent and deduced molecular masses of fragments F1 and F2 showing the same putative N-glycosylation sites suggests the presence of N-linked complex oligosaccharides. This difference in the molecular mass is not observed in the case of fragment F1-1, which is possibly a not glycosylated form of F1 and is only present in the red fruits of this plant.

The fact that, by affinity fishing, we found the vacuolar TIV-1 instead of an apoplastic invertase (LINs) was not totally surprising. Indeed, Miron *et al.* (Miron et al., 2002) proposed that, in mature tomato fruits, cell wall invertase activity is also due to a portion of TIV-1, sorted by

default and localized to the cell wall. In addition, since TIV-1 accounts for most of the total invertase activity in tomato, the possibility cannot be ruled out that the vacuolar enzyme may prevent *in vitro* interactions between the inhibitor and apoplastic invertases

3.3.3. Molecular modeling of tomato vacuolar invertase

The 3D structure of tomato vacuolar invertase was modeled using the crystal structure of *Arabidopsis thaliana* cell-wall invertase as a template(Verhaest et al., 2006). Analysis of the models and crystal structure showed the existence of considerable similarity in the overall folding topology, especially at the active site. Superimposition of the Cα traces of all the aligned residues of the model structure and its crystal template (511 atoms) gave a very low root-mean-square deviation (rmsd of 0.47 Å), which indicates that the sequence well fitted into the structure (superimposed Cα traces are shown in Fig 52/A). The Ramachandran plot indicated that only seven amino acid residues, mainly lying in loop regions, were located outside the allowed regions. The differences between the two structures focused mainly on some peripheral loops and strand lengths, and on the absence in tomato invertase of the α-helix present in the Arabidopsis invertase C-terminal domain. The molecular model for TIV-1 shows that the proteolytic cleavage sites are located in external loop regions, one in the N-terminal five-fold β-propeller domain, and the other in the two β-sheet C-terminal domain. The fragments generated by the two cleavages were found to be strongly interconnected (Fig 52/B). Moreover, the catalytic activity observed in the purified protein is obviously only possible when the fragments are closely associated: the first cleavage (between Asn160 and Gly 161) splits into two halves the catalytic site where two catalytic amino acids Asp26 and Glu 205 lying on two different fragments face each other (Fig 52/B).

3.3.4. Enzymatic properties of TIV-1 and enzyme inhibition by recombinant SolyCIF

TIV-1 showed a normal pattern of Michaelis-Menten kinetics with sucrose as the substrate. Km and Vmax were measured using sucrose in the 2-150 mM concentration range. V max was 2.9 μmol min^{-1} and the Km recorded with sucrose was 6.4 mM, in agreement with the kinetic parameters obtained by other authors on vacuolar enzymes (Lee et al., 1996; Karuppiah et al., 1989; Bracho and Whitaker, 1990b; Unger et al., 1992a; Lin and Sung, 1993; Obenland et al., 1993; Charng et al., 1994; Tang et al., 1996; Isla et al., 1999). The specific activity of TIV-1 was 438.3 U mg^{-1} and the catalytic constant during hydrolysis was found to be $7.25x10^3$ sec^{-1}. The resulting catalytic efficiency (kcat/Km) was $1.08x10^6$ M^{-1} s^{-1}, which indicates that TIV-1 hydrolyses sucrose

very efficiently. Preliminary inhibition assays performed at pH 4.9 at a temperature of 37°C, indicated the very low amount of inhibitor is needed to decrease TIV-1 activity.

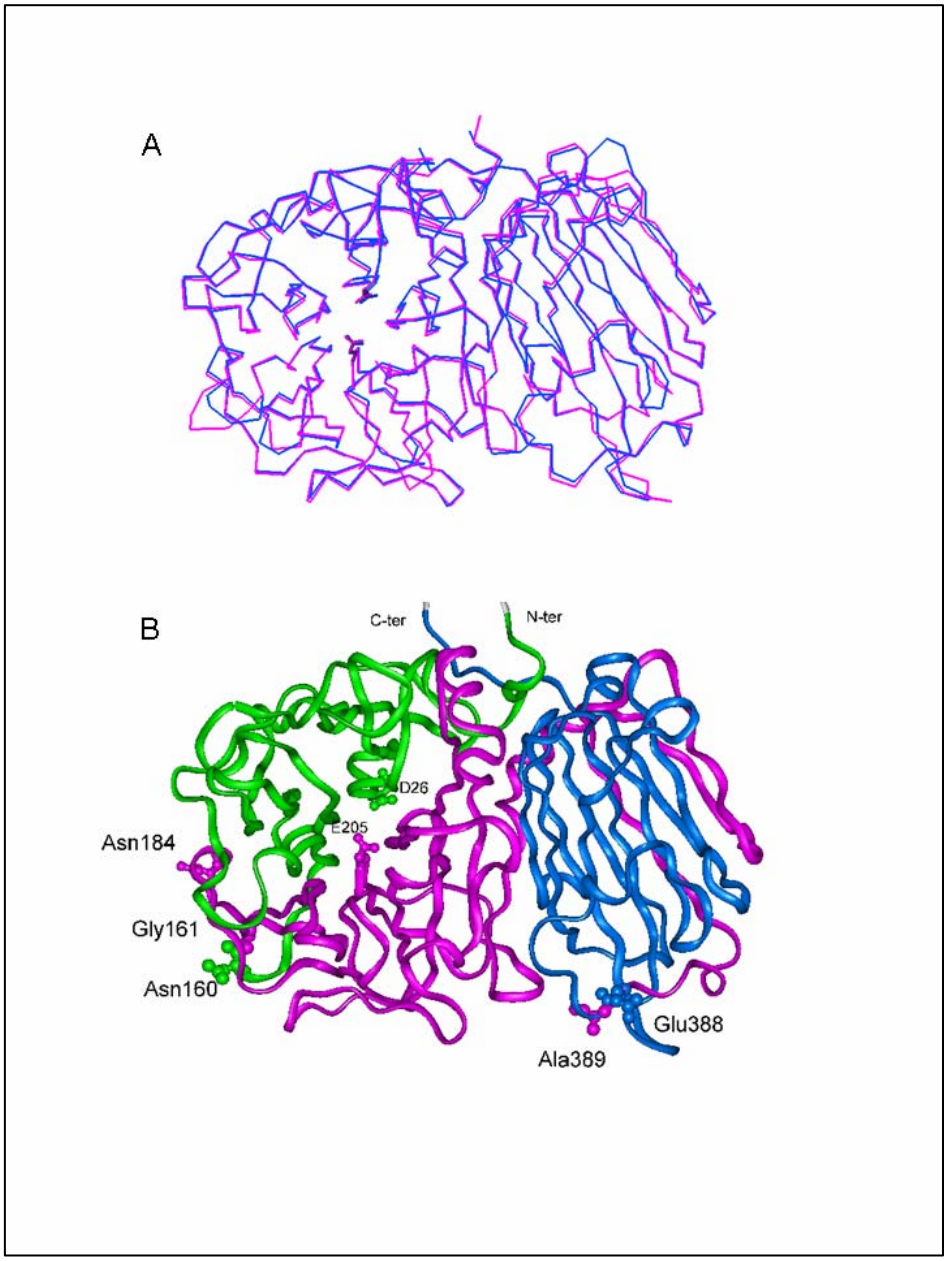

Figure 52. Tomato vacuolar invertase molecular model. (**A**) Trace superimposition of tomato vacuolar invertase model and *A. thaliana* cell-wall invertase crystal structure (PDB code 1GQ8). The model and the crystal template were superimposed by Cα of all the aligned residues (511 atoms) with a root-mean-square deviation (rmsd) of 0.47 Å. (**B**) Ribbon representation of tomato vacuolar invertase model showing the fragments produced by the proteolytic cleavages. The two cleavage site occur between the residues N160-G161 and 388-389 and give rise apparently to three proteolytic fragments. F3 (green) comprises the residues between 1 and 160, F2 (magenta) the residues between 161 and 388 and F4 (blue) the residues between 389 and 544. Incomplete cleavage at the 160-161 proteolytic site give rise to the fragments F1 and F1.1 , both comprising the residues from 1 to 388 (F3+F2). Asn 184, common to fragments F1 and F2, likely carrying an N-linked complex type oligosaccharide is also shown. Catalytic amino acids, Asp26 and Glu 205, are shown to lye on different fragments. The amino acid are represented as ball and stick, molecules have been drawn using the Insight II package from Accelrys Inc.

4. Conclusions

Plants synthesize proteinaceous inhibitors to modulate the activity of a number of carbohydrate active enzymes. Pectin methylesterase and invertase are key enzymes in plant carbohydrate metabolism and are both involved in important developmental processes such as fruit development and ripening.

Invertase inhibitors (INH) and pectin methylesterase inhibitors (PMEI), due to their high structural similarity, are included in the same protein family (Pf04043) nevertheless the respective target enzymes are structurally unrelated.

In this thesis two new members of INH/PMEI family (i.e. SolyCIF and SolyPMEI) have been identified and characterised in tomato. In tomato fruits SolyCIF and SolyPMEI expression correlate with the enzymatic activity indicating the importance of this post-transcriptional mechanism in the modulation of the respective enzymes. Both inhibitors inhibit endogenous plant enzymes and do not inhibit fungal enzymes indicating that they are mainly involved in growth and development instead of plant defence against pathogen.

SolyCIF, was cloned, expressed in two heterologous systems (*Pichia pastoris* and *Nicotiana tabacum)* and functionally characterized. The data obtained here clearly show that SolyCIF is a cell-wall localized proteinaceous thermostable invertase inhibitor which interacts *in vitro* with a vacuolar enzyme, namely TIV-1. The results obtained also show that TIV-1 is a glycosylated monomer composed of several fragments that have to be tightly associated for enzymatic activity to occur.

SolyPMEI was found to be mainly expressed in red fruit and was albeit at lower levels in flower and pollen. All attempts to produce active recombinant SolyPMEI protein for biochemical characterization appear to be unsuccessful nevertheless CD spectra, disulfide bridges indicated a correct folding of the protein in solution.

The isolation of both natural SolyPMEI and PME-1 by the immuno-affinity chromatography from tomato fruits, indicate that SolyPMEIs is *in vivo* engaged in the formation of a stable complex with endogenous PME-1. Gel-filtration experiments, also indicate that in tomato fruits SolyPMEI is not present in free form but totally engaged in the formation of an inactive complex with endogenous PME(s). Due to the lower level of expression in other tissues and to the stability of the PMEI-PME complex the purification of the inhibitor from this tissue is difficult and future investigation will be focused on the ectopic expression of SolyPMEI in *planta*.

Given the crucial role played by invertases and pectin methylesterase in the carbohydrate metabolism and plant growth, studies on the role of the inhibitors on their regulation open new perspective for plant biotechnological applications and for the improvement of agronomic traits in crop species.

5. References

Akimitsu, K., Isshiki, A., Ohtani, K., Yammoto, H., Eshel, D. and Prusky, D. (2004). Sugars and pH: A clue to the regulation of fungal cell wall-degrading enzymes in plants. Physiol. Mol. Plant Pathol., **65**, 271-275.

Al Qsous, S., Carpentier, E., Klein-Eude, D., Burel, C., Mareck, A., Dauchel, H., Gomord, V. and Balange, A.P. (2004). Identification and isolation of a pectin methylesterase isoform that could be involved in flax cell wall stiffening. Planta, **219**, 369-378.

Balestrieri, C., Castaldo, D., Giovane, A., Quagliuolo, L. and Servillo, L. (1990). A glycoprotein inhibitor of pectin methylesterase in kiwi fruit (*Actinidia chinensis*). Eur. J. Biochem., **193**, 183-187.

Balibrea Lara, M.E., Gonzalez Garcia, M.-C., Fatima, T., Ehness, R., Lee, T.K., Proels, R., Tanner, W. and & Roitsch, T. (2004). Extracellular invertase is an essential component of cytokinin-mediated
delay of senescence. Extracellular invertase is an essential component of cytokinin-mediated. Plant Cell, **16**, 1276-1287.

Beaulieu, C., Boccara, M. and Van Gijsegem, F. (1993). Pathogenic behavior of pectinase-defective *Erwinia chrysanthemi* mutants on different plants. Mol. Plant-Microbe Interact., **6**, 197-202.

Bednarek, S.Y. and Raikhel, N.V. (1992). Intracellular Trafficking of Secretory Proteins. Plant Mol. Biol., **20**, 133-150.

Benhamou, N., Grenier, J. and Chrispeels, M.J. (1991). Accumulation of β-fructosidase in the cell walls of tomato roots following infection by a fungal wilt pathogen. Plant Physiol., **97**, 739-750.

Beresovsky, N., Kopelman, I.J. and Mizrahi, S. (1995). The Role of Pulp Interparticle Interaction in Determining Tomato Juice Viscosity. Journal of Food Processing and Preservation, **19**, 133-146.

Bergelson, J., Kreitman, M., Stahl, E.A. and Tian, D. (2001). Evolutionary dynamics of plant R-genes. Science, **292**, 2281-2285.

Blobel, G. (1980). Intracellular protein topogenesis. Proceedings of the National Academy of Sciences USA, **77**, 1496-1500.

Boccara, M. and Chatain, V. (1989). Regulation and role in pathogenicity of *Erwinia chrysanthemi* 3937 pectin methylesterase. J. Bacteriol., **171**, 4085-4087.

Bock, W., Dongowski, G., Göbel, H. and Krause, M. (1975). Nachweis der hemmung mikrobieller pektin- und pektat lyase durch pflanzeneigene inhibitoren. Die Nahrung, **19**, 411-416.

Bordenave, M. and Goldberg, R. (1993). Purification and characterization of pectin methylesterases from Mung bean hypocotyl cell walls. Phytochemistry, **33**, 999-1003.

Bosch, M., Cheung, A.Y. and Hepler, P.K. (2005). Pectin methylesterase, a regulator of pollen tube growth. Plant Physiol, **138**, 1334-1346.

Bosch, M. and Hepler, P.K. (2005). Pectin methylesterases and pectin dynamics in pollen tubes. Plant Cell, **17**, 3219-3226.

Bournay, A., Hedley, P., Maddison, A., Waugh, R. and Machray, G. (1996). Exon skipping induced by cold stress in a potato invertase gene transcript. Nucl Acids Res, **24**, 2347-2351.

Bourne, M. (2002). Food Texture and Viscosity: Concept and Measurement (Food Science and Technology International Series). (Food Science and Technology International Series), Academic Press,New York,

Bracho, G.E. and Whitaker (1990a). Purification and partial characterization of potato (*Solanum tuberosum*) invertase and its endogenous proteinaceous Inhibitor. PlantPhysiol, **92**, -386

Bracho, G.E. and Whitaker, J.R. (1990b). Characteristics of the Inhibition of Potato (Solanum-Tuberosum) Invertase by An Endogenous Proteinaceous Inhibitor in Potatoes. Plant Physiol., **92**, 381-385.

Brady, C.J. (1987). Fruit ripening. Annu. Rev. Plant Physiol., **38**, 155-178.

Brito, N., Espino, J.J. and Gonzalez, C. (2006). The endo-beta-1,4-xylanase xyn11A is required for virulence in Botrytis cinerea. Mol. Plant-Microbe Interact., **19**, 25-32.

Brown, M.M., Hall, J.L. and Ho, L.C. (1997). Sugar uptake by protoplasts isolated from tomato fruit tissues during various stages of fruit growth. Physiologia Plantarum, **101**, 533-539.

Brummell, D.A. and Harpster, M.H. (2001). Cell wall metabolism in fruit softening and quality and its manipulation in transgenic plants. Plant Mol. Biol., **47**, 311-340.

Brutus, A., Reca, I.B., Herga, S., Mattei, B., Puigserver, A., Chaix, J.C., Juge, N., Bellincampi, D. and Giardina, T. (2005). A family 11 xylanase from the pathogen Botrytis cinerea is inhibited by plant endoxylanase inhibitors XIP-I and TAXI-I. Biochem. Biophys. Res. Commun., **337**, 160-166.

Brutus, A., Villard, C., Durand, A., Tahir, T., Furniss, C., Puigserver, A., Juge, N. and Giardina, T. (2004). The inhibition specificity of recombinant Penicillium funiculosum xylanase B towards wheat proteinaceous inhibitors. Biochimica et Biophysica Acta-Proteins and Proteomics, **1701**, 121-128.

Bucheli, P. and Devaud, S. (1994). Sugar Accumulation in Tomato and Partial-Purification of Buffer-Insoluble Invertase. Phytochemistry, **36**, 837-841.

Bugbee, W.M. (1993). A pectin lyase inhibitor protein from cell walls of sugar beet. Phytopathology, **83**, 63-68.

C.Versteeg, F.Romboutos, C.Spansen and W.Pilnik (1980). Thermostability and orange juice cloud destabilizing properties of multiple pectinesterases from orange. J. Food Sci., **45**, 969-971.

Camardella, L., Carratore, V., Ciardiello, M.A., Servillo, L., Balestrieri, C. and Giovane, A. (2000). Kiwi protein inhibitor of pectin methylesterase amino-acid sequence and structural importance of two disulfide bridges. Eur. J. Biochem., **267**, 4561-4565.

Castaldo, D., Laratta, B., Loiudice, R., Giovane, A., Quagliuolo, L. and Servillo, L. (1997). Presence of residual pectin methylesterase activity in thermally stabilized industrial fruit preparations. Food Science and Technology-Lebensmittel-Wissenschaft & Technologie, **30**, 479-484.

Castaldo, D., Lovoi, A., Quagliuolo, L., Servillo, L., Balestrieri, C. and Giovane, A. (1991). Orange juices and concentrates stabilization by a proteic inhibitor of pectin methylesterase. J. Food Sci., **56**, 1632-1634.

Castaldo, D., Villari, G., Laratta, B., Impembo, M., Giovane, A., Fasanaro, G. and Servillo, L. (1996). Preparation of high-consistency diced tomatoes by immersion in calcifying solutions. A pilot plant study. Journal of Agricultural and Food Chemistry, **44**, 2600-2607.

Catoire, L., Pierron, M., Morvan, C., Du Penhoat, C.H. and Goldberg, R. (1998). Investigation of the action patterns of pectinmethylesterase isoforms through kinetic analyses and NMR spectroscopy. Implications In cell wall expansion. J. Biol. Chem., **273**, 33150-33156.

Charng, Y.Y., Juang, R.H., Su, J.C. and Sung, H.Y. (1994). Partial-Purification and Characterization of Invertase Isozymes from Rice Grains (Oryza-Sativa). Biochem. Mol. Biol. Int., **33**, 607-615.

Chen, M.H., Sheng, J., Hind, G., Handa, A.K. and Citovsky, V. (2000). Interaction between the tobacco mosaic virus movement protein and host cell pectin methylesterases is required for viral cell-to-cell movement. EMBO J., **19**, 913-920.

Chen, M.-H. and Citovsky, V. (2003). Systemic movement of a tobamovirus requires host cell pectin methylesterase. Plant J., **35**, 386-392.

Cheng, W.H., Taliercio, E.W. and Chourey, P.S. (1996). The *Miniature 1* seed locus of maize encodes a cell-wall invertase required for natural development of endosperm and maternal cells in the pedicel. Plant Cell, **8**, 971-983.

Chrispeels, M.J. and Raikhel, N.V. (1992). Short Peptide Domains Target Proteins to Plant Vacuoles. Cell, **68**, 613-616.

Christensen, T.M.I.E., Nielsen, J.E., Kreiberg, J.D., Rasmussen, P. and Mikkelsen, J.D. (1998). Pectin methyl esterase from orange fruit: characterization and localization by in-situ hybridization and immunohistochemistry. Planta, **206**, 493-503.

Chun, J.P. and Huber, D.J. (1998). Polygalacturonase-mediated solubilization and depolymerization of pectic polymers in tomato fruit cell walls - Regulation by pH and ionic conditions. Plant Physiol., **117**, 1293-1299.

Ciardiello, M.A., D'Avino, R., Amoresano, A., Tuppo, L., Carpentieri, A., Carratore, V., Tamburrini, M., Giovane, A., Pucci, P. and Camardella, L. (2008). The peculiar structural features of kiwi fruit pectin methylesterase: Amino acid sequence, oligosaccharides structure, and modeling of the interaction with its natural proteinaceous inhibitor. Proteins, **71**, 195-206.

Collmer, A. and Keen, N.T. (1986). The role of pectic enzymes in plant pathogenesis. Annu. Rev. Phytopathol., **24**, 383-409.

Corredig, M., Kerr, W. and Wicker, L. (2001). Particle size distribution of orange juice cloud after addition of sensitized pectin. Journal of Agricultural and Food Chemistry, **49**, 2523-2526.

Côté, F. and Hahn, M.G. (1994). Oligosaccharins: structures and signal transduction. Plant Mol. Biol., **26**, 1379-1411.

Coutinho, P.M. and Henrissat, B. (1999). Carbohydrate-active enzymes: an integrated database approach. In Recent Advances in Carbohydrate Bioengineering (Gilbert, H.J. et al., eds). TheRoyal Society of Chemistry, 3-12.

D'Avino, R., Camardella, L., Christensen, T.M., Giovane, A. and Servillo, L. (2003). Tomato pectin methylesterase: modeling, fluorescence, and inhibitor interaction studies-comparison with the bacterial (Erwinia chrysanthemi) enzyme. Proteins, **53**, 830-839.

D'Ovidio, R., Mattei, B., Roberti, S. and Bellincampi, D. (2004a). Polygalacturonases, polygalacturonase-inhibiting proteins and pectic oligomers in plant-pathogen interactions. Biochim. Biophys. Acta, **1696**, 237-244.

D'Ovidio, R., Raiola, A., Capodicasa, C., Devoto, A., Pontiggia, D., Roberti, S., Galletti, R., Conti, E., O'Sullivan, D. and De Lorenzo, G. (2004b). Characterization of the complex locus of bean encoding polygalacturonase-inhibiting proteins reveals subfunctionalization for defense against fungi and insects. Plant Physiol., **135**, 2424-2435.

De Lorenzo, G., D'Ovidio, R. and Cervone, F. (2001). The role of polygacturonase-inhibiting proteins (PGIPs) in defense against pathogenic fungi. Annu. Rev. Phytopathol., **39**, 313-335.

De Paepe, A., Vuylsteke, M., Van Hummelen, P., Zabeau, M. and van der Straeten, D. (2004). Transcriptional profiling by cDNA-AFLP and microarray analysis reveals novel insights into the early response to ethylene in Arabidopsis. Plant Journal, **39**, 537-559.

Delincee, H. (1976). Thin-layer isoelectric focusing of multiple forms of tomato pectinesterase. Phytochemistry, **15**, 903-906.

Denes, J.M., Baron, A., Renard, C.M., Pean, C. and Drilleau, J.F. (2000). Different action patterns for apple pectin methylesterase at pH 7.0 and 4.5. Carbohydr. Res., **327**, 385-393.

Di Matteo, A., Giovane, A., Raiola, A., Camardella, L., Bonivento, D., De Lorenzo, G., Cervone, F., Bellincampi, D. and Tsernoglou, D. (2005). Structural Basis for the Interaction between Pectin Methylesterase and a Specific Inhibitor Protein. Plant Cell, **17**, 849-858.

Divol, F., Vilaine, F., Thibivilliers, S., Amselem, J., Palauqui, J.C., Kusiak, C. and Dinant, S. (2005). Systemic response to aphid infestation by Myzus persicae in the phloem of Apium graveolens. Plant Mol. Biol., **57**, 517-540.

Dongowski G and Bock W (1984). On the effects of molecular-parameters of pectin-substrates on the activities of pectin-esterases from *Aspergillus niger* and from higher plants. Nahrung-Food, **28**, 507-516.

Dorokhov, Y.L., Frolova, O.Y., Skurat, E.V., Ivanov, P.A., Gasanova, T.V., Sheveleva, A.A., Ravin, N.V., Makinen, K.M., Klimyuk, V.I., Skryabin, K.G., Gleba, Y.Y. and

Atabekov, J.G. (2006a). A novel function for a ubiquitous plant enzyme pectin methylesterase: The enhancer of RNA silencing. FEBS Lett., **580**, 3872-3878.

Dorokhov, Y.L., Skurat, E.V., Frolova, O.Y., Gasanova, T.V., Ivanov, P.A., Ravin, N.V., Skryabin, K.G., Makinen, K.M., Klimyuk, V.I., Gleba, Y.Y. and Atabekov, J.G. (2006b). Role of the leader sequence in tobacco pectin methylesterase secretion. FEBS Lett., **580**, 3329-3334.

Duvetter T, Fraeye I, Sila DN, Verlent I, Smout C, Hendrickx M and Van Loey A (2006). Mode of de-esterification of alkaline and acidic pectin methyl esterases at different pH conditions. J Agric FoodChem, **54**, 7825-7831.

Ehness, R., Ecker, M., Godt, D.E. and Roitsch, T. (1997). Glucose and stress independently regulate source and sink metabolism and defense mechanisms via signal transduction pathways involving protein phosphorylation. Plant Cell, **9**, 1825-1841.

Ehneÿ , R., Ecker, M., Godt, D.E. and Roitsch, T. (1997). Glucose and stress independently regulate source and sink metabolism and defense mechanisms via signal transduction pathways involving protein phosphorylation. Plant Cell, **9**, 1825-1841.

Elliott, G.O., Hughes, R.K., Juge, N., Kroon, P.A. and Williamson, G. (2002). Functional identification of the cDNA coding for a wheat endo-1,4-beta- D-xylanase inhibitor(1). FEBS Lett., **519**, 66-70.

Elliott, K.J., Butler, W.O., Dickinson, C.D., Konno, Y., Vedvick, T.S., Fitzmaurice, L. and Mirkov, T.E. (1993). Isolation and Characterization of Fruit Vacuolar Invertase Genes from 2 Tomato Species and Temporal Differences in Messenger-Rna Levels During Fruit Ripening. Plant Mol. Biol., **21**, 515-524.

Eufinger, J.D. (2006). Regulation of taproot development and sucrose stabilization in sugar beet: Influence of invertase inhibitors and occurrence of mitochondrial energy-dissipating proteins. PhD defensis,

Federici, L., Di Matteo, A., Fernandez-Recio, J., Tsernoglou, D. and Cervone, F. (2006). Polygalacturonase inhibiting proteins: players in plant innate immunity? Trends Plant Sci., **11**, 65-70.

Felsenstein, J. (1985). Confidence limits on phylogenies: An approach using the bootstrap. Evolution, **39**, 783-791.

Fierens, E., Rombouts, S., Gebruers, K., Goesaert, H., Brijs, K., Beaugrand, J., Volckaert, G., van Campenhout, S., Proost, P., Courtin, C.M. and Delcour, J.A. (2007). TLXI, a novel type of xylanase inhibitor from wheat (Triticum aestivum) belonging to the thaumatin family. Biochem. J., **403**, 583-591.

Flatman, R., McLauchlan, W.R., Juge, N., Furniss, C.S., Berrin, J.G., Hughes, R.K., Manzanares, P., Ladbury, J.E., O'Brien, R. and Williamson, G. (2002). Interactions defining the specificity between fungal xylanases and the wheat proteinaceous inhibitor, XIP-I. Biochem. J., **365**, 773-781.

Francis, K.E., Lam, S.Y. and Copenhaver, G.P. (2006). Separation of Arabidopsis pollen tetrads Is regulated by QRT1, a pectin methylesterase gene. Plant Physiol, **, in press**,

Fries, M., Ihrig, J., Brocklehurst, K., Shevchik, V.E. and Pickersgill, R.W. (2007). Molecular basis of the activity of the phytopathogen pectin methylesterase. EMBO J., **26**, 3879-3887.

Furniss, C.S.M., Williamson, G. and Kroon, P.A. (2005). The substrate specificity and susceptibility to wheat inhibitor proteins of Penicillium funiculosum xylanases from a commercial enzyme preparation. J. Sci. Food Agric., **85**, 574-582.

Futamura, N., Mori, H., Kouchi, H. and Shinohara, K. (2000). Male flower-specific expression of genes for polygalacturonase, pectin methylesterase and beta-1,3-glucanase in a dioecious willow (*Salix gilgiana* Seemen). Plant Cell Physiol, **41**, 16-26.

Gaffe, J., Tieman, D.M. and Handa, A.K. (1994). Pectin methylesterase isoforms in tomato (*Lycopersicon esculentum*) tissues. Effects of expression of a pectin methylesterase antisense gene. Plant Physiol., **105**, 199-203.

Gaffe, J., Tiznado, M.E. and Handa, A.K. (1997). Characterization and functional expression of a ubiquitously expressed tomato pectin methylesterase. Plant Physiol., **114**, 1547-1556.

Gebruers, K., Brijs, K., Courtin, C.M., Fierens, K., Goesaert, H., Rabijns, A., Raedschelders, G., Robben, J., Sansen, S., Sorensen, J.F., van Campenhout, S. and Delcour, J.A. (2004). Properties of TAXI-type endoxylanase inhibitors. Biochimica et Biophysica Acta-Proteins and Proteomics, **1696**, 213-221.

Gebruers, K., Debyser, W., Goesaert, H., Proost, P., van Damme, J. and Delcour, J.A. (2001). Triticum aestivum L. endoxylanase inhibitor (TAXI) consists of two inhibitors, TAXI I and TAXI II, with different specificities. Biochem. J., **353**, 239-244.

Geigenberger, P. and Stitt, M. (1993). Sucrose Synthase Catalyzes A Readily Reversible-Reaction Invivo in Developing Potato-Tubers and Other Plant-Tissues. Planta, **189**, 329-339.

Geisler-Lee, J., Geisler, M., Coutinho, P.M., Segerman, B., Nishikubo, N., Takahashi, J., Aspeborg, H., Djerbi, S., Master, E., Andersson-Gunneras, S., Sundberg, B., Karpinski, S., Teeri, T.T., Kleczkowski, L.A., Henrissat, B. and Mellerowicz, E.J. (2006). Poplar carbohydrate-active enzymes. Gene identification and expression analyses. Plant Physiology, **140**, 946-962.

Giovane, A., Servillo, L., Balestrieri, C., Raiola, A., D'Avino, R., Tamburrini, M., Ciardiello, M.A. and Camardella, L. (2004). Pectin methylesterase inhibitor. Biochim. Biophys. Acta, **1696**, 245-252.

Godt, D.E. and Roitsch, T. (1997). Regulation and tissue-specific distribution of mRNAs for three extracellular invertase isoenzymes of tomato suggests an important function in establishing and maintaining sink metabolism. Plant Physiol., **115**, 273-282.

Goesaert, H., Elliott, G., Kroon, P.A., Gebruers, K., Courtin, C.M., Robben, J., Delcour, J.A. and Juge, N. (2004). Occurrence of proteinaceous endoxylanase inhibitors in cereals. Biochimica et Biophysica Acta-Proteins and Proteomics, **1696**, 193-202.

Goetz, M. and Roitsch, T. (1999). The different pH optima and substrate specificities of extracellular and vacuolar invertases from plants are determined by a single amino-acid substitution. Plant Journal, **20**, 707-711.

Grandillo, S. and Tanksley, S.D. (1996). QTL analysis of horticultural traits differentiating the cultivated tomato from the closely related species Lycopersicon pimpinellifolium. Theoretical and Applied Genetics, **92**, 935-951.

Greer, J. (1990). Comparative Modeling of Proteins in the Design of Novel Renin Inhibitors. Biophys. J., **57**, A207

Greiner, S., Koster, U., Lauer, K., Rosenkranz, H., Vogel, R. and Rausch, T. (2000). Plant invertase inhibitors: expression in cell culture and during plant development. Aust. J. Plant Physiol., **27**, 807-814.

Greiner, S., Krausgrill, S. and Rausch, T. (1998). Cloning of a tobacco apoplasmic invertase inhibitor. Proof of function of the recombinant protein and expression analysis during plant development. Plant Physiol, **116**, 733-742.

Greiner, S., Rausch, T., Sonnewald, U. and Herbers, K. (1999). Ectopic expression of a tobacco invertase inhibitor homolog prevents cold-induced sweetening of potato tubers. Nat. Biotechnol., **17**, 708-711.

Grishutin, S.G., Gusakov, A.V., Markov, A.V., Ustinov, B.B., Semenova, M.V. and Sinitsyn, A.P. (2004). Specific xyloglucanases as a new class of polysaccharide-degrading enzymes. Biochimica et Biophysica Acta-General Subjects, **1674**, 268-281.

Hall, L.N., Bird, C.R., Picton, S., Tucker, G.A., Seymour, G.B. and Grierson, D. (1994). Molecular Characterization of Cdna Clones Representing Pectin Esterase Isozymes from Tomato. Plant Mol. Biol., **25**, 313-318.

Hall, L.N., Tucker, G.A., Smith, C.J.S., Watson, C.F., Seymour, G.B., Bundick, Y., Boniwell, J.M., Fletcher, J.D., Ray, J.A., Schuch, W., Bird, C.R. and Grierson, D. (1993). Antisense inhibition of pectin esterase gene expression in transgenic tomatoes. Plant J., **3**, 121-129.

Hall, T.A. (1999). BioEdit: a user-friendly biological sequence alignment editor and analysis program for Windows 95/98/NT. Nucleic Acids Symp. Ser., **41**, 95-98.

Harriman, R.W., Tieman, D.M. and Handa, A.K. (1991). Molecular cloning of tomato pectin methylesterase gene and its expression in Rutgers, ripening inhibitor, nonripening, and never ripe tomato fruits. Plant Physiol., **97**, 80-87.

Hasunuma, T., Fukusaki, E. and Kobayashi, A. (2004). Expression of fungal pectin methylesterase in transgenic tobacco leads to alteration in cell wall metabolism and a dwarf phenotype. J. Biotechnol., **111**, 241-251.

Henrissat, B. (1991). A classification of glycosyl hydrolases based on amino acid sequence similarities. Biochem. J., **280 (Pt 2)**, 309-316.

Henrissat, B. and Davies, G. (1997). Structural and sequence-based classification of glycoside hydrolases. Curr. Opin. Struct. Biol., **7**, 637-644.

Henrissat, B., Heffron, S.E., Yoder, M.D., Lietzke, S.E. and Jurnak, F. (1995). Functional implications of structure-based sequence alignment of proteins in the extracellular pectate lyase superfamily. Plant Physiol., **107**, 963-976.

Hertzberg, M., Aspeborg, H., Schrader, J., Andersson, A., Erlandsson, R., Blomqvist, K., Bhalerao, R., Uhlen, M., Teeri, T.T., Lundeberg, J., Sundberg, B., Nilsson, P. and Sandberg, G. (2001). A transcriptional roadmap to wood formation. Proc. Natl. Acad. Sci. U. S. A, **98**, 14732-14737.

Heyer, A.G., Raap, M., Schroeer, B., Marty, B. and Willmitzer, L. (2004). Cell wall invertase expression at the apical meristem alters floral, architectural, and reproductive traits in Arabidopsis thaliana. Plant Journal, **39**, 161-169.

Hothorn, M., D'Angelo, I., Marquez, J.A., Greiner, S. and Scheffzek, K. (2004a). The invertase inhibitor Nt-CIF from tobacco: a highly thermostable four-helix bundle with an unusual N-terminal extension. J. Mol. Biol., **335**, 987-995.

Hothorn, M., Wolf, S., Aloy, P., Greiner, S. and Scheffzek, K. (2004b). Structural insights into the target specificity of plant invertase and pectin methylesterase inhibitory proteins. Plant Cell, **16**, 3437-3447.

Husain, S.E., Thomas, B.J., Kingston-Smith, A.H. and Foyer, C.H. (2001). Invertase protein, but not activity, is present throughout development of Lycopersicon esculentum and L-pimpinellifolium fruit. New Phytologist, **150**, 73-81.

Irifune, K., Nishida, T., Egawa, H. and Nagatani, A. (2004). Pectin methylesterase inhibitor cDNA from kiwi fruit. Plant Cell Rep.,

Isla, M.I., Vattuone, M.A., Ordonez, R.M. and Sampietro, A.R. (1999). Invertase activity associated with the walls of Solanum tuberosum tubers. Phytochemistry, **50**, 525-534.

Jahr, H., Dreier, J., Meletzus, D., Bahro, R. and Eichenlaub, R. (2000). The endo-beta-1,4-glucanase CelA of Clavibacter michiganensis subsp michiganensis is a pathogenicity determinant required for induction of bacterial wilt of tomato. Mol. Plant-Microbe Interact., **13**, 703-714.

Jaynes, T.A. and Nelson, O.E. (1971). An invertase inhibitor in maize endosperm and factors aecting inactivation. Plant Physiol, **47**, 629-634.

Jenkins, J., Mayans, O., Smith, D., Worboys, K. and Pickersgill, R.W. (2001). Three-dimensional structure of Erwinia chrysanthemi pectin methylesterase reveals a novel esterase active site. J. Mol. Biol., **305**, 951-960.

Jenkins, J. and Pickersgill, R. (2001). The architecture of parallel beta-helices and related folds. Prog. Biophys. Mol. Biol., **77**, 111-175.

Ji X, Van den Ende W, Van Laere A, Cheng S and Bennett J (2005). Structure,evolution and expression of the two invertase gene families of rice. J MolEvol, **60**, 615-634.

Jiang, C.M., Li, C.P., Chang, J.C. and Chang, H.M. (2002). Characterization of pectinesterase inhibitor in jelly fig (Ficus awkeotsang Makino) achenes. J Agric. Food Chem., **50**, 4890-4894.

Jiang, L., Yang, S.L., Xie, L.F., Puah, C.S., Zhang, X.Q., Yang, W.C., Sundaresan, V. and Ye, D. (2005). VANGUARD1 Encodes a Pectin Methylesterase That Enhances Pollen Tube Growth in the Arabidopsis Style and Transmitting Tract. Plant Cell, **17**, 584-596.

Johansson, K., El Ahmad, M., Friemann, R., Jornvall, H., Markovic, O. and Eklund, H. (2002). Crystal structure of plant pectin methylesterase. FEBS Lett., **514**, 243-249.

Juge, N. (2006). Plant protein inhibitors of cell wall degrading enzymes. Trends in plant science, **11**, 359-367.

Juge, N., Payan, F. and Williamson, G. (2004). XIP-I, a xylanase inhibitor protein from wheat: a novel protein function. Biochimica et Biophysica Acta-Proteins and Proteomics, **1696**, 203-211.

Karuppiah, N., Vadlamudi, B. and Kaufman, P.B. (1989). Purification and characterization of soluble (cytosolic) and bound (cell wall) isoforms of invertases in barley (Hordeum vulgare) elongating stem tissue. Plant Physiol., **91**, 993-998.

Klann, E.M., Hall, B. and Bennett, A.B. (1996). Antisense acid invertase (TIV1) gene alters soluble sugar composition and size in transgenic tomato fruit. Plant Physiol., **112**, 1321-1330.

Kohn R, Dongowski G and Bock W (1985). The distribution of free and esterified carboxyl groups within the pectin molecule after the influence of pectin esterase from Aspergillus niger and oranges. Nahrung-Food, **29**, 75-85.

Konno, Y., Vedvick, T., Fitzmaurice, L. and Mirkov, T.E. (1993). Purification, Characterization, and Subcellular-Localization of Soluble Invertase from Tomato Fruit. J. Plant Physiol., **141**, 385-392.

Krall, S.M. and McFeeters, R.F. (1998). Pectin hydrolysis: Effect of temperature, degree of methylation, pH, and calcium on hydrolysis rates. Journal of Agricultural and Food Chemistry, **46**, 1311-1315.

Krausgrill, S., Greiner, S., Koster, U., Vogel, R. and Rausch, T. (1998a). In transformed tobacco cells the apoplasmic invertase inhibitor operates as a regulatory switch of cell wall invertase. Plant Journal, **13**, 275-280.

Krausgrill, S., Greiner, S., Koster, U., Vogel, R. and Rausch, T. (1998b). In transformed tobacco cells the apoplasmic invertase inhibitor operates as a regulatory switch of cell wall invertase. Plant Journal, **13**, 275-280.

Le Roy, K., Lammens, W., Verhaest, M., De Coninck, B., Rabijns, A., Van Laere, A. and Van den Ende, W. (2007). Unraveling the difference between invertases and fructan exohydrolases: A single amino acid (Asp-239) substitution transforms Arabidopsis cell wall invertase1 into a fructan 1-exohydrolase. Plant Physiol., **145**, 616-625.

Lee, H.S., Karunanandaa, B., McCubbin, A., Gilroy, S. and Kao, T. (1996). *PRK1*, a receptor-like kinase of *Petunia inflata*, is essential for postmeiotic development of pollen. Plant Journal, **9**, 613-624.

Lee, H.S. and Sturm, A. (1996). Purification and characterization of neutral and alkaline invertase from carrot. Plant Physiol., **112**, 1513-1522.

Lee, J.Y. and Lee, D.H. (2003). Use of serial analysis of gene expression technology to reveal changes in gene expression in Arabidopsis pollen undergoing cold stress. Plant Physiol., **132**, 517-529.

Lev, S. and Horwitz, B.A. (2003). A mitogen-activated protein kinase pathway modulates the expression of two cellulase genes in Cochliobolus heterostrophus during plant infection. Plant Cell, **15**, 835-844.

Li, Y.Q., Mareck, A., Faleri, C., Moscatelli, A., Liu, Q. and Cresti, M. (2002). Detection and localization of pectin methylesterase isoforms in pollen tubes of Nicotiana tabacum L. Planta, **214**, 734-740.

Limberg, G., Korner, R., Buchholt, H.C., Christensen, T.M., Roepstorff, P. and Mikkelsen, J.D. (2000). Analysis of different de-esterification mechanisms for pectin by enzymatic fingerprinting using endopectin lyase and endopolygalacturonase II from A. niger. Carbohydr. Res., **327**, 293-307.

Lin, S.S. and Sung, H.Y. (1993). Partial-Purification and Characterization of Soluble Acid Invertases from Rice (Oryza-Sativa) Leaves. Biochem. Mol. Biol. Int., **31**, 945-953.

Link, M., Rausch, T. and Greiner, S. (2004). In Arabidopsis thaliana, the invertase inhibitors AtC/VIF1 and 2 exhibit distinct target enzyme specificities and expression profiles. FEBS Lett., **573**, 105-109.

Lionetti, V., Raiola, A., Camardella, L., Giovane, A., Obel, N., Pauly, M., Favaron, F., Cervone, F. and Bellincampi, D. (2007). Overexpression of pectin methylesterase inhibitors in Arabidopsis restricts fungal infection by *Botrytis cinerea*. Plant Physiol, **143**, 1871-1880.

Lord, E. (2000). Adhesion and cell movement during pollination: cherchez la femme. Trends Plant Sci., **5**, 368-373.

Lorenz, K., Lienhard, S. and Sturm, A. (1995). Structural Organization and Differential Expression of Carrot Beta-Fructofuranosidase Genes - Identification of A Gene Coding for A Flower Bud-Specific Isozyme. Plant Mol. Biol., **28**, 189-194.

Loreti, E., Bellincampi, D., Millet, C., Alpi, A. and Perata, P. (2002). Elicitors of defence responses repress a gibberellin signalling pathway in barley embryos. J. Plant Physiol., **159**, 1383-1386.

Ly-Nguyen, B., Van Loey, A.M., Fachin, D., Verlent, I., Duvetter, T., Vu, S.T., Smout, C. and Hendrickx, M.E. (2002a). Strawberry pectin methylesterase (PME): Purification, characterization, thermal and high-pressure inactivation. Biotechnology Progress, **18**, 1447-1450.

Ly-Nguyen, B., Van Loey, A.M., Fachin, D., Verlent, I., Indrawati and Hendrickx, M.E. (2002b). Partial purification, characterization, and thermal and high-pressure inactivation of pectin methylesterase from carrots (Daucus carrota L.). Journal of Agricultural and Food Chemistry, **50**, 5437-5444.

Ly-Nguyen, B., Van Loey, A.M., Smout, C., Verlent, I., Duvetter, T. and Hendrickx, M.E. (2004). Effect of intrinsic and extrinsic factors on the interaction of plant pectin methylesterase and its proteinaceous inhibitor from kiwi fruit. J. Agric. Food Chem., **52**, 8144-8150.

M.Chii, C.Ming, H.W. and M.Hung (2001). Change in particle size of pectin reacted with pectinesterase isozymes from pea (Pisum sativum L.)

sprout. J. Agric. Food Chem*,* **49**, 4383-4387.

Markovic, O. and Janecek, S. (2004). Pectin methylesterases: sequence-structural features and phylogenetic relationships. Carbohydr. Res*.,* **339**, 2281-2295.

Marty, P., Jouan, B., Bertheau, Y., Vian, B. and Goldberg, R. (1997). Charge density in stem cell walls of solanum tuberosum genotypes and susceptibility to blackleg. Phytochemistry*,* **44**, 1435-1441.

Matsouka, K.n.K. (1991). Propeptide of a precursor to a plant vacuolar protein required for vacuolar targeting. Proceedings of the National Academy of Sciences USA*,* **88**, 843-838.

Matsudaira, P. (1987). Sequence from picomole quantities of proteins electroblotted onto polyvinylidene difluoride membranes. J. Biol. Chem*.,* **262**, 10035-10038.

Mattei, B., Raiola, A., Caprari, C., Federici, L., Bellincampi, D., De Lorenzo, G., Cervone, F., Giovane, A., and Camardella, L. (2002). Studies on plant inhibitors of pectin modifying enzymes: polygalacturonase-inhibiting protein (PGIP) and pectin methylesterase inhibitor (PMEI). In Carbohydrate Bioengineering - Interdisciplinary approaches, T.T.Teeri, B.Svensson, H.J.Gilbert, and T.Feizi, eds pp. 160-167.

McMillan, G.P., Hedley, D., Fyffe, L. and Pérombelon, M.C.M. (1993a). Potato resistance to soft-rot erwinias is related to cell wall pectin esterification. Physiol. Mol. Plant Pathol*.,* **42**, 279-289.

McMillan, G.P., Hedley, D. and Pérombelon, M.C.M. (1993b). Activation of pectate lyase from *Erwinia carotovora* subsp. *atroseptica* by potato tuber tissue extract. Physiol. Mol. Plant Pathol*.,* **42**, 1-8.

Mei, X.H., Hao, Y.L., Zhu, H.L., Gao, H.Y. and Luo, Y.B. (2007). Cloning of pectin methylesterase inhibitor from kiwi fruit and its high expression in Pichia pastoris. Enzyme Microb. Technol*.,* **40**, 1001-1005.

Micheli, F. (2001). Pectin methylesterases: cell wall enzymes with important roles in plant physiology. Trends Plant Sci*.,* **6**, 414-419.

Micheli, F., Sundberg, B., Goldberg, R. and Richard, L. (2000). Radial distribution pattern of pectin methylesterases across the cambial region of hybrid aspen at activity and dormancy. Plant Physiol*,* **124**, 191-199.

Miron, D., Petreikov, M., Carmi, N., Shen, S., Levin, I., Granot, D., Zamski, E. and Schaffer, A.A. (2002). Sucrose uptake, invertase localization and gene expression in developing fruit of Lycopersicon esculentum and the sucrose-accumulating Lycopersicon hirsutum. Physiol. Plant*.,* **115**, 35-47.

Moscatiello, R., Mariani, P., Sanders, D. and Maathuis, F.J.M. (2006). Transcriptional analysis of calcium-dependent and calcium-independent signalling pathways induced by oligogalacturonides. Journal of Experimental Botany*,* **57**, 2847-2865.

Moustacas, A.-M., Nari, J., Borel, M., Noat, G. and Ricard, J. (1991). Pectin methylesterase, metal ions and plant cell-wall extension. The role of metal ions in plant cell-wall extension. Biochem. J*.,* **279**, 351-354.

Obenland, D.M., Simmen, U., Boller, T. and Wiemken, A. (1993). Purification and Characterization of 3 Soluble Invertases from Barley (Hordeum-Vulgare L) Leaves. Plant Physiol., **101**, 1331-1339.

Ohyama, A., Ito, H., Sato, T., Nishimura, S., Imai, T. and Hirai, M. (1995). Suppression of Acid Invertase Activity by Antisense Rna Modifies the Sugar Composition of Tomato Fruit. Plant and Cell Physiology, **36**, 369-376.

Payan, F., Flatman, R., Porciero, S., Williamson, G., Juge, N. and Roussel, A. (2003). Structural analysis of XIP-1, a proteinaceous xylanase inhibitor from wheat. Biochem. J., **Pt**,

Payan, F., Leone, P., Porciero, S., Furniss, C., Tahir, T., Williamson, G., Durand, A., Manzanares, P., Gilbert, H.J., Juge, N. and Roussel, A. (2004). The dual nature of the wheat xylanase protein inhibitor XIP-I - Structural basis for the inhibition of family 10 and family 11 xylanases. Journal of Biological Chemistry, **279**, 36029-36037.

Pelloux, J., Rusterucci, C. and Mellerowicz, E.J. (2007). New insights into pectin methylesterase structure and function. Trends in plant science, **12**, 267-277.

Penuelas, J., Filella, I., Stefanescu, C. and Llusia, J. (2005). Caterpillars of Euphydryas aurinia (Lepidoptera : Nymphalidae) feeding on Succisa pratensis leaves induce large foliar emissions of methanol. New Phytol., **167**, 851-857.

Pfaffl, M.W. (2001). A new mathematical model for relative quantification in real-time RT-PCR. Nucleic Acids Res., **29**, e45

Pilling, J., Willmitzer, L., Bucking, H. and Fisahn, J. (2004). Inhibition of a ubiquitously expressed pectin methyl esterase in Solanum tuberosum L. affects plant growth, leaf growth polarity, and ion partitioning. Planta, **219**, 32-40.

Pilling, J., Willmitzer, L. and Fisahn, J. (2000). Expression of a Petunia inflata pectin methyl esterase in Solanum tuberosum L. enhances stem elongation and modifies cation distribution. Planta, **210**, 391-399.

Pina, C., Pinto, F., Feijo, J.A. and Becker, J.D. (2005). Gene family analysis of the Arabidopsis pollen transcriptome reveals biological implications for cell growth, division control, and gene expression regulation. Plant Physiol, **138**, 744-756.

Pressey R and Avants JK (1972). Multiple forms of pectinesterase in tomatoes. Phytochemistry, **11**, 3139-3142.

Pressey, R. (1966). Separation and properties of potato invertase and invertase inhibitor. Arch. Biochem. Biophys., **113**, 667-674.

Pressey, R. (1968). Invertase inhibitor from red beet, sugar beet and sweet potato roots. PlantPhysiol, **43**, 1430-1434.

Pressey, R. (1994). Invertase inhibitor in tomato fruit. Phytochemistry, **36**, 543-546.

Qin, Q., Bergmann, C.W., Rose, J.K., Saladie, M., Kolli, V.S., Albersheim, P., Darvill, A.G. and York, W.S. (2003). Characterization of a tomato protein that inhibits a xyloglucan-specific endoglucanase. Plant J, **34**, 327-338.

R.Baker (1977). Process to control juice cloud. Proc. Int. Soc. Citric., **3**, 751-752.

Raiola, A., Camardella, L., Giovane, A., Mattei, B., De Lorenzo, G., Cervone, F. and Bellincampi, D. (2004). Two Arabidopsis thaliana genes encode functional pectin methylesterase inhibitors. FEBS Lett., **557**, 199-203.

Ramloch-Lorenz, K., Knudsen, S. and Sturm, A. (1993). Molecular characterization of the gene for carrot cell wall β- fructosidase. Plant J., **4**, 545-554.

Rausch, T. and Greiner, S. (2004). Plant protein inhibitors of invertases. Biochim. Biophys. Acta, **1696**, 253-261.

Ray, J., Knapp, J., Grierson, D., Bird, C. and Schuch, W. (1988). Identification and sequence determination of a cDNA clone for tomato pectin esterase. Eur. J. Biochem., **174**, 119-124.

Ren, C. and Kermode, A.R. (2000). An increase in pectin methyl esterase activity accompanies dormancy breakage and germination of yellow cedar seeds. Plant Physiol, **124**, 231-242.

Ricard, J. and Noat, G. (1986). Electrostatic effects and the dynamics of enzyme reactions at the surface of plant cells. 1. A theory of the ionic control of a complex multi-enzyme system. Eur. J. Biochem., **155**, 183-190.

Rockel, N., Wolf, S., Kost, B., Rausch, T. and Greiner, S. (2008). Elaborate spatial patterning of cell-wall PME and PMEI at the pollen tube tip involves PMEI endocytosis, and reflects the distribution of esterified and de-esterified pectins. Plant Journal, **53**, 133-143.

Roitsch, T.&.G.M. (2004). Function and regulation of plant invertases: sweet sensations. Trends Plant Sci, **9**, 606-613.

Ruan, Y.L., Chourey, P.S., Delmer, D.P. and PerezGrau, L. (1997). The differential expression of sucrose synthase in relation to diverse patterns of carbon partitioning in developing cotton seed. Plant Physiology, **115**, 375-385.

Ruan, Y.L. and Patrick, J.W. (1995). The Cellular Pathway of Postphloem Sugar-Transport in Developing Tomato Fruit. Planta, **196**, 434-444.

Saitou, N. and Nei, M. (1987). The neighbor-joining method: A new method for reconstructing phylogenetic trees. *Molecular Biology and Evolution*. Mol. Biol. Evol., **4**, 406-425.

Sali, A. and Blundell, T.L. (1993). Comparative Protein Modeling by Satisfaction of Spatial Restraints. J. Mol. Biol., **234**, 779-815.

Sambrook, J., Fritsch, E.F., and Maniatis, T. (1989). Molecular Cloning, A Laboratory Manual. In Anonymous(Cold Spring Harbor, NY, USA: Cold Spring Harbor Laboratory Press),

Sander, A., Krausgrill, S., Greiner, S., Weil, M. and Rausch, T. (1996). Sucrose protects cell wall invertase but not vacuolar invertase against proteinaceous inhibitors. Febs Letters, **385**, 171-175.

Sansen, S., De Ranter, C.J., Gebruers, K., Brijs, K., Courtin, C.M., Delcour, J.A. and Rabijns, A. (2004). Structural basis for inhibition of Aspergillus niger xylanase by Triticum aestivum xylanase inhibitor-I. J. Biol. Chem., **279**, 36022-36028.

Scognamiglio, M.A., Ciardiello, M.A., Tamburrini, M., Carratore, V., Rausch, T. and Camardella, L. (2003). The plant invertase inhibitor shares structural properties and disulfide bridges arrangement with the pectin methylesterase inhibitor. J. Prot. Chem., **22**, 363-369.

Shanmugam, V. (2005). Role of extracytoplasmic leucine rich repeat proteins in plant defence mechanisms. Microbiological Research, **160**, 83-94.

Sicilia, F., Mattei, B., Cervone, F., Bellincampi, D. and De Lorenzo, G. (2005). Characterization of a membrane-associaiated apoplastic lipoxygenase in *Phaseolus vulgaris* L. Biochim. Biophys. Acta, **1748**, 9-19.

Simpson, C.G., Hedley, P.E., Watters, J.A., Clark, G.P., McQuade, C., Machray, G.C. and Brown, J.W.S. (2000). Requirements for mini-exon inclusion in potato invertase mRNAs provides evidence for exon-scanning interactions in plants. Rna-A Publication of the Rna Society, **6**, 422-433.

Smeekens, S. (2000). Sugar-induced signal transduction in plants. Annu Rev Plant Physiol Plant Mol Biol, **51**, 49-81.

Sonnewald, U., Hajirezaei, M.R., Kossmann, J., Heyer, A., Trethewey, R.N. and Willmitzer, L. (1997). Increased potato tuber size resulting from apoplastic expression of a yeast invertase. Nat. Biotechnol., **15**, 794-797.

Sonnewald, U., Kossman, J., Mullerrober, B. and Willmitzer, L. (1991). Molecular Approaches to Influence Sink-Source Interactions in Transgenic Plants. Biological Chemistry Hoppe-Seyler, **372**, 757

Sorensen, J.F., Kragh, K.M., Sibbesen, O., Delcour, J., Goesaert, H., Svensson, B., Tahir, T.A., Brufau, J., Perez-Vendrell, A.M., Bellincampi, D., D'Ovidio, R., Camardella, L., Giovane, A., Bonnin, E. and Juge, N. (2004). Potential role of glycosidase inhibitors in industrial biotechnological applications. Biochim. Biophys. Acta, **1696**, 275-287.

Spadoni, S., Zabotina, O., Di Matteo, A., Mikkelsen, J.D., Cervone, F., DL, G., Mattei, B. and Bellincampi, D. (2006). Polygalacturonase-inhibiting protein (PGIP) interacts with pectin through a binding site formed by four clustered residues of arginine and lysine. Plant Physiol, **141**, 557-564.

Stephenson, M.B. and Hawes, M.C. (1994). Correlation of pectin methylesterase activity in root caps of pea with root border cell separation. Plant Physiol., **106**, 739-745.

Sturm, A. (1999). Invertases. Primary structures, functions, and roles in plant development and sucrose partitioning. Plant Physiol, **121**, 1-8.

Sturm, A. and Chrispeels, M.J. (1990). cDNA cloning of carrot extracellular β-fructosidase and its expression in response to wounding and bacterial infection. Plant Cell, **2**, 1107-1119.

Sturm, A., Sebkova, V., Lorenz, K., Hardegger, M., Lienhard, S. and Unger, C. (1995). Development-Specific and Organ-Specific Expression of the Genes for Sucrose Synthase and 3 Isoenzymes of Acid Beta-Fructofuranosidase in Carrot. Planta, **195**, 601-610.

Sturm, A. and Tang, G.Q. (1999). The sucrose-cleaving enzymes of plants are crucial for development, growth and carbon partitioning. Trends in plant science, **4**, 401-407.

Tahir, T.A., Berrin, J.G., Flatman, R., Roussel, A., Roepstorff, P., Williamson, G. and Juge, N. (2002). Specific characterization of substrate and inhibitor binding sites of a glycosyl hydrolase family 11 xylanase from Aspergillus niger. Journal of Biological Chemistry, **277**, 44035-44043.

Tamura, K., Dudley, J., Nei, M. and Kumar, S. (2007). MEGA4: Molecular Evolutionary Genetics Analysis (MEGA) software version 4.0. Mol. Biol. Evol., **24**, 1596-1599.

Tang, G.Q., Lüscher, M. and Sturm, A. (1999). Antisense repression of vacuolar and cell wall invertase in transgenic carrot alters early plant development and sucrose partitioning. Plant Cell, **11**, 177-189.

Tang, X.W., Ruffner, H.P., Scholes, J.D. and Rolfe, S.A. (1996). Purification and characterisation of soluble invertases from leaves of Arabidopsis thaliana. Planta, **198**, 17-23.

Tanksley, S.D., Grandillo, S., Fulton, T.M., Zamir, D., Eshed, Y., Petiard, V., Lopez, J. and BeckBunn, T. (1996). Advanced backcross QTL analysis in a cross between an elite processing line of tomato and its wild relative L-pimpinellifolium. Theoretical and Applied Genetics, **92**, 213-224.

Thakur, B.R., Singh, R.K. and Handa, A.K. (1996). Effect of an antisense pectin methylesterase gene on the chemistry of pectin in tomato (*Lycopersicon esculentum*) juice. Journal of Agricultural and Food Chemistry, **44**, 628-630.

Thompson, G.A. and Goggin, F.L. (2006). Transcriptomics and functional genomics of plant defence induction by phloem-feeding insects. Journal of Experimental Botany, **57**, 755-766.

Tian, G.W., Chen, M.H., Zaltsman, A. and Citovsky, V. (2006). Pollen-specific pectin methylesterase involved in pollen tube growth. Dev. Biol., **294**, 83-91.

Tieman, D.M. and Handa, A.K. (1994). Reduction in pectin methylesterase activity modifies tissue integrity and cation levels in ripening tomato (*Lycopersicon esculentum* Mill.) fruits. Plant Physiol., **106**, 429-436.

Tieman, D.M., Harriman, R.W., Ramamohan, G. and Handa, A.K. (1992). An antisense pectin methylesterase gene alters pectin chemistry and soluble solids in tomato fruit. Plant Cell, **4**, 667-679.

Tucker, G.A., Robertson, N.G. and Grierson, D. (1982). Purification and changes in activities of tomato pectinesterase isoenzymes. J. Sci. Fd. Agric., **33**, 396-400.

Tymowska-Lalanne, Z. and Kreis, M. (1998). The plant invertases: physiology, biochemistry and molecular biology. Adv. Bot. Res., **28**, 71-117.

Unger, C., Hardegger, M., Lienhard, S. and Sturm, A. (1994). cDNA cloning of carrot (Daucus carota) soluble acid beta-fructofuranosidases and comparison with the cell wall isoenzyme. PlantPhysiol, **104(4)**, 1351-1357.

Unger, C., Hofsteenge, J. and Sturm, A. (1992a). Purification and Characterization of A Soluble Beta-Fructofuranosidase from Daucus-Carota. Eur. J. Biochem., **204**, 915-921.

Unger, C., Hofsteenge, J. and Sturm, A. (1992b). Purification and Characterization of A Soluble Beta-Fructofuranosidase from Daucus-Carota. Eur. J. Biochem., **204**, 915-921.

van Alebeek, G.J., van Scherpenzeel, K., Beldman, G., Schols, H.A. and Voragen, A.G. (2003). Partially esterified oligogalacturonides are the preferred substrates for pectin methylesterase of Aspergillus niger. Biochem. J., **372**, 211-218.

Verde, C., Malorni, A. and Parente, A. (1989). The primary structure of papaya mosaic virus coat protein: a revision 795±805. J. Protein Chem, **8**, 795-805.

Verhaest, M., Lammens, W., Le Roy, K., De Coninck, B., De Ranter, C.J., Van Laere, A., Van den Ende, W. and Rabijns, A. (2006). X-ray diffraction structure of a cell-wall invertase from Arabidopsis thaliana. Acta Crystallographica Section D-Biological Crystallography, **62**, 1555-1563.

von Dahl, C.C., Havecker, M., Schlogl, R. and Baldwin, I.T. (2006a). Caterpillar-elicited methanol emission: a new signal in plant-herbivore interactions? Plant Journal, **46**, 948-960.

von Dahl, C.C., Havecker, M., Schlogl, R. and Baldwin, I.T. (2006b). Caterpillar-elicited methanol emission: a new signal in plant-herbivore interactions? Plant Journal, **46**, 948-960.

Von Schaewen, A., Stitt, M., Schmidt, R., Sonnewald, U. and Willmitzer, L. (1990). Expression of a yeast-derived invertase in the cell wall of tobacco and *Arabidopsis* plants leads to accumulation of carbohydrate and inhibition of photosynthesis and strongly influences growth and phenotype of transgenic tobacco plants. EMBO J., **9**, 3033-3044.

Vorwerk, S., Somerville, S. and Somerville, C. (2004). The role of plant cell wall polysaccharide composition in disease resistance. Trends Plant Sci, **9**, 203-209.

Wakeley, P.R., Rogers, H.J., Rozycka, M., Greenland, A.J. and Hussey, P.J. (1998). A maize pectin methylesterase-like gene, ZmC5, specifically expressed in pollen. Plant Mol. Biol., **37**, 187-192.

Warrilow, A.G.S., Turner, R.J. and Jones, M.G. (1994). A novel form of pectinesterase in tomato. Phytochemistry, **35**, 863-868.

Wei, Y.D., Shih, J., Li, J.R. and Goodwin, P.H. (2002). Two pectin lyase genes, pnl-1 and pnl-2, from Colletotrichum gloeosporioides f. sp malvae differ in a cellulose-binding domain and in their expression during infection of Malva pusilla. Microbiology-Sgm, **148**, 2149-2157.

Weil, M., Krausgrill, S., Schuster, A. and Rausch, T. (1994). A 17-kDa *Nicotiana tabacum* cell-wall peptide acts as an in-vitro inhibitor of the cell-wall isoform of acid invertase. Planta, **193**, 438-445.

Wen, F.S., Zhu, Y.M. and Hawes, M.C. (1999). Effect of pectin methylesterase gene expression on pea root development. Plant Cell, **11**, 1129-1140.

Weschke, W., Panitz, R., Gubatz, S., Wang, Q., Radchuk, R., Weber, H. and Wobus, U. (2003). The role of invertases and hexose transporters in controlling sugar ratios in maternal and filial tissues of barley caryopses during early development. Plant Journal, **33**, 395-411.

Wicker, L., Ackerley, J.L. and Corredig, M. (2002). Clarification of juice by thermolabile Valencia pectinmethylesterase is accelerated by cations. Journal of Agricultural and Food Chemistry, **50**, 4091-4095.

Wietholter, N., Graessner, B., Mierau, M., Mort, A.J. and Moerschbacher, B.M. (2003). Differences in the methyl ester distribution of homogalacturonans from near-isogenic wheat lines resistant and susceptible to the wheat stem rust fungus. Mol. Plant Microbe Interact., **16**, 945-952.

Wolf, S., Grsic-Rausch, S., Rausch, T. and Greiner, S. (2003). Identification of pollen-expressed pectin methylesterase inhibitors in Arabidopsis. FEBS Lett., **555**, 551-555.

Wu, L.C., Tseng, K.C., Huang, T.H. and Chang, H.M. (2002). Pectinesterase inhibitor in rubbery banana (*Musa sapientum* L.). J. Food Sci., **67**, 1337-1340.

Wu, L.L., Mitchell, J.P., Cohn, N.S. and Kaufman, P.B. (1993). Gibberellin (Ga3) Enhances Cell-Wall Invertase Activity and Messenger-Rna Levels in Elongating Dwarf Pea (Pisum-Sativum) Shoots. Int. J. Plant Sci., **154**, 280-289.

Yang, J.T. (1986). Calculation of protein conformation from circular dichroism. Methods Enzymol., **130**, 208-269.

Yoder, M.D., Keen, N.T. and Jurnak, F. (1993). New domain motif: The structure of pectate lyase C, a secreted plant virulence factor. Science, **260**, 1503-1507.

Zeng, Y., Wu, Y., Avigne, W.T. and Koch, K.E. (1999). Rapid repression of maize invertases by low oxygen. Invertase/sucrose synthase balance, sugar signaling potential, and seedling survival. Plant Physiol., **121**, 599-608.

Zhang, L., Cohn, N.S. and Mitchell, J.P. (1996). Induction of a pea cell-wall invertase gene by wounding and its localized expression in phloem. Plant Physiol., **112**, 1111-1117.

Zuppini, A., Navazio, L., Sella, L., Castiglioni, J., Favaron, F. and Mariani, P. (2005). An endopolygalacturonase from Sclerotinia sclerotiorum induces calcium-mediated signaling and programmed cell death in soybean cells. Mol. Plant-Microbe Interact., **18**, 849-855.